MATHEMATICAL MODELING THE EFFECT OF ANTIMICROBIALS ON HETEROGENEOUS BACTERIAL POPULATIONS

A Dissertation

Presented to

the Faculty of the Department of Chemical and Biomolecular Engineering

University of Houston

In Partial Fulfillment

of the Requirements for the Degree

Doctor of Philosophy

in Chemical Engineering

by

Pratik Rangnath Bhagunde

August 2012

MATHEMATICAL MODELING THE EFFECT OF ANTIMICROBIALS ON HETEROGENEOUS BACTERIAL POPULATIONS

Pratik R. Bhagunde

Approved:

Chairman of the Committee
Michael Nikolaou, Professor,
Chemical and Biomolecular Engineering

Committee Members:

Jacinta Conrad, Assistant Professor,
Chemical and Biomolecular Engineering

Navin Varadarajan, Assistant Professor,
Chemical and Biomolecular Engineering

Vincent H. Tam, Associate Professor,
Department of Clinical Sciences and
Administration

Kevin Garey, Associate Professor and Chair,
Department of Clinical Sciences and
Administration

Suresh K. Khator, Associate Dean,
Cullen College of Engineering

Ramanan Krishnamoorti, Professor and Chair,
Chemical and Biomolecular Engineering

Dedicated

to

my parents for their love and support.

ACKNOWLEDGEMENTS

I would like to thanks my advisor Dr. Michael Nikolaou and my co-advisor Dr. Vincent Tam. It is their support and motivation which kept me always excited and enthusiastic toward my research work. Without their guidance and patience this work would not have been possible. Both of them helped me to develop as an independent researcher, a better speaker and technical writer.

I would also like to thanks my thesis committee members, Dr Jacinta Conrad, Dr. Navin Varadarajan and Dr. Kevin Garey for their suggestions. I would like to express my gratitude to Nahor Haddish Berhane, Alison Betts, John O'Donnell and Mike Kuhn for their support and guidance during my internship at Pfizer. The financial support from the National Science Foundation, Pfizer, AstraZeneca PLC, and Merck and Co. is gratefully acknowledged.

I would like to dedicate my dissertation to my parents and sisters. I am blessed with their love, care and support which has always inspired me and kept me motivated towards my research work.

I have been very lucky to have wonderful friends/roommates around me during my PhD. Pankaj(*Batman Fan*), Arun(*Koterberg*), Pranit(*Pandu*) and Ajay(*APS*) with whom I spent most of the time during my PhD period helped me experience life in Houston would not be that exciting, joyful and memorial.

I would like to mention my thanks to all of my friends: Sameer & Helly, Ashok & Kantaji, Saurabh, Divesh, Ratandeep, Avinash, Charu, Teja, Kshitij, Balagam, Santosh, Rahul jain / Kumar, Srimoyee, Aaditya, Robin, Illa, Manoj, Yogendra, Ashu, Priyank, and Bijesh.

MATHEMATICAL MODELING THE EFFECT OF ANTIMICROBIALS ON HETEROGENEOUS BACTERIAL POPULATIONS

An Abstract

of a

Dissertation

Presented to

the Faculty of the Department of Chemical and Biomolecular Engineering

University of Houston

In Partial Fulfillment

of the Requirements for the Degree

Doctor of Philosophy

In Chemical Engineering

by

Pratik Rangnath Bhagunde

August 2012

ABSTRACT

This dissertation comprises of six chapters with chapters 2-4 being individual case studies, each case study corresponding to a project involving use of mathematical modeling to characterize the effect of antimicrobials on bacterial populations.

In the second chapter a novel mathematical modeling framework to characterize the inoculum effect is proposed. In our approach the inoculum effect was solely attributed to reduced effective drug exposure. Accordingly, a simplified model pharmacodynamic model was developed where the reduced effective drug exposure was expressed as a function of initial bacterial burden. A case of *Escherichia coli* against a combination of piperacillin and tazobactum was used to characterize the model and validate the model assumptions.

In the third chapter, a pharmacodynamic model was used to characterize the biphasic killing profiles observed for the effect of flouroquinolones against both gram-positive and gram-negative bacteria. Time-kill experiment data for the *Escherichia coli* against moxifloxacin and *Staphyloccocus aureus* against levofloxacin was used to characterize the model. Further, the model was used to make predictions regarding the design of the optimal dosing strategy which was selectively validated in the Hollow Fiber Infection Model.

In chapter four, the issue of fluctuating bacterial susceptibilities in the presence of a combination antibiotic and inhibitor was addressed using a novel modeling approach. Instantaneous Minimum Inhibitory Concentration (MIC_i) was defined to capture fluctuating susceptibilities. A theoretical concept capturing fluctuating susceptibility over time was used to define a novel pharmacodynamic index (Time above instantaneous MIC

[T > MIC_i]). The approach was illustrated using a novel beta-lactamase inhibitor MK-7655 in combination with imipenem against a clinical isolate of Klesiella pneumonia *Klebseilla pneumoniae*.

Finally in the fourth chapter mathematical modeling was used to characterize immune-response (granulocyte clearance) against bacterial infections. The semi-mechanistic immune response model was then integrated with a drug effect model to characterize bacterial dynamics in the presence of both immune and drug pressure. The immune-response model was used to characterize bacterial time-kill dynamics for naïve and neutropenic mice. The immune-drug integrated model was later used to model the invivo time-kill data for naïve and neutropenic mice infected with *Klebsiella pneumoniae* (KP-1470) treated with PF-05081090.

TABLE OF CONTENTS

LIST OF FIGURES

LIST OF TABLES

CHAPTER 1

INTRODUCTION AND MOTIVATION

1.1 MODELING BACKGROUND

Bacterial resistance to antibiotics has reached alarming proportions, with potentially grave consequences for public health (13, 17, 26, 32, 38, 40, 64). The need to preserve the efficacy of existing antibiotics against bacterial pathogens and to rapidly develop new antibiotics is imperative. For either task, it is essential to identify effective dosing regimens, such that an antibiotic can safely cure bacterial infections. Identification of effective dosing regimens may start with standard time-kill experiments, namely a set of in vitro experiments where a bacterial population is exposed to a number of different time-invariant concentrations of an antibiotic, and the size of the population is monitored over time (e.g.., 24 hours). The data collected can be used to design effective dosing regimens for realistic antibiotic pharmacokinetics (variation of antibiotic concentration over time in humans). Extrapolation from time-kill experimental data to realistic dosing regimen design can be substantially aided by mathematical modeling of time-kill dynamics. Such modeling aims to determine whether part of a bacterial population is resistant to an antibiotic at a certain concentration. Therefore, it is logical to think of a bacterial population as comprised of subpopulations that are susceptible or resistant to the antibiotic. While this dichotomy is intuitively appealing, using it to model time-kill dynamics may lead to erroneous predictions. Specifically, it has been shown that fitting time-kill data over 24 hours with a model comprising two (resistant and

susceptible) subpopulation balances may fail to predict eventual regrowth of the entire population due to growth of the resistant subpopulation (43).

To remedy this problem, Nikolaou et al. (43) introduced a new model structure to describe time-kill dynamics. Rather than considering two distinct subpopulations, this structure employs a distribution of the bacterial kill rate over an entire bacterial population exposed to an antibiotic concentration. The resulting infinite differential equations for the cumulants of the kill rate distribution were shown to fully capture time-kill dynamics. Under heuristic simplifying assumptions, a finite number of differential equations was obtained, yielding a closed-form expression for the size of a bacterial population over time. This expression allows relatively simple parameter estimation from experimental data and subsequent use of the model for extrapolation of population size over time.

The heuristic approach to handling the cumulant equations referred to in the preceding paragraph was shown to work on experimental data (43) i.e., it was capable of using time-kill data over 24 hours to predict regrowth of the corresponding bacterial population beyond 24 hours.

Consider a bacterial population of N_0 bacteria in an environment of an antibiotic at a fixed concentration *C*. This is the setting in standard in vitro experiments, where the effect of an antibiotic at a series of twofold dilutions is investigated. Under the assumption that all bacteria have the same susceptibility to the antibiotic at concentration *C*, one can write the standard population balance equations.

Physiological growth rate: Because a growing bacterial population will eventually saturate, the *logistic* growth equation for the physiological growth rate can be used in eqn. for long growing populations, to yield

$$\frac{dN}{dt} = \underbrace{K_g N(t)\left[1 - \frac{N(t)}{N_{\max}}\right]}_{\text{physiological growth rate}} - \underbrace{r(C(t))N(t)}_{\substack{\text{kill rate} \\ \text{due to antibiotic}}}, \quad N(0) = N_0 \ . \tag{1}$$

The logistic growth equation is based upon the fact that bacterial population in absence of antibacterial antibiotic would not continue to grow exponentially forever. Any bacterial inoculum in presence of limited nutrient would follow the lag-log-stationary growth pattern. The stationary growth phase is the saturation phase wherein the growth rate becomes negligible.

Kill rate: The kill rate term $r(C(t))$ varies with every drug and bacteria combination. A commonly used expression for kill rate is the Hill expression where $r(C(t))$ is defined as

$$r(C) = \frac{KC^H}{C^H + C_{50}{}^H} \ , \tag{2}$$

where K_k is the maximal kill rate achieved as $C \to \infty$; C_{50} is a constant equal to the antibacterial antibiotic concentration at which 50% of the maximal kill rate is achieved; and H is the Hill exponent, corresponding to how inflected $r(C(t))$ is as a function of C. Consider now a heterogeneous bacterial population in which resistance to an antibacterial antibiotic varies among bacteria, with more resistant bacteria corresponding to lower kill rate constants $r(C)$. For a given antibacterial antibiotic concentration *C*, one may consider a distribution of $r(C)$ over the bacterial population. Considering such a distribution is plausible from a physiological viewpoint, given that variability is expected

within any given species. From a therapeutic viewpoint, the desired outcome for a given antibacterial antibiotic concentration is the eventual killing of all bacteria and avoidance of any regrowth. The following theorem provides the basis for an analysis that can help extrapolate ordinary 24-hour in vitro experimental data, to make predictions about eventual elimination or regrowth of heterogeneous populations.

Consider a population of $N(t)$ bacterial cells exposed to an antibiotic at concentration C. Discretize this population into subpopulations, each having $N_i(t)$ cells, such that

$$N(t) = \sum_i N_i(t) . \tag{3}$$

Each subpopulation satisfies the cell balance

$$\frac{dN_i}{dt} = \left(K_g \left[1 - \frac{N(t)}{N_{\max}} \right] - r_i(C) \right) N_i(t) . \tag{4}$$

with a corresponding kill rate constant $r_i(C)$. All subpopulations are assumed to share the same physiological growth rate constant K_g, because they correspond to the same basic species. Further, growth saturation is assumed to be governed by the same term $1 - N(t)/N_{\max}$. Even though eqn. 4 is conceptually appealing, it is of little use for modeling experimental data, because the size of individual subpopulations, $N_i(t)$, cannot realistically be measured in time-kill experiments. What is routinely measured in such experiments is the size of the entire population, $N(t)$, over time, for which summation of eqn. 4 over all i yields

$$\begin{aligned}\frac{dN}{dt} &= \sum_i \left(K_g \left[1 - \frac{N(t)}{N_{\max}} \right] - r_i(C) \right) N_i(t) \\ &= \left(K_g \left[1 - \frac{N(t)}{N_{\max}} \right] - \mu(t) \right) N(t)\end{aligned} \quad . \tag{5}$$

where the average $\mu(t)$ of the kill rate constant $r_i(C)$ is defined in a standard way as

$$\mu(t) \hat{=} \sum_i r_i(C) \, f\left(r_i(C), t\right) \tag{6}$$

with

$$f\left(r_i(C), t\right) \hat{=} \frac{N_i(t)}{N(t)} \tag{7}$$

The quantity $f\left(r_i(C), t\right)$ can be thought of as the probability distribution function for the kill rate constant $r_i(C)$ over the entire population at a given antibiotic concentration C and at time t.

The above eqn. 5 makes intuitive sense, since it suggests that the dynamics of the entire population is similar to the dynamics of individual subpopulations, the only difference being that the average kill rate over the entire population affects the overall population dynamics. The population average of the kill rate constant, $\mu(t)$, decreases over time, as the percentage of more resistant subpopulations in the overall population increases.

Consider the following kill rate average which declines exponentially with time

$$\mu(t) \approx \underbrace{\mu(0) - \frac{\sigma(0)^2}{A}}_{b} + \underbrace{\frac{\sigma(0)^2}{A}}_{R} e^{-At} \quad , \tag{8}$$

$$\mu(t) \approx Re^{-At} + b \,. \tag{9}$$

For heterogeneous populations subjected to a time invariant concentration C the average kill rate coefficient would eventually reach a value b for each C. This is because whatever mixture of susceptible population we start with eventually all the susceptible would be killed by the drug to leave just the resistant one as $t \to \infty$. This population at $t \to \infty$ would eventually be homogeneous. It is assumed that the initial average kill rate and the kill rate as $t \to \infty$ follow the functional form given by eqn.(2). The initial average kill rate and kill rate average as $t \to \infty$ are thus given as

$$R + b = \frac{K_k C^H}{C^H + C_{50}^H}, \tag{10}$$

$$b = \frac{K_b C^{Hb}}{C^{Hb} + C_{50b}^{Hb}} \quad . \tag{11}$$

1.2 BASIC MICROBIOLOGY PROCEDURES AND TERMINOLOGY

1.2.1 Minimum Inhibitory Concentration (MIC)

Minimum inhibitory concentration (MIC) is the minimum concentration of the antimicrobial which will inhibit visible growth of microorganism after overnight incubation. A pictorial representation of MIC is shown in Figure 1-1. MIC is the most basic laboratory measurement of activity of an antimicrobial against a microorganism. MIC is important to confirm resistance of a microorganism against an antimicrobial agent (4). A better antimicrobial agent has lower MIC values.

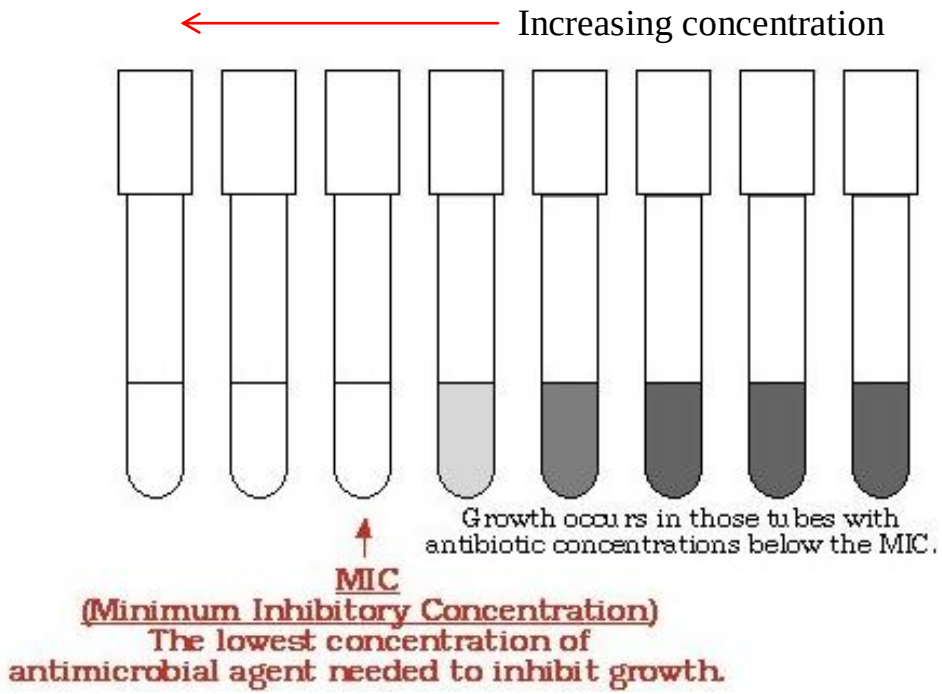

Figure 1-1 Broth dilution method for measuring MIC

1.2.2 Time-kill study

Time-kill study is an experimental procedure used to measure the dynamics of antimicrobial pressure on bacterial populations. In a typical time-kill study a fixed bacterial burden is exposed to time-invariant escalating concentrations of antimicrobial and the change in bacterial burden with time is observed. Such a change in bacterial burden with time could be quantified by collecting bacterial samples at fixed time points (eg. 0, 2, 4, 6, 8, 12 and 24 h) and plating the samples to observe the colony forming units per ml (cfu/ml) after 24 h incubation.

While MIC is important to measure the susceptibility of a microorganism to an antimicrobial, it does not give any information on the kill kinetics. Time-kill studies help in measuring the rate of killing by the antimicrobial. Such a study is useful in understanding the onset of resistance and suboptimal drug pressures that may be causing it. A typical time-kill study data is shown in Figure 1-2.

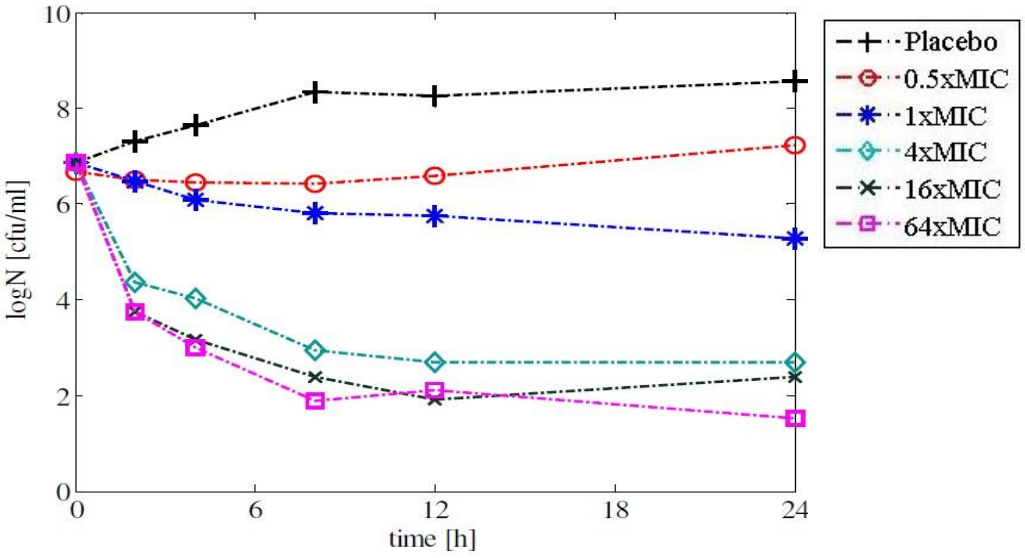

Figure 1-2 A typical time-kill data for levofloxacin against *Staphylococcus aureus* (SA-29213). N is bacterial population measured as colony forming units per ml (cfu/ml) Concentration of levofloxacin is scaled in multiples of MIC.

1.3 INOCULUM EFFECT

Inoculum effect is the reduced bacterial kill observed at higher bacterial burden. A typical example of inoculum effect is shown in Figure 1-3. In this time-kill study it is clearly evident that as the baseline (initial) bacterial inoculum is increased from 10^5 CFU/ml to 10^8 CFU/ml, the same concentrations of drug are unable to kill the bacteria with same effect. For baseline inoculum of 10^5 CFU/ml higher drug concentrations are able to contain the bacteria. However, for 10^8 CFU/ml all of the drug concentrations fail to completely eradicate the bacteria. This reduction in killing effect is observed gradually for baseline inoculum of 10^6 CFU/ml and 10^7 CFU/ml.

The inoculum effect is a phenomenon that has been described for many different antibiotics and how they affect several different organisms after it was first discovered in 1945 (65). A general observation is that a higher concentration of organisms requires a higher concentration of antibiotic to achieve the same degree of bacterial killing. Simplistically, it would make sense that the more organisms there are to kill; the more antibiotic molecules are needed to do so. However, the mechanisms for the inoculum effect could be much more complex, depending upon the number of antibiotic molecules necessary to kill a single organism, the various resistance mechanisms employed by bacteria, the quantity of inactivating enzymes produced by the organisms, the growth cycle characteristics of the organisms, and so forth. Regardless of the mechanism, it appears that in most cases, a higher concentration of bacteria i.e. a greater number of bacteria in any given volume of fluid or tissue will decrease the effectiveness of antibiotics.

A

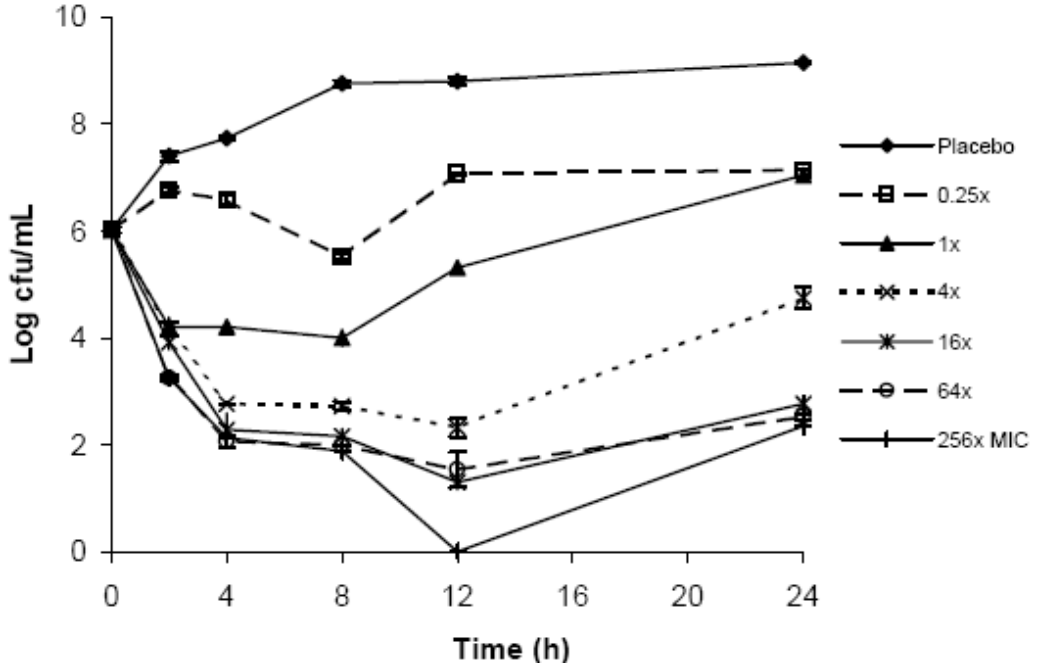

B

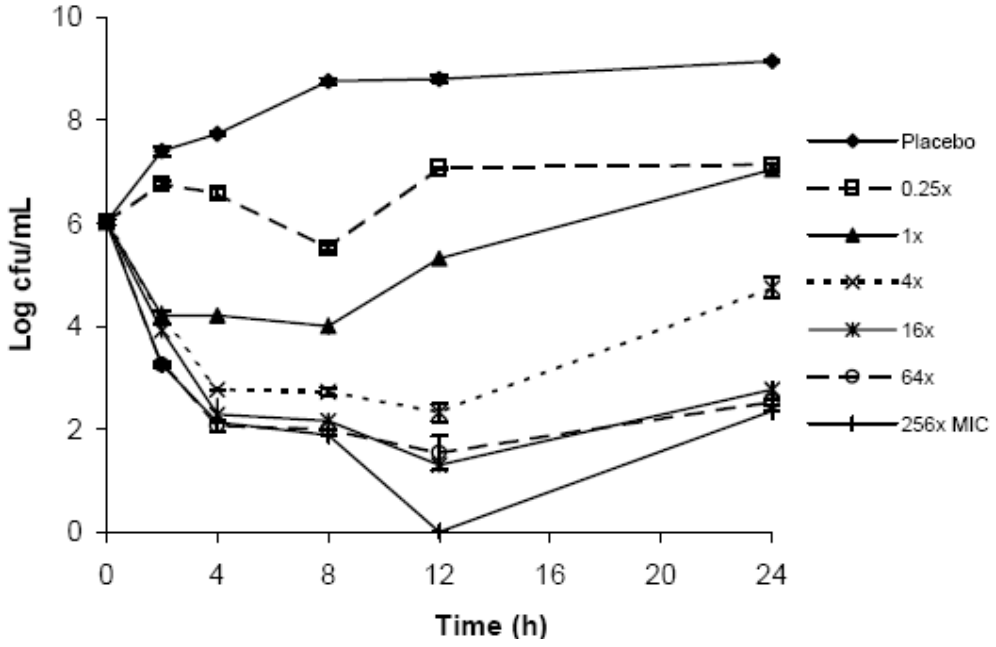

Figure 1-3 Time kill studies of piperacillin / tazobactam against *E. coli* ATCC 25922. Data shown as mean ± standard deviation. Baseline inoculum (A) 10^5 CFU/ml; (B) 10^6 CFU/ml.

C

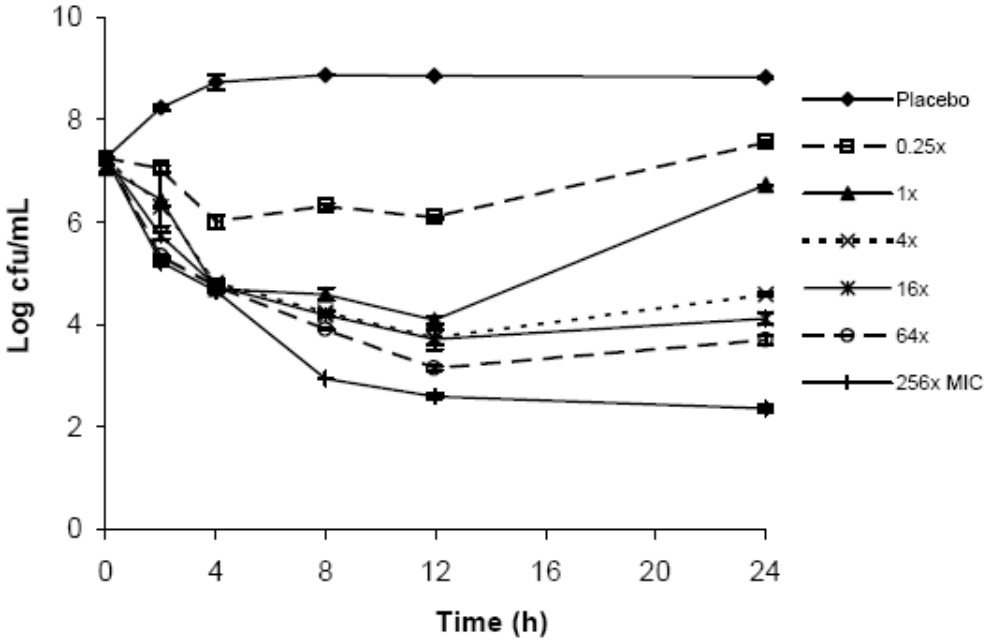

D

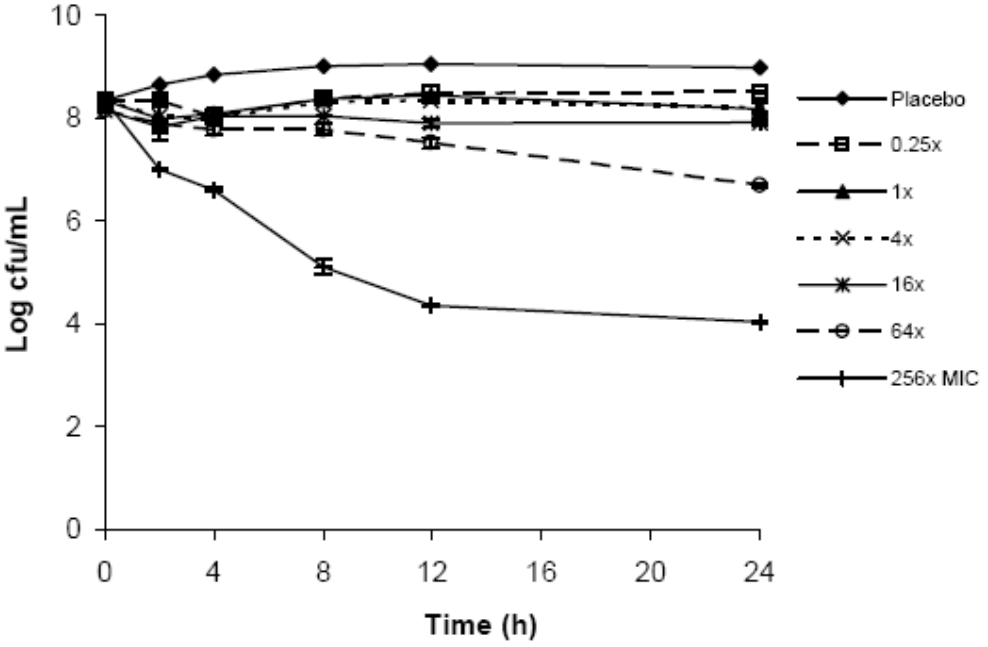

Figure 1-3 Time kill studies of piperacillin / tazobactam against *E. coli* ATCC 25922. Data shown as mean ± standard deviation. Baseline inoculum (C) 10^7 CFU/ml; (D) 10^8 CFU/ml. (Continued).

1.4 PHARMACODYNAMICS OF DIFFERENT CLASSES OF ANTIMICROBIALS

For an antibiotic to eradicate an organism, three major factors must occur. First, the antibiotic must bind to its target site(s) in the bacterium. To reach the binding site is no easy matter. It must penetrate the outer membrane of the organism (penetration resistance), avoid being pumped out of the membrane (efflux pump resistance), and remain intact as a molecule (e.g., avoid hydrolysis by beta-lactamases). Once the target is reached, the antibiotic can still be useless if the binding site has changed its molecular configuration and no longer allows the drug to attach. A range of different binding sites has been identified including ribosomes, penicillin-binding proteins, DNA topoisomerase/gyrase, and the cell membrane itself. The crucial binding site will vary with the antibiotic class. These binding sites can be defined as points of biochemical reaction crucial to the survival of the bacterium. Thus, by binding to these sites, the antibiotic interferes with the chemical reaction resulting in the death of the bacterium.

Second, the drug must not only attach to its binding target but also must occupy an adequate number of binding sites, which is related to its concentration within the microorganism.

Third, for an antibiotic to work effectively, the antibiotic should remain at the binding site for a sufficient period of time in order for the metabolic processes of the bacteria to be sufficiently inhibited.

Thus, the two major determinants of bacteria killing include the concentration and the time that the antibiotic remains on these binding sites. The area under the concentration curve (AUC) after a dose of antibiotic measures how high (concentration)

and how long (time) the antibiotic levels remain above the target MIC during any one dosing interval. In essence, the AUC indirectly measures the two major factors for bacterial eradication and quantifies the amount of exposure of the organism to the antibiotic during any one dosing interval.

Time-Dependent Killing:

For certain classes of antibiotics, the major killing effect against an organism is produced by either the time or the concentration of the drug at the binding site. In fact, of these two factors of bacterial killing, the killing process may be so minimal that it can be ignored in the prediction of a clinical response. For instance, certain antibiotics, like beta-lactams (penicillins, cephalosporins, carbapenems, monobactams), clindamycin, macrolides (erythromycin, clarithromycin), oxazolidinones (linezolid), can be effective because of the extensive amount of time the antibiotic binds to the microorganism. The inhibitory effect can be effective because their concentration exceeds the MIC for the microorganism. Hence, these antibiotics are referred to as time-dependent antibiotics. For time-dependent drugs, the pharmacodynamic parameter can be simplified to the time that serum concentrations remain above the MIC during the dosing interval (T>MIC) , Figure 1-4.

Concentration-Dependent Killing:

Other classes of antibiotics, such as aminoglycosides and quinolones, have high concentrations at the binding site which eradicates the microorganism and, hence, these drugs are considered to have a different kind of bacterial killing, named concentration-dependent killing. For concentration-dependent agents, the pharmacodynamic parameter can be simplified as a C_{max}/MIC ratio.

These concepts have been even further refined from studies performed in animal models of sepsis, in-vitro pharmacokinetic models and volunteer studies. For instance, for antibiotics with time-dependent killing, the optimal responses occur when the time that the drug remains above the MIC is equal or greater than 50% of the dosing interval. For agents with concentration-dependent killing, the best responses occur when the concentrations are $\geq$ 10 times above the MIC for their target organism (s) at the site of infection (15) For agents with concentration-dependent killing, it has also been shown that clinical responses can be predicted as well as the peak/MIC ratio by measuring the AUC over the dosing interval and dividing that value by the antibiotic's MIC against the target organism. In essence, the AUC/MIC ratio becomes a "default" pharmacodynamic concept for the peak/MIC ratio for antibiotics with concentration-dependent killing.

This concept has been studied best with the fluoroquinolones. For instance, certain organisms require modest AUC/MIC ratio for their prompt eradication, *Streptococcus pneumoniae*and most other Gram-positive bacteria are typically rapidly killed by quinolones at an AUC/MIC_{24hr} ratio $\geq$ 30) whereas others, like *Pseudomonas aeruginosa* and most other aerobic Gram-negative bacteria, require much greater exposure of time to quinolones (AUC/MIC_{24hr} ratios $\geq$ 100-125) (20, 67).

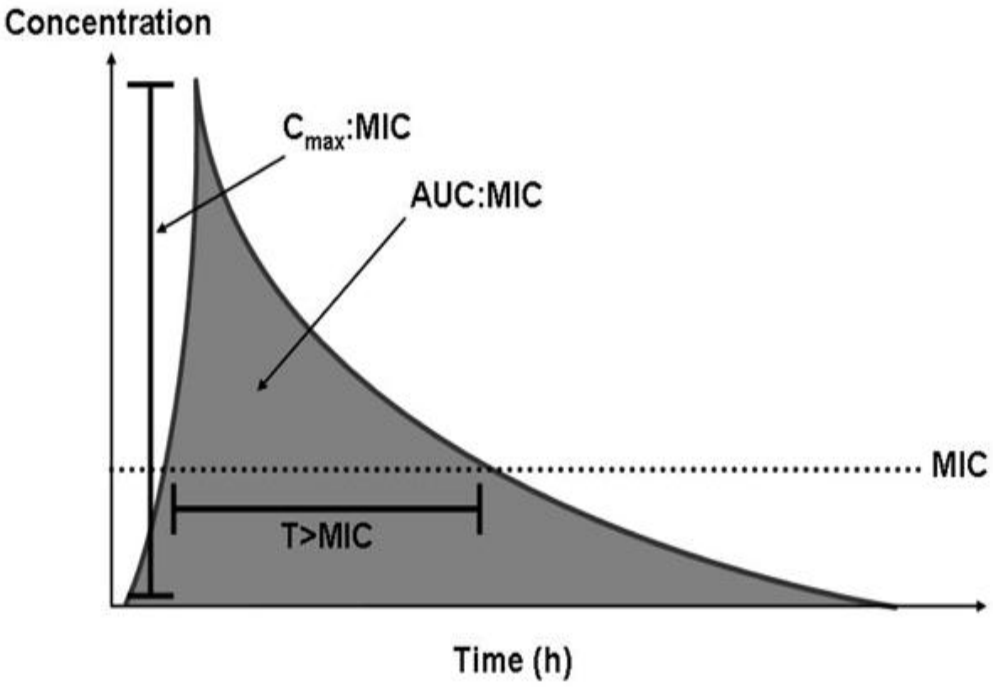

Figure 1-4 Plot showing the area under the concentration curve and MIC. Different pharmacodynamic indices are also shown.

1.5 ANTIBIOTIC-INHIBITOR COMBINATION PHARMACODYNAMICS

Since the development of new drugs is a long, non-trivial process unable to meet the current demand (21), alternative to restore the effectiveness of existing drugs should be investigated. A viable approach towards that end is the development of inhibitors designed to target specific resistance mechanism(s). For instance, it has long been known that resistance mediated by production of beta-lactamases could be tackled by an inhibitor which inhibits the function of the beta-lactamases (drug hydrolysis). Similarly, efflux pump inhibitors could be used against bacteria that over-express efflux pumps to extrude drugs from the bacterial cells, thereby decreasing intracellular drug concentration.

Despite inhibitors being developed since a long time, the design of optimal dosing strategy for them is unprecedented. Depending on the class of antibiotics different pharmacodynamic indices such as C_{max}/MIC, AUC/MIC and T > MIC could be useful in determine optimal dosing strategies (1). However, such indices may not be immediately applicable to inhibitors since the susceptibility of the bacteria increases with inhibitor concentration. In contrast the MIC for drug-bacteria combination is determined in absence of inhibitor (intrinsic MIC). This calls into question the use T > MIC where in presence of inhibitor the MIC may be significantly lower than intrinsic MIC. This issue is further aggravated when both the drug and inhibitor concentrations fluctuate with time governed by their respective pharmacokinetics. In such a case ideally, the MIC is changing with every instant of time thus giving rise to fluctuating susceptibilities. As in the case of a single antimicrobial agent, variables such as dose, dosing interval and inter-

subject pharmacokinetic differences make the process of determining optimal dosing regimens for drug/inhibitor combinations non-trivial. Therefore, comprehensive assessment of all possible dosing strategies is impractical in pre-clinical and clinical investigations. In empirical selection of dosing regimens the full potential of these new inhibitor candidates may not be realized. The use of mathematical modeling and simulation comes in extremely handy to address some of these complicated issues for antibiotic-inhibitor combinations.

1.6 IMMUNE RESPONSE AND ANTIMICROBIAL EFFECT

For any infected individual immune system is body's intrinsic defense mechnism against the infection. The innate immune response primarily involves granulocytes as the first line of such defense. Granulocytes play a major in clearing many bacterial infections. In-spite of this, there are few efforts to delineate the role of granulocytes in clearing infection.

With the concern of bacterial resistance to antibiotics, the race to develop new antibiotics with optimal dosing strategies has taken pace. Mathematical modeling is one of the decision support tools which could help in speeding up the pre-clinical and clinical development of new antibiotics. While there have been numerous efforts to characterize the effect of antibiotics on dynamic bacterial populations, little attention has been paid to the role of immune system. In-vivo experiments to characterize the drug effect were done primarily on neutropenic animals undermining the role of immune system. If the contribution of immune system is overlooked, there is a possibility that the dose predictions are suboptimal; further aggravating the issue of resistance.

Integrating the immune response with drug effect would help in demarcating how much of the curing ability is due to antibiotics and how much is due to immune response. An ideal experimental series to integrate the immune response with drug effect would be first to characterize the immune response with no-drug in-vivo experiments and then integrate the resulting immune response with drug effect in-vivo data. Such an exercise would also help to determine if there is any interaction between the immune system and drug. When such integration is achieved at in-vivo level it could be extrapolated to

complex human like systems. Our work is a small step forward in quantifying the contributions of immune system and drug effect.

1.7 OBJECTIVES OF RESEARCH

In summary the present research work has four objectives:

A) Development of a mathematical modeling framework to characterize the inoculum effect.

B) Development of a pharmacodynamic model to characterize resistance against fluoroquinolones and make optimal dosing strategy predictions.

C) Development of a novel mathematical modeling and simulation framework to guide design of optimal dosing regimens for antibiotic-inhibitor combination.

D) Development of semi-mechanistic modeling framework to characterize immune response and integrate the immune response with drug effect.

The entire thesis is divided into four case studies making 4 core chapters as follows. Chapter 2 discussed the novel mathematical framework to explain inoculum effect. Chapter 3 is about a modeling of flouroquinolones and making optimal predictions. 4^{th}chapter consists of novel mathematical modeling framework to describe dynamics of antibiotic-inhibitor combination. Finally chapter 5 comprises of modeling framework to characterize immune response and integrate the immune response with drug effect. Finally all case studies are concluded in chapter 6.

CHAPTER 2

MATHEMATICAL MODELING FRAMEWORK TO CHARACTERIZE INOCULUM EFFECT

2.1 INTRODUCTION

Escherichia coli is part of the human gastrointestinal flora and a common pathogen implicated in intra-abdominal infections such as perforated appendicitis and peritonitis. Beta-lactams are often the empiric drug of choice for the management of severe intra-abdominal infections, in view of their spectrum of activity and safety profile. In intra-abdominal infections, a heavy bacterial burden is commonly encountered and the clinical utility of the beta-lactams may be limited by the inoculum effect. This phenomenon is believed to be due to the physiologic state of the bacterial cells, or preferential expression of different penicillin-binding proteins, rendering the bacteria less susceptible to beta-lactams (53). Biofilm production and quorum sensing may also be involved.

We and others have previously developed mathematical models to capture the dynamic relationship between a heterogeneous microbial population and constant drug concentrations (33, 41, 43, 48, 60, 66). Our models were further refined to predict the microbial response to multiple antimicrobial agent dosing regimens (fluctuating drug concentration over time) efficiently (42, 62). Such a modeling approach could be used as a decision-support tool for dosing regimen design, and it may be used at different stages of drug development. It is often observed that killing could be more pronounced against a lower bacterial burden than with a higher bacterial burden (8, 10, 55). Capturing this

phenomenon in a mathematical model would require a killing function dependent on bacterial burden. However, one common assumption in most modeling approaches is that the killing function is independent of the bacterial burden (11, 36, 57). This modeling assumption is often restrictive and is only useful when there is not a very significant change in bacterial susceptibility to antimicrobials, as the bacterial burden changes. In other cases, it may be misleading in making accurate predictions about the bacterial behaviors. For example, an experiment with a higher bacterial burden may suggest a dosing exposure requirement to suppress regrowth, but this may overestimate the requirement to suppress regrowth at lower bacterial burdens. In order to capture the overall picture satisfactorily, we need a more robust model which conclusions can be extended over a wide range of bacterial burden.

2.2 MATERIALS AND METHODS

The objective of this study was to extend our mathematical modeling approach proposed previously, to further account for the reduced in-vitro killing observed. For illustrative purposes, a standard wild-type *E. coli* strain with various baseline inocula was used in this investigation.

2.2.1 Antimicrobial agents

Piperacillin and tazobactam were purchased from Sigma (St. Louis, MO). A stock solution of each antimicrobial agent in sterile water was prepared, aliquoted, and stored at -70°C. Prior to each susceptibility testing, an aliquot of the drug was thawed and diluted to the desired concentrations with cation-adjusted Mueller-Hinton broth (Ca-MHB) (BBL, Sparks, MD).

2.2.2 Microorganisms

E. coli ATCC 25922 (American Type Culture Collection, Rockville, MD) was used in the study. The bacteria were stored at -70°C in Protect® (Key scientific products, Round Rock, TX) storage vials. Fresh isolates were sub-cultured twice on 5% blood agar plates (Hardy Diagnostics, Santa Maria, CA) for 24 hours at 35°C prior to each experiment.

2.2.3 Susceptibility studies

Minimum inhibitory concentration (MIC) / minimum bactericidal concentration (MBC) were determined in Ca-MHB using a modified macrobroth dilution method as described by the CLSI.(5) The final concentration of bacteria in each macrobroth dilution tube was approximately 5×10^5 CFU/ml of Ca-MHB. Serial twofold dilutions of

drugs were used. The MIC was defined as the lowest concentration of drug that resulted in no visible growth after 24 hours of incubation at 35°C in ambient air. Samples (50 μl) from clear tubes and the cloudy tube with the highest drug concentration were plated on Mueller-Hinton agar (MHA) plates (Hardy Diagnostics, Santa Maria, CA). The MBC was defined as the lowest concentration of drug that resulted in ≥ 99.9% kill of the initial inoculum. Drug carry-over effect was assessed by visual inspection of the distribution of colonies on media plates. The studies were conducted in duplicate and repeated at least once on a separate day.

2.2.4 Time kill experiments

Time-kill studies were performed using different inocula ranging from approximately 1×10^5 to 1×10^8 CFU/ml at baseline. A clinically achievable unbound concentration range of piperacillin (0 – 512 mg/l) / tazobactam (4 mg/l in all investigations to minimize effect of any constitutive beta-lactamase, if present), were used, and the drug concentrations were normalized to multiples of MIC. Serial samples (baseline, 2, 4, 8, 12 and 24 hours) were obtained in duplicate over 24 hours; viable bacterial burden was determined by quantitative culture. Prior to culturing the bacteria quantitatively, the bacterial samples were centrifuged at 10000× G for 15 minutes, and reconstituted with sterile normal saline in order to minimize drug carry-over effect. Total bacterial populations were quantified by spiral plating (Spiral Biotech, Bethesda, MD) 10× serial dilutions of the samples (50 μl) onto MHA plates. The media plates were incubated at 35°C for up to 24 hours, then bacterial density from each sample was enumerated visually. The theoretical reliable lower limit of detection was 400 CFU/ml.

2.2.5 Mathematical modeling

Based on our previous work (43), all time-kill profiles of *E. coli* over 24 hours were modeled collectively. During our investigation, several related mathematical model structures were evaluated. The modified structure of the final growth dynamics model is shown in Figure 2-1. Briefly, the rate of change of bacteria over time was expressed as the difference between the intrinsic bacterial growth rate and the (sigmoidal) kill rate provided by the antimicrobial agent. Decline in kill rate over time and regrowth were attributed to adaptation, which was modeled as reduction in the kill function, using a saturable function of antimicrobial agent selective pressure [both piperacillin effective concentration (C) and time (t)]. In addition, to account for the inoculum effect, an effective drug concentration was used in all killing and adaptation terms, which was explicitly modeled as a sigmoidal function of the initial inoculum. The effective drug concentration can be conceptualized as the result of a biofilm barrier put up by a dense bacterial population (i.e., the greater the bacterial population, the greater the drug barrier, and thus the less effective drug concentration). Biofilm is basically an aggregate of bacteria in a matric of external polymeric substance. The modeling estimation process involved 2 steps. The intrinsic bacterial growth rate (K_g) and maximal bacterial population size (N_{max} - to account for contact inhibition) were first determined from placebo (control) experiments. Using these parameter estimates, the parameter values in the killing function were subsequently determined using data from all active treatment experiments simultaneously. The performance of different model candidates were assessed by visual fit to the data, and discriminated using the Akaike's information

criterion. The rule of parsimony was used. All modeling was performed with MATLAB version 7.5 (The MathWorks, Inc., Natick, MA).

Figure 2-1 Bacterial growth dynamics model and various model parameters

Population balance for a bacterial population:

Rate of change of bacteria over time = Intrinsic growth rate – Kill rate by antimicrobial agent

$$\frac{dN(t)}{dt} = G[N(t)] - K[C_{eff}(t), N(t)]$$

where:

$$G[N(t)] = K_g \cdot [1 - \frac{N(t)}{N_{\max}}] \cdot N(t)$$

$$K[C_{eff}(t), N(t)] = \{(\{[\frac{C_{eff}(t)^H \cdot K_k}{C_{eff}(t)^H + (C_{50k})^H}] - [\frac{C_{eff}(t)^H \cdot K_k}{C_{eff}(t)^H + (C_{50b})^H}]\} \cdot e^{-A \cdot t}) + [\frac{C_{eff}(t)^H \cdot K_k}{C_{eff}(t)^H + (C_{50b})^H}]\} \cdot N(t)$$

G – growth rate function

K – kill rate function

K_g – growth rate constant for bacterial population

$N(t)$ – concentration of bacterial population at time t

$N_{\max}$ – maximum population size

$C(t)$ – concentration of drug at time t

$C_{eff}(t)$ – effective concentration of drug at time t

K_k – maximal kill rate constant for bacterial population

C_{50k} – concentration to achieve 50% maximal kill rate of the initial population

C_{50b} – concentration to achieve 50% maximal kill rate of the most resistant population

H – sigmoidicity constant for bacterial population

A – adaptation function

and

$$C_{eff}(t) = [1 - \frac{LogN(0)^{Q}}{LogN(0)^{Q} + LogN_{50}{}^{Q}}] \cdot C(t)$$

$$A = \frac{C_{eff}(t)^{Ha}}{C_{eff}(t)^{Ha} + (C_{50a})^{Ha}}$$

N_{50} – bacterial population which 50% of actual drug concentration is in effect

Q – sigmoidicity constant for drug concentration

C_{50a} – concentration to achieve 50% maximal adaptation rate

Ha – sigmoidicity constant for bacterial adaptation

2.2.6 Sensitivity analysis

After the model fitting, selected parameters were evaluated for sensitivity with respect to their best fit estimates. This was done by plotting the 95% joint confidence intervals for a selected group of parameters. The joint confidence plots were produced using the Fischer test. If (1-α) is the confidence level and $S(\theta)$ is residual sum of squares at the point estimate θ, the (1-α) confidence region for P-parameters in the vector θ is the region where θ satisfies the inequality:

$$S(\theta) \leq S(\theta)\ (1 + P * \frac{F(P, N-P; \alpha)}{(N-P)}\ ) \qquad (12)$$

2.2.7 Experimental validation

The association of a bacterial population size with biomass was assessed semi-quantitatively using a modified colorimetric assay as described previously (25). Briefly, a late log-phase growth culture of *E. coli* was diluted and inoculated into 1/4 strength Ca-MHB (final density of 1×10^{5} or 1×10^{8} CFU/ml). The bacteria were incubated in an in-vitro assay (Calgary Biofilm device, MBEC, Calgary, AB) at 37 °C on a platform shaker

for 24 hours. Three pegs were randomly removed from the lid of the assay. Media and non-adherent planktonic bacteria were removed by vortexing briefly in saline, after which they were transferred and fully immersed in 0.1% crystal violet for 15 minutes. After removing the excessive dye solution, the attached dye was eluted using 95% ethanol, and the absorbance at 580 nm was determined using a spectrophotometer. Uninoculated growth medium was used as a negative control. *Pseudomonas aeruginosa* ATCC 700888 (a known biofilm hyperproducer) was used as a positive control.

2.3 RESULTS

2.3.1 Susceptibility studies

`The MIC/MBC of the *E. coli* isolate to piperacillin were found to be 2/2 mg/l, respectively. The susceptibilities to piperacillin did not change in the presence of tazobactam.

2.3.2 Time-kill experimets

Data from the time-kill studies are as shown in Figure 2-2. As anticipated from other previous investigations (2, 3, 8, 13, 22), the killing of piperacillin was considerably reduced as the baseline inoculum increased from 1×10^5 to 1×10^8 CFU/ml. Significant reduction in bacterial burden (> 2 log drop at 24 hours) was observed with 4× MIC when the baseline inoculum was 1×10^5 CFU/ml (Figure 2-2A), compared to 256× MIC when the baseline inoculum was 1×10^8 CFU/ml (Figure 2-2D).

A

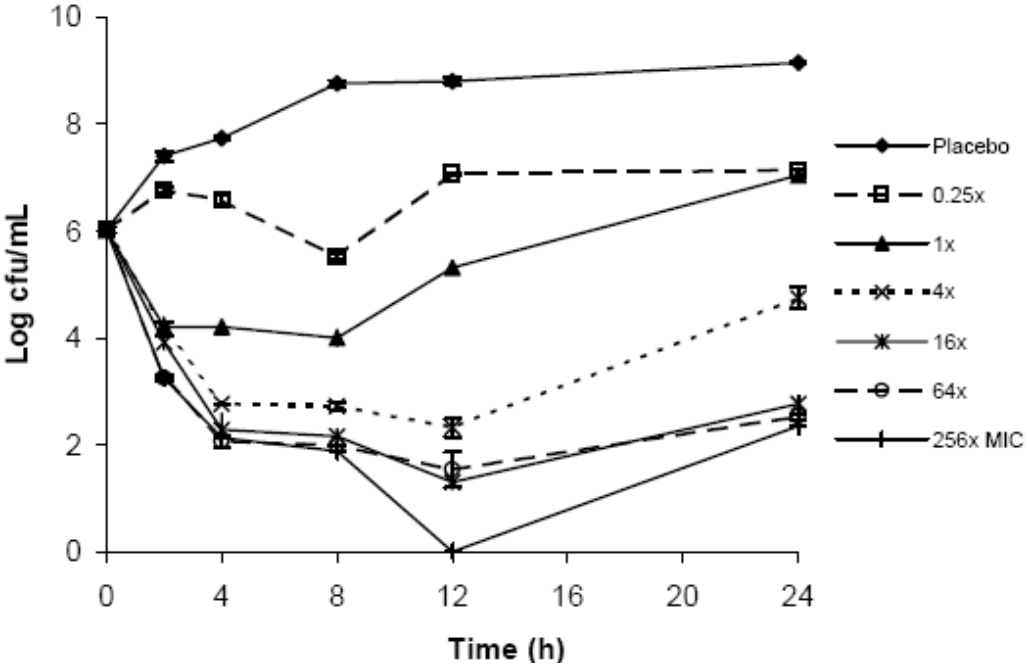

B

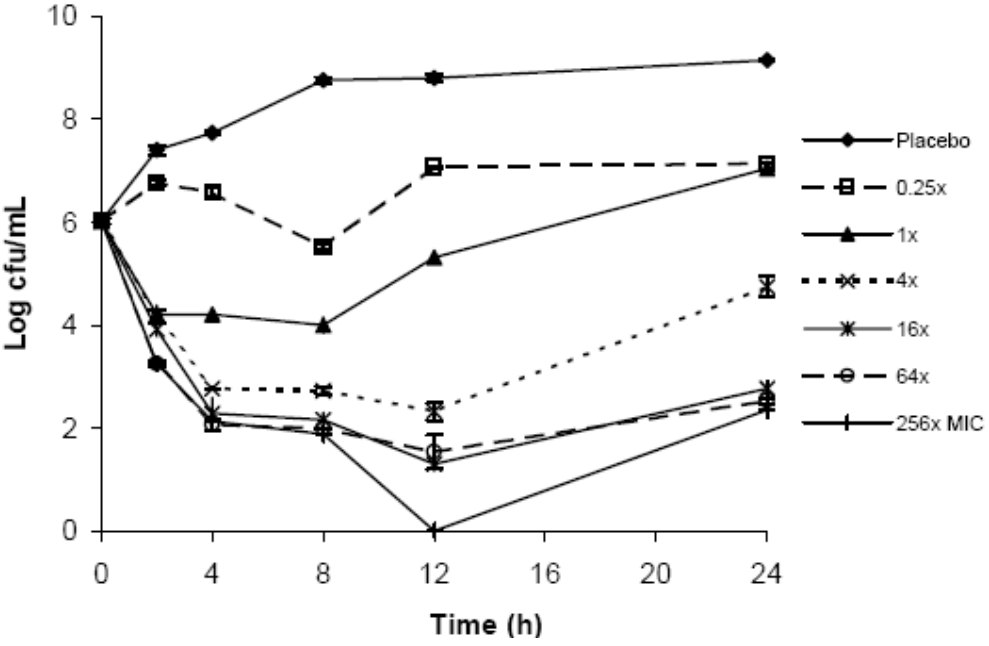

Figure 2-2 Time kill studies of piperacillin / tazobactam against *E. coli* ATCC 25922. Data shown as mean ± standard deviation. Baseline inoculum (A) 10^5 CFU/ml; (B) 10^6 CFU/ml. Continued..

C

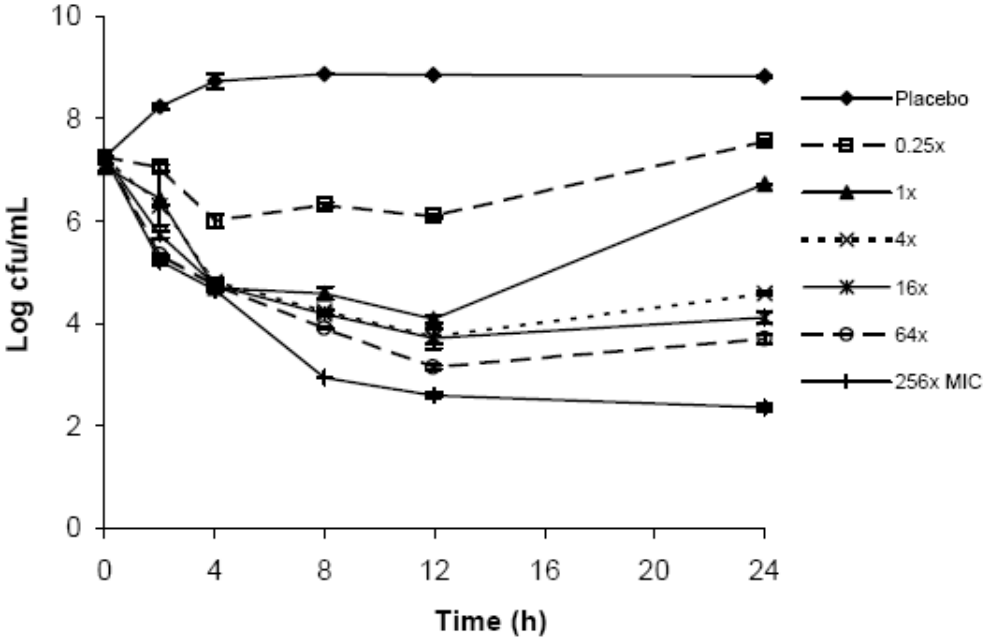

D

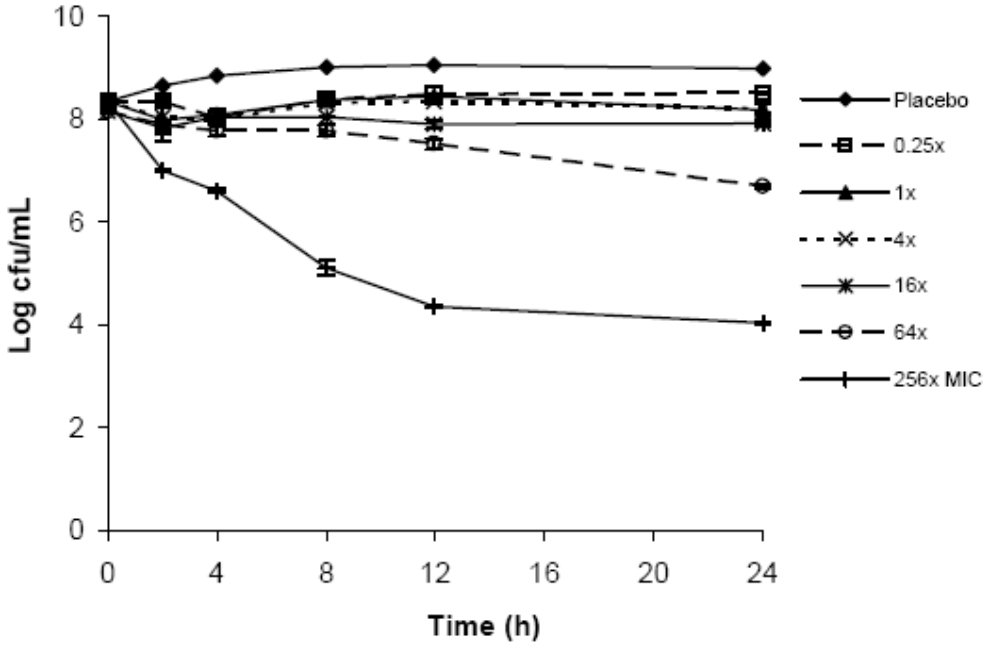

Figure 2-2 Time kill studies of piperacillin / tazobactam against *E. coli* ATCC 25922. Data shown as mean ± standard deviation. Baseline inoculum (C) 10^7 CFU/ml; (D) 10^8 CFU/ml.

2.3.3 Mathematical modeling

The model best-fits to the data are as shown in Figure 2-3. The estimates of the best-fit model parameters are as shown in Table 2–1. Taken as a whole, the observations in bacterial burdens over time were reasonably described by the model. Several alternative model candidates were explored (data not shown). Generally, the fits of these alternative models to the experimental data were less satisfactory when: (1) the adaptation function was condensed to a single parameter (as expected); and (2) the actual (instead of effective) drug concentration was used in the killing / adaptation functions. Additionally, we attempted to incorporate drug degradation in the model as (i) a zero order decay with a degradation constant of 0.01 h^{-1} and (ii) a first order decay with a degradation rate constant of 0.015 h^{-1}. The final best-fit parameter estimates were not found to be significantly different from the original estimates when the drug degradation was not considered.

A

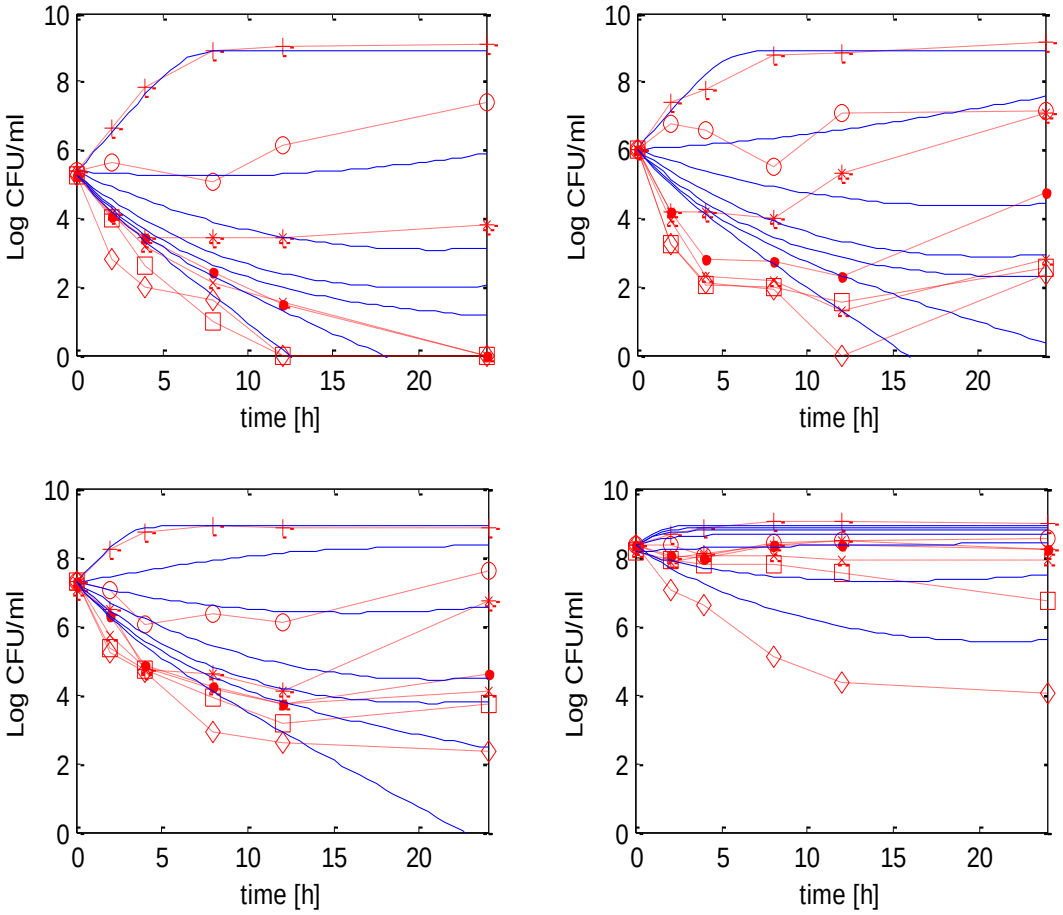

Figure 2-3 Model fits to the experimental data. (A) Overlay of experimental data with the best-fit model. Red symbols (and dotted lines) represent experimental data: +, placebo; ○, 0.25×MIC; *, 1×MIC; ●, 4×MIC; ×, 16×MIC; □, 64×MIC; ◊, 256×MIC. Blue (solid) lines depict the best fit model.

B

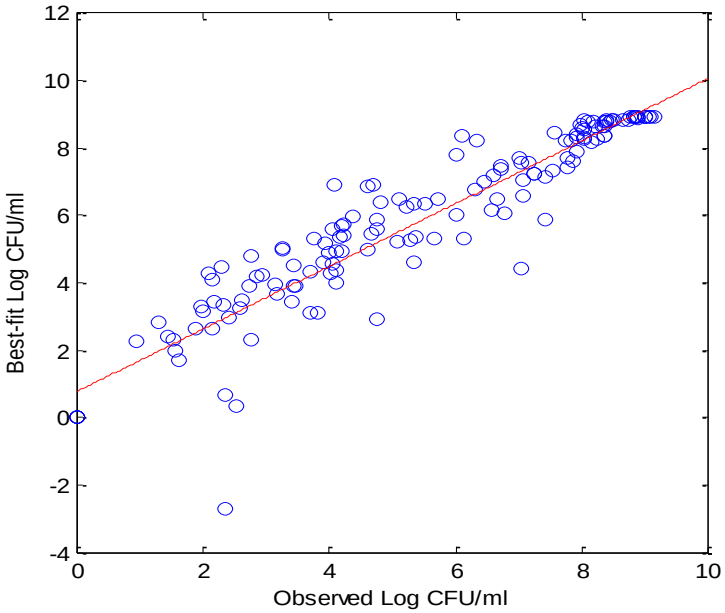

$R^2 = 0.88$

The best-fit regression line is given by:

Best-fit = 0.94 * Observed + 0.68

Figure 2-3 Model fits to the experimental data (B) Correlation between observed and best-fit bacterial burden.

2.3.4 Sensitivity analysis

The 95% confidence intervals are shown in Table 1.1, and the corresponding confidence regions for selected parameter groups are shown in Figure 2-4. The lower and upper confidence limits have been deduced from confidence regions. It was done by examining the plot and finding the maximum variation in each parameter within the plot.

A

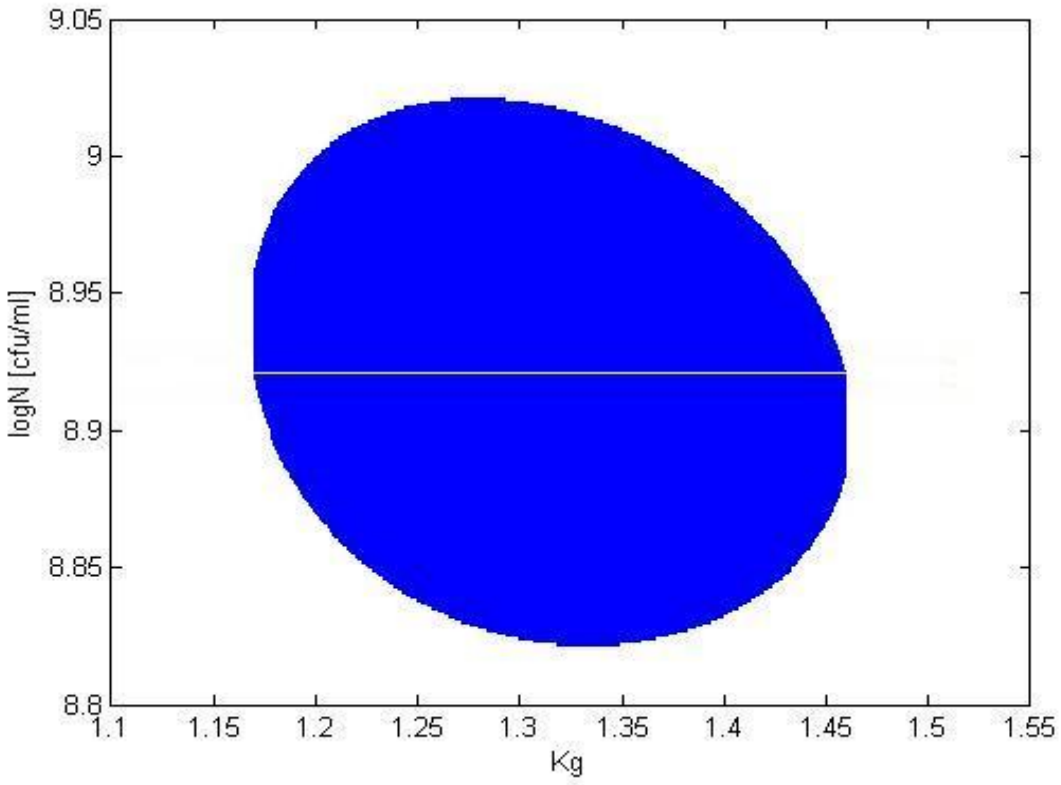

Figure 2-4 95% joint confidence region for: (A) K_g and $logN_{max}$;.

B

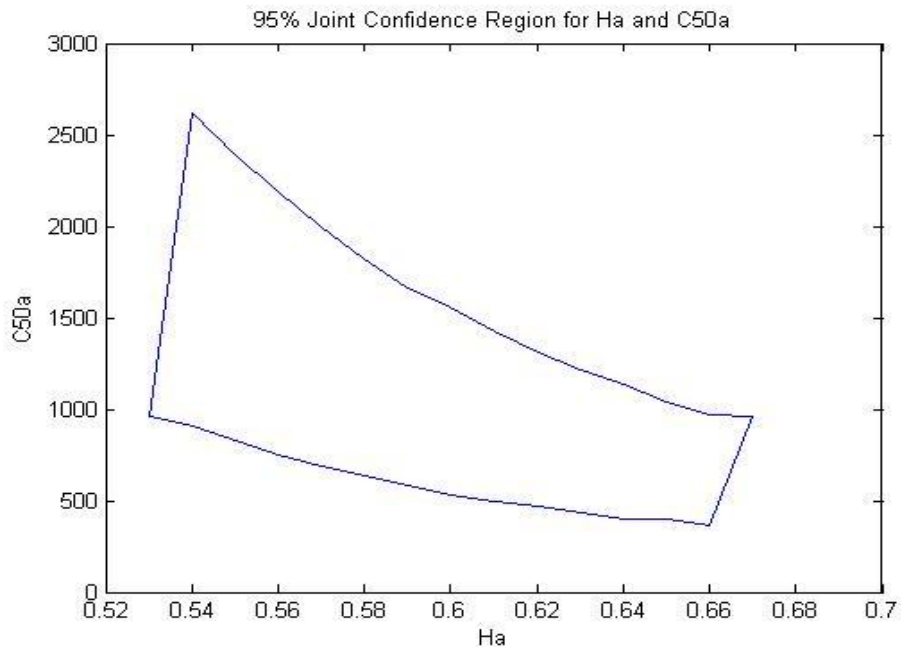

Figure 2-4 95% joint confidence region for: (B) C_{50a} and H_a

C

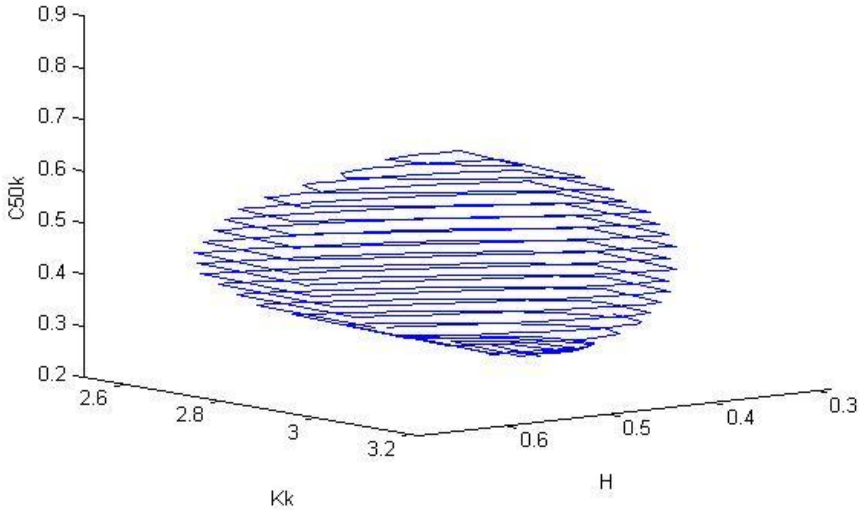

Figure 2-4 95% joint confidence region for: (C) K_k, C_{50k} *and H.*

Table 2-1 Final estimates of the best-fit model parameters

	Point estimates	95% Confidence limits	
		Upper Limit	Lower Limit
K_g (h^{-1})	1.3078	1.17	1.47
N_{max} (10^8 CFU/ml)	8.3357	6.886	10.715
K_k (h^{-1})	2.79	2.5	3.05
C_{50k} (mg/l)	0.51	0.22	0.68
C_{50b} (mg/l)	40.31	*	
H	0.5	0.3	0.62
C_{50a} (mg/l)	962.19	367.2	2615
H_a	0.592	0.542	0.662
Log N_{50} (CFU/ml)	6.55	*	
Q	0.8	*	

K_g – growth rate constant for bacterial population

$N_{\max}$ – maximum population size

K_k – maximal kill rate constant for bacterial population

C_{50k} – concentration to achieve 50% maximal kill rate of the initial population

C_{50b} – concentration to achieve 50% maximal kill rate of the most resistant population

H – sigmoidicity constant for bacterial population

C_{50a} – concentration to achieve 50% maximal adaptation rate

Ha – sigmoidicity constant for bacterial adaptation

N_{50} – bacterial population which 50% drug concentration is in effect

Q – sigmoidicity constant for effective drug concentration

* Unable to determine. The non-linear confidence region plotting method was found to be inadequate. The sum of squares flattened off in case of these parameters.

2.3.5 Experimental validation

The results of the colorimetric assay are shown in Figure 2-5. There was a significant difference in biomass formation as the initial bacterial density was increased from 1×10^5 CFU/ml to 1×10^8 CFU/ml ($p = 0.002$, student's t-test).

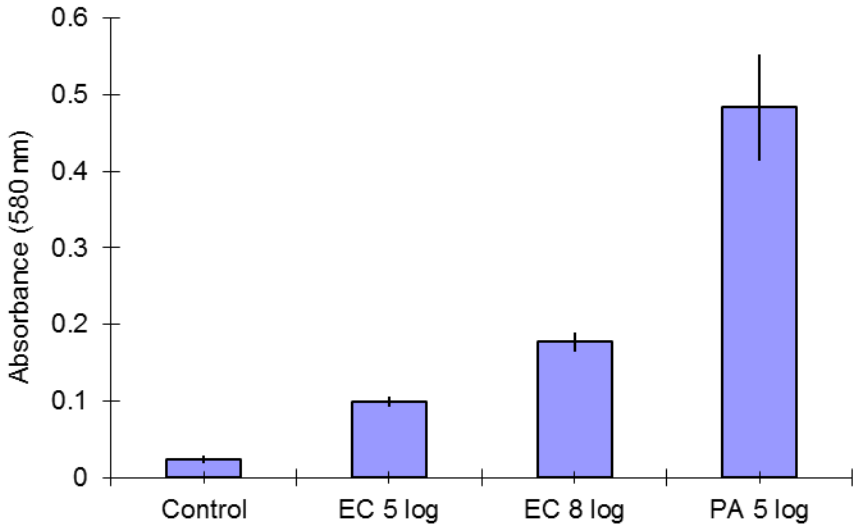

Figure 2-5 Comparison of absorbance values in biofilm assay.

Each condition was examined in triplicate

Control – bacteria-free media (negative control)

EC – *E. coli* ATCC 25922

PA – *P. aeruginosa* ATCC 700888 (a known biofilm hyperproducer - positive control)

2.4 DISCUSSION

Inoculum effect has been the subject of study for several recent investigations. Different researchers have attempted to characterize the phenomenon in various ways. Udekwu et al. conducted experiments with a wide variety of antimicrobial agents against a wild-type *Staphylococcus aureus* and witnessed a consistent reduction in antibiotic efficacy at high cell densities (63). Using a series of escalating inocula (ranging from 2×10^4 CFU/ml to 9×10^7 CFU/ml), the effect on MIC was not linear and was not noticed until the starting inoculum was in the order of 10^7. One logical concept was the reduction in the effective concentration of the drug available to the bacteria. Consequently, mechanisms such as decrease in drug molecules per bacterium or denaturing drug at high bacterial densities were proposed to explain the reduced efficacy observed. However, the bacterial burdens were only assessed at specific time points (e.g., 3 and 18 hours) and the mathematical models were not fit to actual experimental data over time to substantiate these theoretical concepts.

These experimental observations reported previously were similar to our experience. The functional forms of the relationship between the bacterial density and efficacy of an antimicrobial agent were also consistent in both studies, as reflected by the model parameter estimate of $Log\ N_{50}$ (6.55) in this study. Our work further extended on their conceptual framework, and expressed the specific density (inoculum) effect as the effective antimicrobial agent concentration available for bacterial kill. Specifically, the killing function was assumed to be inversely dependent on initial bacterial burden in a nonlinear fashion (i.e., bacterial killing was expected to increase with decreasing initial

burden). In addition, we also included a model fit to serial bacterial burden data over time.

On the other hand, Bulitta et al. tried to explain the inoculum effect with the help of mechanistic-based models (9). The proposed modeling approach was shown to be useful in predicting the growth of resistant *P. aeruginosa* in external datasets, which could facilitate effective design of dosing regimens. However, the proposed model was of moderate to high complexity; a total of 17 parameters were involved and with several interconnected steps. Furthermore, no experimental evidence was put forth to support some of the underlying mechanistic modeling assumptions. In contrast, our model structure was much less complex, and the functional relationship between initial inoculum and effective drug concentration proposed in our model was more straight forward. As a result, the identifiability of the model and the confidence interval of the parameter estimates would likely be improved. Also, some experimental evidence was provided to support the key conceptual framework.

There are several limitations with this study. Modeling was performed in only one drug-pathogen in this study. We have previously performed similar time-kill studies with several beta-lactams against a variety of *E. coli* isolates expressing different beta-lactamases (55), and the drug-pathogen combination reported in this study was the most dramatic illustrating the inoculum effect. As a result, we expect the same mathematical model would be relevant to other drug-pathogen combinations as well.

From the mechanistic perspective, the inoculum effect was solely attributed to the reduced effective drug exposure. We provided some experimental data as shown in Figure 2-5 to substantiate the validity of our postulation. However, we recognized that

this might still be an oversimplification of the complex interaction between an antimicrobial agent and a bacterial population. Individual bacterial cell in a dense population could be in a different physiological state (e.g., slower growth, metabolism or in an inactive state), in addition to being encased in a biofilm barrier. Despite that, in search of a useful mathematical model to predict bacterial response to an antimicrobial exposure, it is not always necessary to capture all the physiological processes comprehensively in the model. The role of quorum sensing was not investigated. From the modeling perspective, the inoculum effect was attributed to the baseline inoculum only. In reality, the effective drug concentration may be dependent on additional variable(s) other than the baseline inoculum. For example, it might also be a function of evolving bacterial burden. Although we are not describing effective concentration as a function of instantaneous population in this study, the modeling framework is one step towards this direction. Investigations are in progress to explore if effective drug concentration should be expressed as a function of instantaneous bacterial burden.

CHAPTER 3

MODELING OF BIPHASIC KILLING OF FLUOROQUINOLONES: GUIDING OPTIMAL DOSING REGIMEN DESIGN

3.1 INTRODUCTION

The problem of bacterial resistance against antimicrobials has reached alarming proportions in recent decades. Evidence suggests that resistance development could be correlated to the use of suboptimal dosing regimens (29, 57, 27, 56, 62, 34, 68). On the other hand, optimal dosing regimens are associated with a higher likelihood to suppress the development of resistance. However, determining the optimal dosing regimen for a new antimicrobial is not a trivial task, since a large number of control variables can result in number of different scenarios to be considered. As a result, only a restricted number of dosing regimens are usually evaluated experimentally for new antimicrobial candidates. Thus, a purely experimental approach to antimicrobial development is restrictive, in that it may result in inefficiency or missed opportunities. Mathematical modelling can be a useful aid in antimicrobial development and use. It can offer unique and valuable guidance towards the design and testing of dosing regimens at various stages of development. This can significantly reduce the number of experiments necessary in pre-clinical and clinical investigations.

In our previous work, we developed a modelling approach to characterize the effect of antimicrobials on heterogeneous bacterial populations (43). In addition, we developed a modelling framework that can predict the efficacy of different dosing regimens (42). So far, the modelling approach has been so far validated on only selective drug-bacteria combinations and has been found to be reasonably accurate. To ensure the robustness of the approach (so that it can be used with confidence in guiding the design of clinical trials), it is necessary to evaluate it for a broader range of drug-bacteria combinations. The objective of this study was to evaluate the performance of the modelling approach on predicting the impact of quinolone (moxifloxacin and levofloxacin) exposures on resistance development in Gram positive (*Staphylococcus aureus*) and Gram negative (*Escherichia coli*) bacteria

3.2 MATERIALS AND METHODS

3.2.1 Antimicrobial agents

Moxifloxacin powder was provided by Bayer Pharmaceuticals (West Haven, CT) and levofloxacin powder was purchased from Waterstone Technologies (Carmel, IN). A stock solution of each antimicrobial agent in sterile water was prepared, aliquoted, and stored at -70°C. Prior to each experiment, an aliquot of the agent was thawed and diluted to the desired concentrations with cation-adjusted Mueller-Hinton broth (Ca-MHB) (BBL, Sparks, MD) or sterile water.

3.2.2 Microorganisms

Two standard wild-type microorganisms: *Escherichia coli* MG1655 and *Staphylococcus aureus* ATCC 29213 (American Type Culture Collection, Rockville, MD) were used in the study. The bacteria were stored at -70°C in Protect® (Key scientific products, Round Rock, TX) storage vials. Fresh isolates were sub-cultured twice on 5% blood agar plates (Hardy Diagnostics, Santa Maria, CA) for 24 hours at 35°C prior to each experiment.

3.2.3 Susceptibility studies

Minimum inhibitory concentration (MIC) was determined in Ca-MHB using a modified macrobroth dilution method as described by the CLSI (12). The final concentration of bacteria in each macrobroth dilution tube was approximately 5×10^5 cfu/mL of Ca-MHB. Serial twofold dilutions of drugs were used. The MIC was defined as the lowest concentration of drug that resulted in no visible growth after 24 hours of incubation at 35°C in ambient air. To determine the minimum bactericidal concentration

(MBC), samples (50 μL) from clear tubes and the cloudy tube with the highest drug concentration were plated on Mueller-Hinton agar (MHA) plates (Hardy Diagnostics, Santa Maria, CA). The MBC was defined as the lowest concentration of drug that resulted in ≥ 99.9% kill of the initial inoculum. Drug carry-over effect was assessed by visual inspection of the distribution of colonies on media plates. The studies were conducted in duplicate and repeated at least once on a separate day.

3.2.4 Mutation frequency

Suspensions of *E. coli* MG 1655 and *S. aureus* ATCC 29213 were allowed to grow overnight. The suspensions were diluted serially (10×) and plated onto drug-free MHA and MHA supplemented with 3× MIC of moxifloxacin (for *E. coli*) or levofloxacin (for *S. aureus*), respectively. The media plates were incubated for up to 72 hours at 35°C. Colonies were counted and the mutation frequency of resistance was determined by dividing the bacterial burden on drug-supplemented plates by the bacterial burden on drug-free plates. The studies were conducted three times on separate days.

3.2.5 Time-kill studies

Time-kill studies were performed in 20 mL, using inocula of approximately 1×10^8 cfu/mL at baseline for *E. coli* MG1655 and approximately 1×10^7 cfu/mL at baseline for *S. aureus* ATCC 29213, respectively. A concentration range of moxifloxacin (0-8 mg/L) and levofloxacin (0-16 mg/L) were used for *E. coli* MG1655 and *S. aureus* ATCC 29213, respectively. The drug concentrations were normalized to multiples of the respective MIC. Serial samples (baseline, 2, 4, 8, 12 and 24 hours) were obtained in duplicate over 24 hours; viable bacterial burden was determined by quantitative culture. Prior to culturing the bacteria quantitatively, the bacterial samples were centrifuged at 10 000× G

for 15 minutes, and reconstituted with sterile normal saline to minimize drug carry-over effect. Total bacterial populations were quantified by spiral plating (Spiral Biotech, Bethesda, MD) 10× serial dilutions of the samples (50 μL) onto MHA plates. The media plates were incubated for up to 24 hours at 35°C; bacterial density from each sample was enumerated visually. The theoretical (reliable) lower limit of detection was 400 cfu/mL.

3.2.6 Mathematical modeling

For each bacterium, all time-kill profiles were modeled collectively to derive a model fit and model parameter estimates. Briefly, the rate of change of bacteria over time was expressed as the difference between the intrinsic bacterial growth rate and the (sigmoidal) kill rate (provided by the antimicrobial agent). In both time-kill data sets, a biphasic killing profile was observed. Initially there was a rapid decline in bacterial burden, followed by a much more gradual reduction. This feature prompted the need for different maximal kill rates for the initial phase and latter phase, namely K_k and K_b respectively. Similarly, the concentrations needed to achieve half the maximal kill rates were different for both phases, namely C_{50} and C_{50b}. The decline in kill rate and regrowth over time was attributed to adaptation, expressed by a coefficient A. Several hierarchical model candidates (using identical maximal kill rates, concentration-dependent adaptation, etc.) were evaluated. The mathematical structure of the final population dynamics model is as shown in Figure 3-1. The parameter estimation process involved two steps. The intrinsic bacterial growth rate (K_g) and maximal bacterial population size ($N_{\max}$ - to account for contact inhibition) were first derived from placebo control experiments. Using these fixed growth parameter estimates, the parameter values in the killing function were subsequently derived using data from all active treatment

experiments simultaneously. All modelling was performed with MATLAB version 7.5 (The MathWorks, Inc., Natick, MA). The MATLAB differential equation solver ode45 was used together with fmincon for optimisation.

Figure 3-1 Bacterial growth dynamics model and various model parameters

Population balance for a bacterial population:

Rate of change of bacteria = Intrinsic growth rate – Kill rate by antimicrobial agent

$$\frac{dN(t)}{dt} = G[N(t)] - K[C(t), N(t)]$$

where:

$$G[N(t)] = K_g \cdot [1 - \frac{N(t)}{N_{\max}}] \cdot N(t)$$

$$K[C(t), N(t)] = [(\frac{C(t)^H \cdot K_k}{C(t)^H + (C_{50})^H} - \frac{C(t)^H \cdot K_b}{C(t)^H + (C_{50b})^H}) \cdot e^{-A \cdot t} + \frac{C(t)^H \cdot K_b}{C(t)^H + (C_{50b})^H}] \cdot N(t)$$

G – growth rate function

K – kill rate function

K_g – growth rate constant for bacterial population

$N(t)$ – concentration of bacterial population at time t

$N_{\max}$ – maximum population size

$C(t)$ – concentration of drug at time t

K_k – maximal kill rate constant for susceptible bacterial population

K_b – maximal kill rate constant for most resistant bacterial population

C_{50} – concentration to achieve 50% maximal kill rate of the initial population

C_{50b} – concentration to achieve 50% maximal kill rate of the most resistant population

H – sigmoidicity constant for bacterial population

A – adaptation function

3.2.7 Computer model predictions

Using the best-fit model parameter values derived, qualitative microbial responses (with respect to whether resistance would develop over time) to various clinically relevant drug exposures were predicted. Briefly, the average kill rate (D) of different dosing regimens against the most resistant population was derived as shown previously (43), and compared to the growth rate (K_g) of bacterial population. Resistance development over time is anticipated if $D/K_g<1$. The pharmacokinetic parameters of moxifloxacin and levofloxacin were derived from previous studies (15). All simulations were performed with MATLAB version 7.5 (The MathWorks, Inc., Natick, MA) and Mathematica 6.0 (Wolfram Research, Inc., champaign, IL).

3.2.8 Experimental validation

The computer simulations were compared to experimental data from an *in-vitro* hollow-fiber infection model with selected antimicrobial agent exposures for up to 120 hours. The experimental setup has been described elsewhere (59). A human-like elimination half-life [approximately 12 hours for moxifloxacin (24, 51) and 5-7 hours for levofloxacin (46)] was simulated in the infection models. Serial samples were obtained from circulatory loop of the infection models over time to ascertain the simulated pharmacokinetic exposures by a validated HPLC assay (49, 50).

In addition, serial samples were obtained at baseline, 4, and 8 hours and daily (predose) in duplicate from each hollow-fiber system for quantitative culture as described above (to define the effects of various drug exposures on the bacterial population). In addition to total bacterial population, subpopulations with reduced susceptibility were quantified by culturing samples on cation-adjusted MHA plates supplemented with the

exposed agent (moxifloxacin or levofloxacin) at a concentration of 3× MIC. The medium plates were incubated at 35°C for up to 24 hours (total population) and 72 hours (subpopulations with reduced susceptibility), and the bacterial density of each sample was enumerated visually. Susceptibilities of the isolates recovered from the drug-supplemented medium plates at the end of the experiments to the exposed agent were repeated to confirm the emergence of resistance. The mechanism of resistance was confirmed by PCR of the quinolone resistant determining regions (QRDR) of *gyrA* and *parC* (or *grlA* in *S. aureus*) genes of the resistant isolates (49, 50).

3.2.9 Biofitness

In the mathematical modelling analysis, the growth rate constant was assumed to be the same for all bacteria, regardless of fluoroquinolone susceptibility. To support this assumption, parallel time-growth experiments were performed on the parent (susceptible) and a randomly-selected daughter (resistant) strain which has undergone molecular investigations. A baseline inoculum of approximately 1×10^5 cfu/mL was used. Serial time samples (baseline, 1, 2, 3, 4, 6, 8, 24 hours) were taken in triplicate. Viable bacterial burden for each time sample was obtained by quantitative culture as described above. The growth function of the mathematical model (Figure 1) was fit to the bacterial burden-time profiles to derive the growth rates, and they were compared using student's t-test.

3.2.10 Resistance amplification

To substantiate resistance amplification as a plausible cause of regrowth, levofloxacin time-kill experiments (control, 0.125 mg/L and 0.25 mg/L) were repeated as described above. After 24 hours, each suspension (10 mL) was washed, diluted and plated onto drug-free MHA and MHA supplemented with 3× MIC of levofloxacin. The

proportion of the bacterial population with reduced susceptibility was determined as described above and compared.

3.3 RESULTS

3.3.1 Susceptibility studies and mutation frequency

The MIC and MBC of moxifloxacin for the *E. coli* MG1655 isolate were found to be 0.0625 and 0.0625 mg/L, respectively. On the other hand, the MIC and MBC of levofloxacin for the *S. aureus* ATCC 29213 isolate were found to be 0.25 and 1 mg/L, respectively. The mutation frequency of moxifloxacin / levofloxacin resistance (at 3× MIC) was approximately 0.5-3 x 10^{-9} in *E. coli* MG1655, and 2-8 x 10^{-9} in *S. aureus* ATCC 29213. Based on these mutation frequencies, pre-existing mutants could be present and the inocula used in time-kill / hollow fiber model studies are therefore deemed to be heterogeneous.

3.3.2 Time-kill studies

In both sets of time-kill studies, a biphasic killing profile was observed. These bacterial burden-time profiles were reasonably described by the model. Data from the time-kill studies and model fits to the data are shown as overlay plots in Figure 3-2. The correlation plots are shown in Figure 3-3. The estimates of the best-fit model parameters are shown in Table 3–1.

A

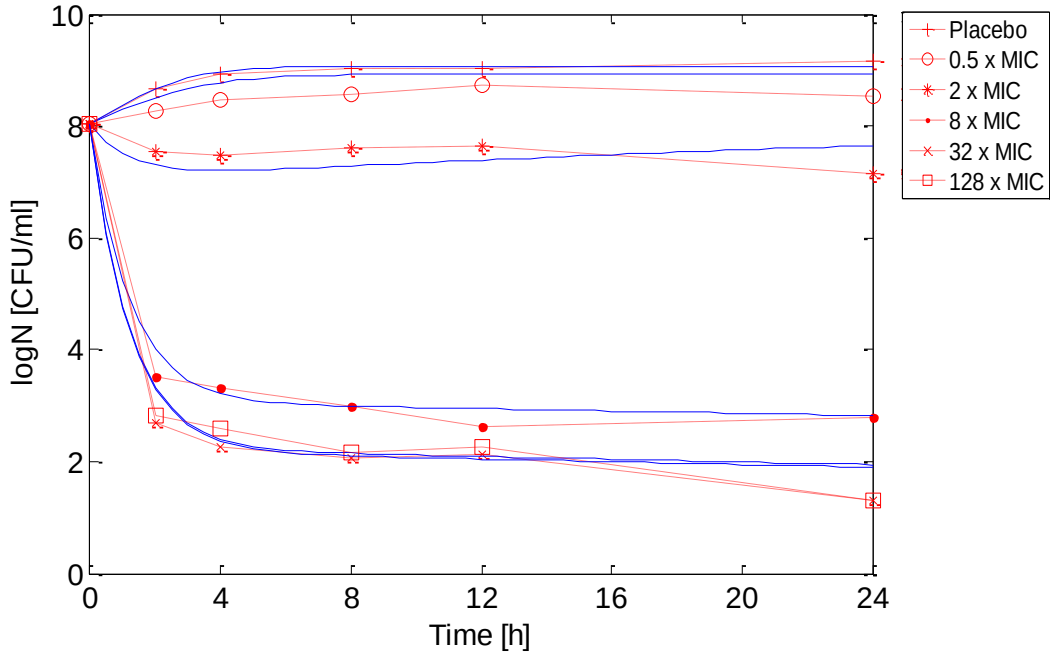

Figure 3-2 Model fits to the experimental data in time kill studies. Symbols are observed experimental data and solid lines are best fit model predictions. (A) Moxifloxacin against *Escherichia coli* MG1655.

B

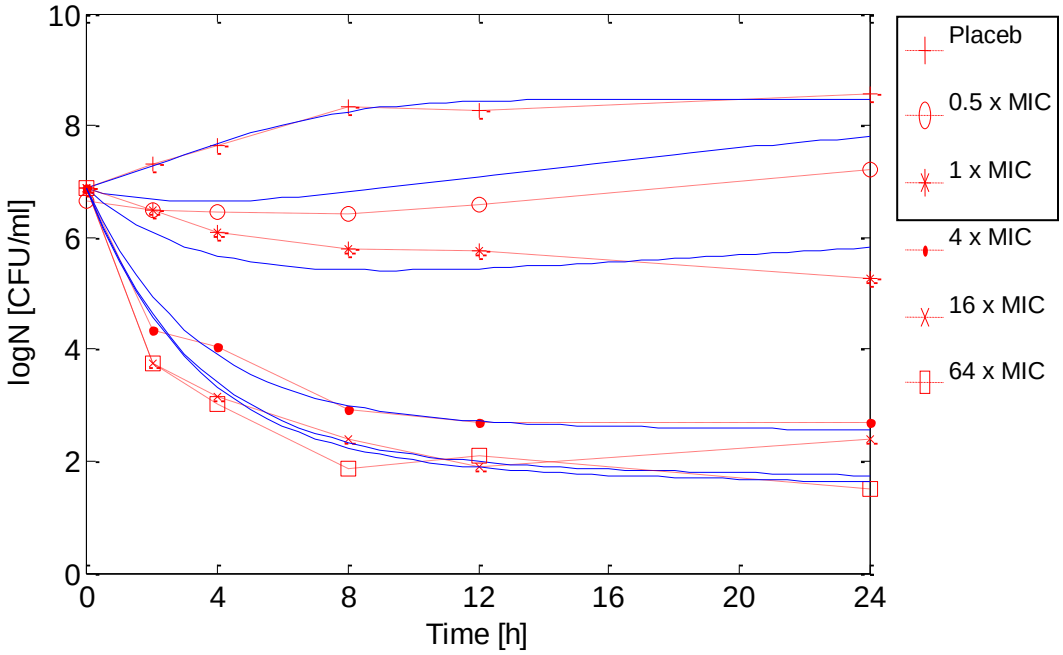

Figure 3-2 Model fits to the experimental data in time kill studies. Symbols are observed experimental data and solid lines are best fit model predictions. (B) levofloxacin against *Staphylococcus. aureus* ATCC 29213.

A

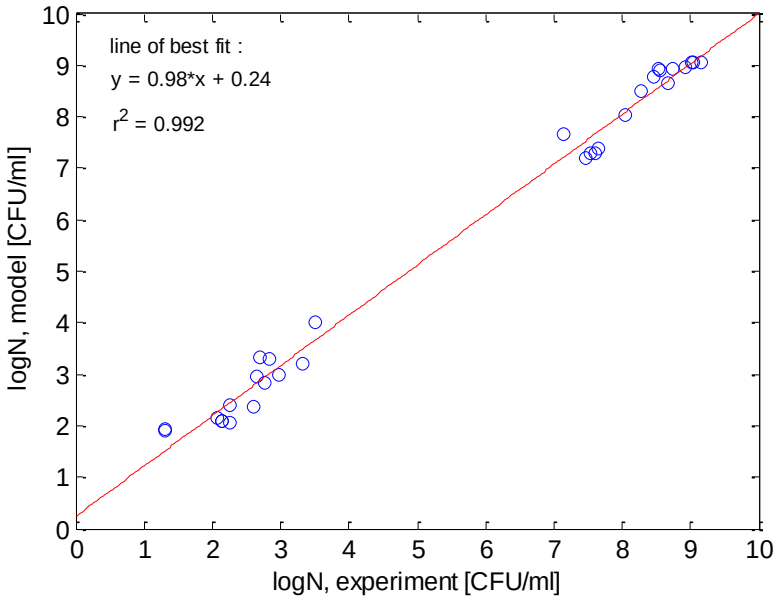

Figure 3-3 Correlation plots between experiment and model. (A) Moxifloxacin against *Escherichia coli* MG1655.

B

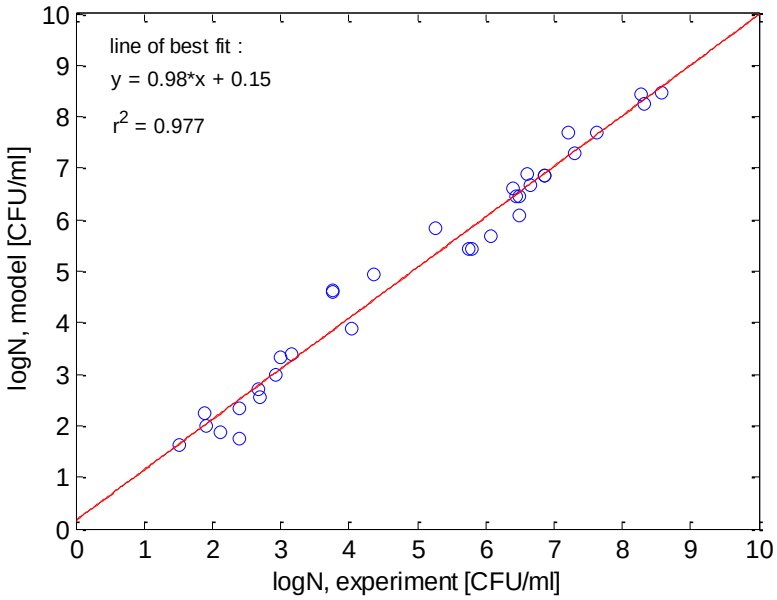

Figure 3-3 Correlation plots between experiment and model. (B) levofloxacin against *Staphalococcus aureus* ATCC 229213.

Table 3-1 Estimates of the best-fit model parameters (95% confidence intervals)

Parameter	*E. coli* MG1655	*S. aureus* 29213
K_g (h^{-1})	0.89 (0.58-1.58)	0.51 (0.32-0.81)
N_{max} (10^9 cfu/mL)	1.15 (0.83-1.66)	0.29 (0.13-0.83)
K_k (h^{-1})	12.00 (11.18-13.03)	4.01 (3.78-4.46)
K_b (h^{-1})	0.93 (0.90-1.01)	0.52 (0.48-0.59)
C_{50} (mg/L)	0.22 (0.19-0.26)	0.30 (0.23-0.36)
C_{50b} (mg/L)	0.05 (0.011-0.0704)	0.10 (0.01-0.14)
H	2.23 (1.77-3.81)	1.43 (1.07-2.2)
A (h^{-1})	0.82 (0.76-0.85)	1.29 (0.27-0.32)

3.3.3 Computer model prediction and experimental validation

Using the best-fit model parameter estimates, predictions were made relating to emergence of resistance as a function of daily dose and dosing interval. In all cases, there was a significant reduction in bacterial burden initially. Regrowth and resistance emergence was subsequently observed with suboptimal dosing regimens, but not with optimal regimens. For both bacteria, the mathematical model predictions were in general agreement with experimental results. A moxifloxacin dose of 85 mg once daily (q24h) would be necessary to suppress *E coli* resistance (Appendix 1 – for reviewing purpose only). We have previously shown that a simulated dose of moxifloxacin 80 mg once daily resulted in emergence of resistance over time, whereas resistance suppression was observed with 120 mg once daily (49).

A more comprehensive analysis was performed for levofloxacin as shown in Figure 3-4. Based on the model predictions, a dose of 166 mg twice daily and 487 mg once daily was necessary to suppress the emergence of resistance. A total of 8 different and escalating dosing regimens were used to experimentally verify the predictive performance of the model. The predictive performance of the model is as shown in Figure 3-4. Overall from Figure 3-4, the model prediction was reasonably reliable in predicting resistance emergence in 75% (6 out of 8) of the dosing experiments. For instance in Figure 3-4, if the model were perfect all the dark circles (levofloxacin exposures found to suppress bacterial population) would have been in non-shaded zone whereas the white circles (levofloxacin exposures found to be associated with regrowth) would have been in the shaded zone. However, 2 of the dark circles miss the expected zone which overall would results in 6 out of 8 experiments (75%) being predicted correctly. Typical pharmacokinetic profiles and bacterial responses observed are as shown in Figure 3-5.

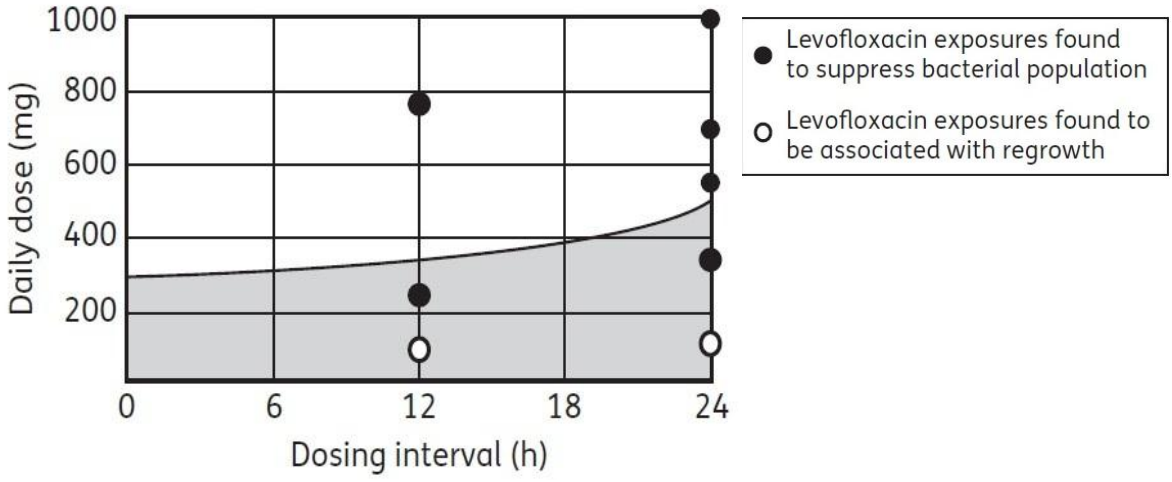

Figure 3-4 Predictive performance of levofloxacin dosing strategy to suppress resistance in *S. aureus* ATCC 29213.

The non-shaded area depicts dosing regimens (combinations of daily dose and dosing frequency) predicted to suppress resistance selection; shaded area depicts dosing regimens predicted to be associated with regrowth (resistance selection) over time. Analytically, the exposures required to suppress resistance predicted were: 487 mg q24h (daily dose = 487 mg); 166 mg q12h (daily dose = 332 mg); and 103 mg q8h (daily dose = 309 mg). The open and filled circles depict the selective validation experiments preformed, superimposed on the model predictions. All filled circles should ideally be in the white area, and all open circles in the shaded area. Overall, 6 out of 8 experiments were consistent with the model prediction (75% prediction success).

A

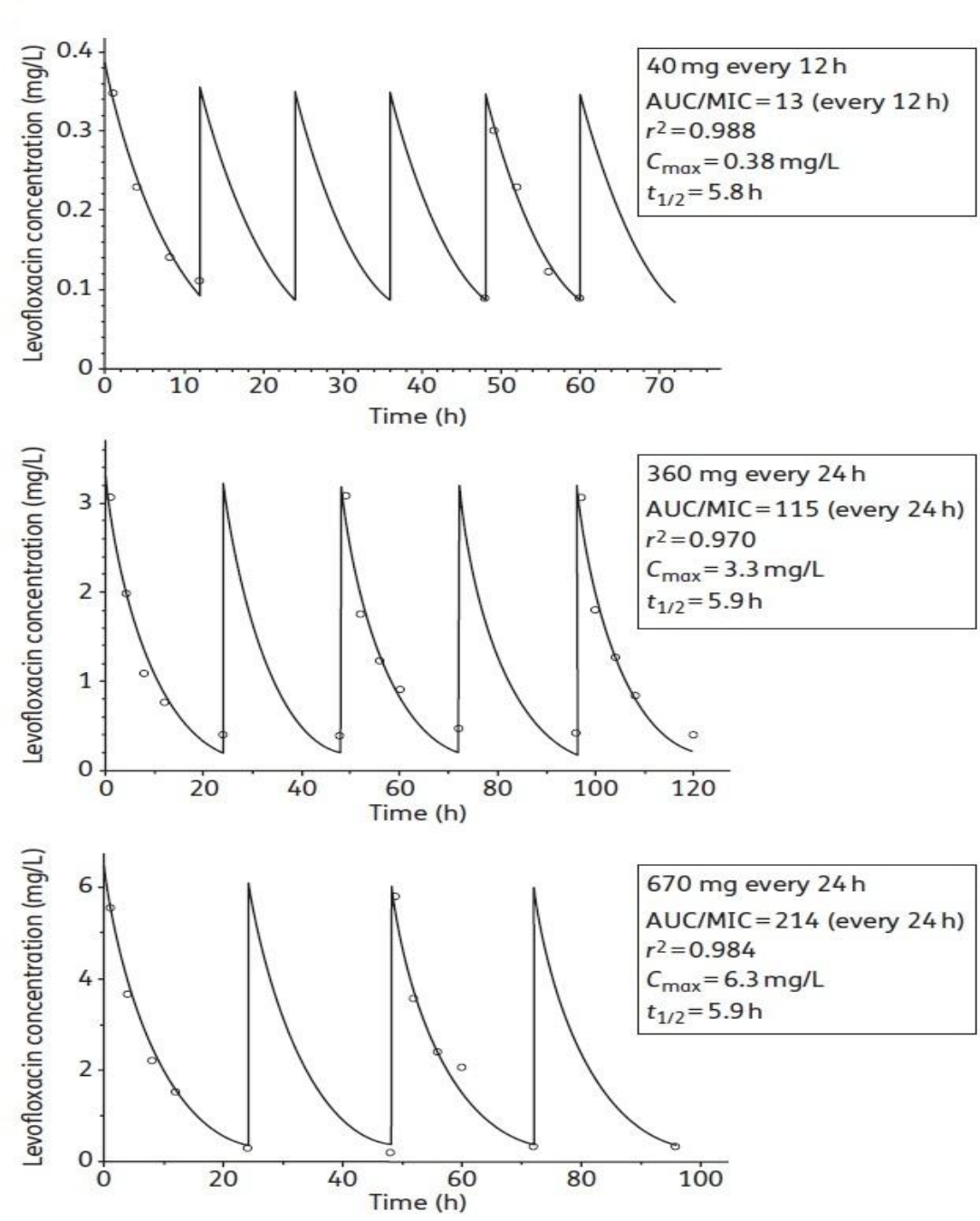

Figure 3-5 Representative observed levofloxacin pharmacokinetic simulations (A) in the infection models. (A) Open circles are experimental observations and continuous lines are model best-fit. The experiments were performed up to 120 hours or when the hollow-fiber cartridge could no longer confine the bacteria, whichever occurred earlier.

B

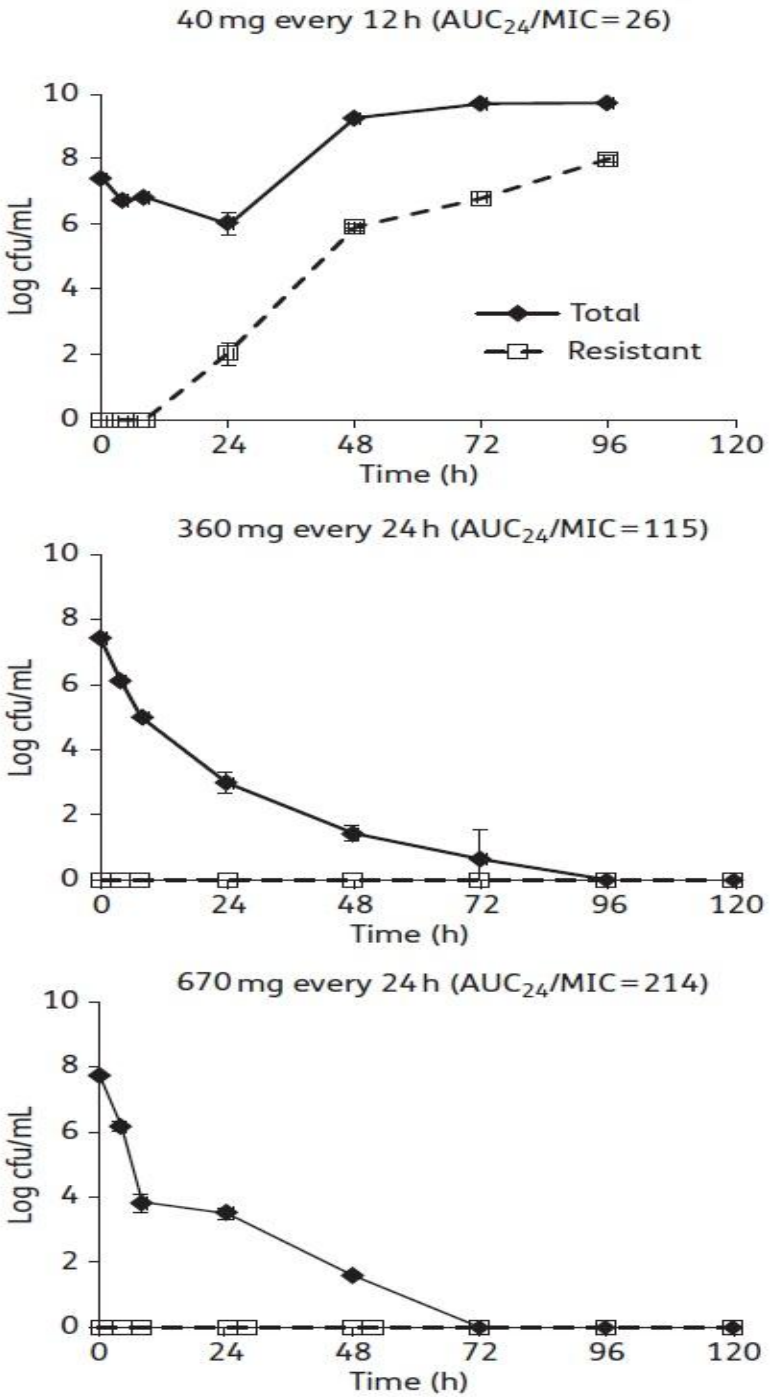

Figure 3-5 Representative observed bacterial (*S. aureus*) responses (B) in the infection models. (B) Data shown as mean ± standard deviation. The experiments were performed up to 120 hours or when the hollow-fiber cartridge could no longer confine the bacteria, whichever occurred earlier.

3.3.4 Confirmation of resistance

The mechanism of moxifloxacin resistance in *E. coli* (Ser 83 Leu substitution in *gyrA*) has been previously published (49). Three randomly selected resistant isolates of *S. aureus* were recovered from the drug-supplemented plates at the end of experiment corresponding to levofloxacin 40 mg q12h. Susceptibility studies revealed levofloxacin resistance with 6- to 8- fold elevation in MIC; subsequent sequencing of QRDR showed substitution of Ser 80 Phe in *grlA*, and no mutation was observed in *gyrA*. In addition, 4 resistant isolates were recovered from the drug-supplemented plates from the experiment corresponding to levofloxacin 100 mg q24h. Levofloxacin resistance was observed with 96- to 128-fold increase in MIC. Sequencing of QRDR revealed substitution of Ser 84 Leu in *gyrA* and Ser 80 Phe in *grlA*.

3.3.5 Accounting for Biofitness and amplification of resistance

For both bacteria, time-growth studies revealed there was no significant difference in the growth rates between the parent (wild-type) and daughter (resistant) strains. The growth rates (mean ± SD) were $0.58 \pm 0.01\ h^{-1}$ vs $0.56 \pm 0.012\ h^{-1}$ in *E. coli* ($p = 0.11$) and $0.53 \pm 0.01\ h^{-1}$ vs $0.49 \pm 0.024\ h^{-1}$ in *S. aureus* ($p = 0.07$). Under sub-inhibitory levofloxacin concentrations, the proportion of the bacterial (*S. aureus*) population with reduced susceptibility was found to be higher after 24 hours. Under sub-inhibitory levofloxacin concentrations;0 mg/L (control), 0.125 mg/L and 0.25 mg/L the proportion of the bacterial (*S. aureus*) population with reduced susceptibility after 24 hours was 1.8×10^{-9}, 5.9×10^{-9} and 1.9×10^{-8} respectively.

3.4 DISCUSSION

Fluoroquinolone pharmacodynamics has been investigated extensively and it is well accepted that fluoroquinolones exhibit concentration-dependent antimicrobial activity (14, 3). Both AUC/MIC and C_{max}/MIC have been recognized to be the most important pharmacodynamic indices for quinolones (23, 47, 19). However, the exposure necessary for favorable outcomes may not be the same for different bacteria. A pharmacodynamic study of fluoroquinolones on *Streptococcus pneumoniae* revealed that an AUC/MIC ratio > 33.7 was necessary for clinical and microbiological responses (2), but a significantly higher AUC/MIC ratio (> 125) was necessary against Gram negative bacteria (23). Furthermore, significantly different drug exposures were necessary to suppress resistance in *S. pneumoniae* and *Pseudomonas aeruginosa* (34).

The feasibility of fluoroquinolones to suppress resistance has also been examined by our group. *In-vitro* studies on the effect of moxifloxacin against a high inoculum of *E. coli* indicated that a clinical dose higher than 80 mg/day (AUC/MIC > 117) was associated with resistance suppression (49). A more general study has reported an inverted-U relationship between fluoroquinolone exposures and resistance amplification (56), resistance amplification is minimal at low drug exposures, which rises to a peak at intermediate exposures, and eventually becoming negligible again at high enough exposures. Similarly, *in-vivo* studies have demonstrated that resistance emergence in *P. aeruginosa* and *S. pneumoniae* could be related to fluoroquinolone exposures (29, 22).

In this work we modeled the effect of two different fluoroquinolones on both Gram negative and Gram positive bacteria. In time-kill studies, the classical concentration-dependent activity of fluoroquinolone was not observed. Instead a

biphasic killing profile was seen. There was concentration-dependent killing during the initial phase (i.e., bacterial burden reduction can be directly correlated to the drug concentration). However, during the latter phase there seemed to be little or no correlation between the reduction in bacterial burden and concentration of drug. Most of the killing profiles emerged as a bundle towards an asymptote. A similar phenomenon was observed in both Gram positive and Gram negative bacteria. Such an observation revealed that fluoroquinolone activity could be a complex combination of concentration-dependent and independent killing. To describe the population dynamics for both bacteria, an alternative modelling structure rather than the general structure developed previously was necessary.[8] Thus, keeping the key aspects of the previous framework, we have developed a model structure which was able to describe the bacterial population dynamics for such complex phenomena. Instead of assuming the presence of two discrete populations, we described a heterogeneous population with infinite number of sub-populations with different drug susceptibilities. Under a drug selective pressure, there was a gradual change from one type (concentration dependent) of profile to another (bundling) over time. This is a novel and unique feature of a single population model that we propose. Previous attempts of allowing just the maximum kill rate to vary did not result in satisfactory predictions (data not shown).

We demonstrated that the model was satisfactory to describe the dynamics of bacterial population under the effect of fluoroquinolones. Furthermore, selective validation showed that the model predictions in the extended time frame (with respect to resistance development) were in reasonable agreement with experiments using clinically relevant drug exposures (i.e., fluctuating concentration over time). In the model, we

made an assumption of similar growth rates for all bacteria regardless of susceptibility. This was later substantiated via time-growth experiments showing that there was no significant difference between the growth rates of parent (susceptible) and a daughter (resistant) strain. However, if there was a small biofitness cost associated with resistance, it could have explained the bias we observed in the model predictions. A lower drug exposure than anticipated would be needed to suppress resistance development over time. Additionally, resistance amplification was proposed as a mechanism contributing to bacterial regrowth. This assumption was also supported by our experimental data. Finally, the mechanism of quinolone resistance was also confirmed by relevant molecular studies. We recognized that the biphasic killing profiles in time-kill studies could have been modeled using the non-susceptible persister concept (41). However, the emergence of resistance observed in hollow-fiber infections models over time would not have been predicted.

An attractive feature of the model presented is that it does not require detailed knowledge of the mechanism of resistance as inputs. Based on data from simple time-kill studies, we were able to make reasonable predictions on the likelihood of resistance development for both the drug-bacteria combinations. This aspect of the model is especially useful in early drug development, since very often little is known about the resistance mechanism for novel entities. In short, our model was validated for two more drug-bacteria combinations, strengthening the robustness of the modelling approach. We also showed how slight changes in the model structure could help to explain the dynamics for different drug-bacteria combinations without a significant loss of predictive performance.

However as with all other modeling approaches our approach is not perfect. It can extract only that information which is contained in the data. If the data lacks dynamics necessary for the model to make sound predictions, it may not be able to give predictions exactly in agreement with experiment. These limitations could be partly overcome by quantifying the uncertainty in model parameters and model predictions.The confidence intervals that have been determined for individual parameters are one –way to address this uncertainty. Another way is to compute bootstrapped distributions for individual parameters and model predictions using repeated sampling from the original data.

In conclusion, we extended the modelling framework to describe the activity of fluoroquinolones against both Gram positive and Gram negative bacteria, which allow optimal dosing regimens to be designed. Our modelling approach is a promising decision support tool to guide investigation of new drug candidates. Further *in-vivo* investigations are ongoing to further extend our modelling approach.

CHAPTER 4

NOVEL MATHEMTICAL MODELING FRAMEWORK TO GUIDE DESIGN OF OPTIMAL DOSING STRATEGIES FOR BETA-LACTAMASE INHIBITORS

4.1 INTRODUCTION

Bacterial resistance to antimicrobial agents has been rising at an alarming rate, and may result in many common infections becoming untreatable in the future. The cost of treatment as well as the risk of mortality will increase with resistance (35). This has led to an urgent demand for new molecular entities attacking novel molecular targets via completely different pathways. However, the development of new drugs is a long, non-trivial process which has not been able to meet the current demand (54). An alternative is to restore the effectiveness of existing drugs. A viable approach towards that end is the development of inhibitors designed to target specific resistance mechanism(s). For instance, it has long been known that resistance mediated by production of beta-lactamases could be tackled by an inhibitor which inhibits the function of the beta-lactamases (drug hydrolysis). Similarly, efflux pump inhibitors could be used against bacteria that over-express efflux pumps to extrude drugs from the bacterial cells, thereby decreasing intracellular drug concentration.

Despite the fact that inhibitors have been clinically available for a long time, optimal dosing strategies for inhibitors are not well established. Pharmacokinetic and pharmacodynamic (PK/PD) indices such as AUC/MIC, C_{max}/MIC and time above MIC

(T>MIC) have been used widely to guide the optimal dosing of antibiotics (1). However, such indices may not be immediately applicable to inhibitors, since these inhibitors themselves have relatively weak to no intrinsic antimicrobial activity (16) and are generally administered in combination with an antimicrobial agent. As in the case of a single antimicrobial agent, variables such as dose, dosing interval and inter-subject pharmacokinetic differences make the process of determining optimal dosing regimens for drug/inhibitor combinations non-trivial. Therefore, comprehensive assessment of all possible dosing strategies is impractical in pre-clinical and clinical investigations. On the other hand, the full potential of these new inhibitor candidates may not be realized with empirical selection.

Mathematical modeling and computer simulation could greatly reduce the amount of experimental work involved in optimal dosing regimen design, simultaneously allowing comprehensive evaluation of numerous dosing strategies for drug / inhibitor combinations. It can be used as a decision support tool in guiding dosing strategy for the combination. Starting with feasible dosing strategies, modeling can produce a short list of the most promising strategies, which can then be evaluated experimentally. In this study, we propose such a modeling framework, and apply it to guide the design of optimal dosing strategies of a beta-lactamase inhibitor used in combination with an antimicrobial agent. To demonstrate our approach, a novel beta-lactamase inhibitor MK-7655, was used in combination with imipenem against a clinical strain of *Klebsiella pneumoniae*.

4.2 MATERIALS AND METHODS

4.2.1 Antimicrobial agents and Inhibitors

Imipenem was used in combination with an experimental beta lactamase inhibitor, MK-7655. Both imipenem and MK-7655 were obtained from Merck (Whitehouse Station, NJ). The first order elimination half life for both imipenem (44) and MK-7655 (data on file, available on request) in healthy volunteers was approximately 1-1.5 h.

4.2.2 Microorganisms

A *Klebsiella pneumoniae* carbapenemase (KPC-2)-producing clinical isolate of *Klebsiella pneumoniae* (KP6339 / CL6339) was provided by Merck (Whitehouse Station, NJ) and used in the study. Details of molecular confirmations were published previously (12). The bacterium was stored at –70°C in Protect® (Key Scientific Products, Round Rock, TX) storage vials. Fresh isolates were sub-cultured twice on 5% blood agar plates (Hardy Diagnostics, Santa Maria, CA) for 24 h at 35°C prior to each experiment.

4.2.3 Susceptibility studies

Susceptibility of KP6339 to imipenem was assessed in the presence of escalating concentrations of MK-7655 (0-32 mg/l) in two-fold increments, using a modified broth dilution method (2). MIC was defined as the minimum drug concentration which resulted in no visible growth after incubation for 24 h at 35^{o}C. All MIC experiments were conducted in triplicate and repeated at least once on a separate day.

4.2.4 Mathematical modeling and simulations

The dependency of MIC reduction on inhibitor concentration was characterized using a modified sigmoid Emax type model (39), as shown.

$$\log_2(MIC) = \log_2(MIC_0) - I_{\max}\frac{I^H}{I^H + I_{50}{}^H} \quad (13)$$

MIC = Minimum inhibitory concentration in presence of inhibitor

MIC_0 = Intrinsic minimum inhibitory concentration

I = Inhibitor concentration

I_{max}= Maximum inhibitor effect

H = Sigmoidicity co-efficient

I_{50} = Inhibitor concentration for 50% of maximum inhibitory effect

Logarithms of MIC taken to base 2 were used to fit the data and estimate the best-fit parameters. Taking logarithms of MIC taken to base 2 ensures prevention of overweighing in fitting a heteroskedastic data. The model was then used to simulate an instantaneous MIC (MIC_i) profile, as a function of MK-7655 concentration. Conceptually, MIC_i could be thought of as a measure of imipenem susceptibility when MK-7655 concentration fluctuates with time. The instantaneous MIC profile was then superimposed on a clinically achievable imipenem serum concentration profile (corresponding to a clinical dose of 500 mg every 6 h), as shown in Figure 4-1. The time above MIC_i ($T>MIC_i$) was assessed quantitatively. When both imipenem concentration and MIC_i fluctuated within their respective dosing intervals, $T>MIC_i$ was the total time when drug concentration was higher than MIC_i, and reported as percentage of the dosing interval. The effect of different magnitudes of $T>MIC_i$ were assessed subsequently for different inhibitor dosing strategies (dose and dosing intervals). The pharmacokinetic profiles for the imipenem and MK-7655 are governed by following equations,

$$\frac{dC_D}{dt} = \underset{\text{infusion rate}}{R_{inD}} - \underset{\text{elimination}}{k_{eD}C_D}\Bigg|_{\frac{t}{T}-\left[\frac{t}{T}\right]\le 0.5}, \tag{15}$$

$$\frac{dC_I}{dt} = \underset{\text{infusion rate}}{R_{inI}} - \underset{\text{elimination}}{k_{eI}C_I}\Bigg|_{\frac{t}{T}-\left[\frac{t}{T}\right]\le 0.5}, \tag{16}$$

$$\frac{dC_D}{dt} = -k_{eD}C_D\Big|_{\frac{t}{T}-\left[\frac{t}{T}\right]>0.5}, \tag{17}$$

$$\frac{dC_I}{dt} = -k_{eI}C_I\Big|_{\frac{t}{T}-\left[\frac{t}{T}\right]>0.5}. \tag{18}$$

C_D = Drug concentration

C_I = Inhibitor concentration

R_{inD} = Drug infusion rate

R_{inI} = Inhibitor infusion rate

k_{eD} = Drug elimination constant

k_{eI} = Inhibitor elimination constant

T = Dosing interval

$\frac{t}{T}-\left[\frac{t}{T}\right]\le 0.5$ = first half hour of every interval

All pharmacokinetics for half hour zero order infusion

A

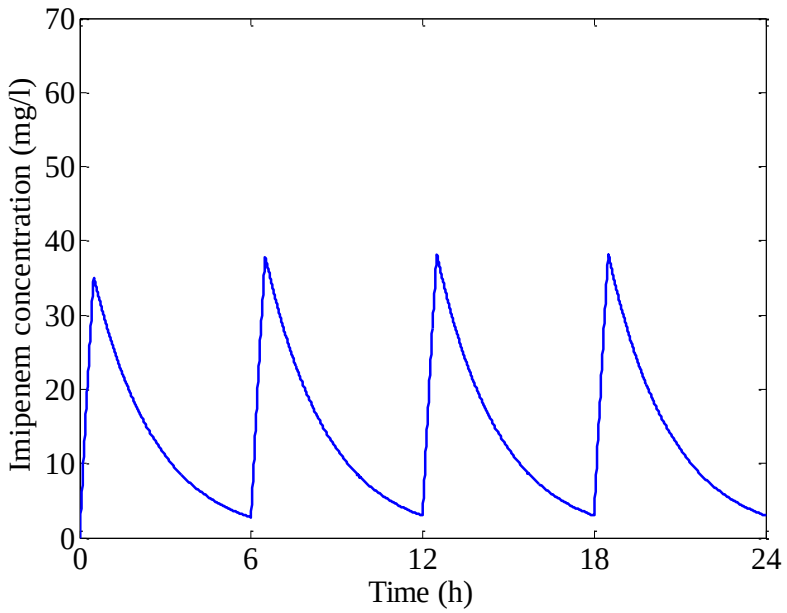

Figure 4-1 Different concentration-time profiles. (A) Imipenem concentrations resulting from a clinical dose of 500 mg every 6 h.

B

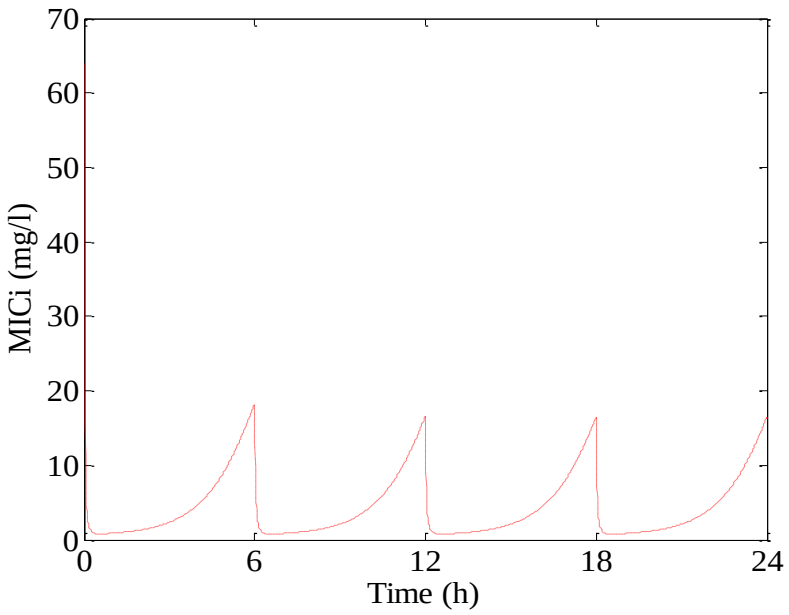

Figure 4-1 (B) A typical instantaneous MIC (MIC_i) profile with fluctuating MK-7655 concentrations.

C

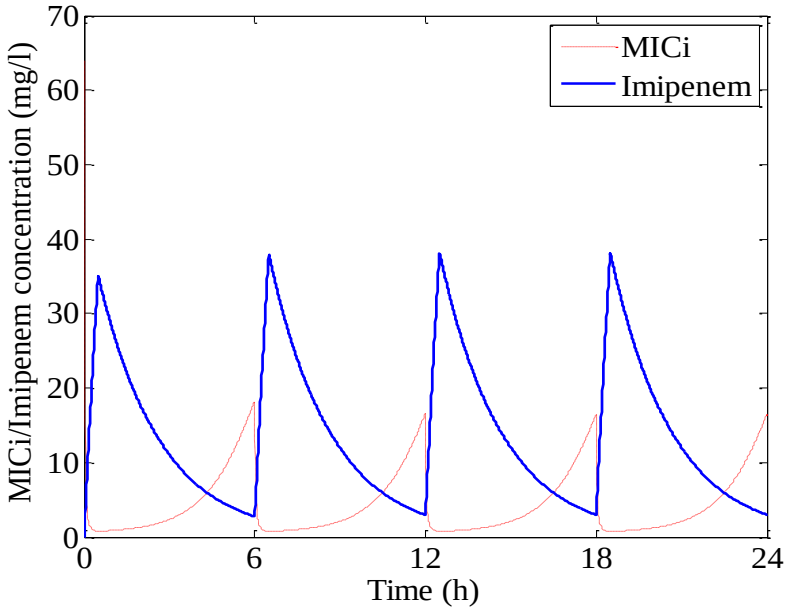

Figure 4-1 (C) Imipenem concentration profile superimposed with MIC_i

The AUC for imipenem was computed by integrating the area under the imipenem profile for 24 h divided by 24. Similarly, average MIC_i was computed by integrating the area under the instantaneous MIC profile for 24 h divided by 24. However, when analyzed, a trend in bacterial response was not observed with increasing AUC/average MIC_i.

4.2.5 Experimental validation

An *in vitro* hollow fiber infection model (HFIM) was used to validate model predictions for clinically achievable concentrations of imipenem / MK-7655. The details of the HFIM setup were described elsewhere (57). An imipenem concentration profile equivalent to 500 mg every 6 h was maintained in the background; the dosing interval and C_{max} (40 mg/l) of imipenem were kept the same for all experiments. A series of HFIM experiments were performed with different C_{max} and dosing intervals of MK-7655, corresponding to escalating predicted $T>MIC_i$ values (0%, 45%, 69% and 99%) as shown in Table 3.1.

An overnight culture of KP6339 was inoculated into pre-warmed cation-adjusted Mueller-Hinton broth (Ca-MHB) (BBL, Sparks, MD) and incubated further at 35°C until log-phase growth. The bacterial suspension was diluted to approximately 1×10^5 CFU/ml with Ca-MHB based on absorbance at 630 nm. Twenty ml of the diluted suspension was used in each experiment. At the start of each dosing interval, imipenem and MK-7655 were administered as infusions over 30 minutes. All experiments were run for 48 h and serial samples were obtained in duplicate (0, 6, 12, 24 and 48 h) to determine viable bacterial burden. Bacterial samples were centrifuged and washed once, before plating (50 µl) on drug-free Mueller-Hinton Agar (MHA) plates (BD Diagnostics, Sparks, MD). The

MHA plates were incubated for 24 h at 35^{o}C and colony forming units were visually enumerated. To ascertain the simulated pharmacokinetic profiles of imipenem / MK-7655, samples were withdrawn from the circulatory loop of the system and assayed in selected experiments. Subsequently a one-compartment model was fit to the concentration-time profiles of both imipenem and MK-7655.

4.3 RESULTS

4.3.1 Susceptibility studies and Mathematical modeling

In the absence of MK-7655, imipenem MIC of KP6339 was 64 mg/l. A MK-7655 concentration dependent decrease in imipenem MIC was observed, which was well characterized using parameter estimates shown in Figure 4-2. Different MK-7655 dosing regimens were simulated and the corresponding $T>MIC_i$ are as shown in Table 4–1 and Figure 4-4. Additionally, two different dosing regimens of MK-7655 resulting in a similar $T>MIC_i$ (69%) were also identified.

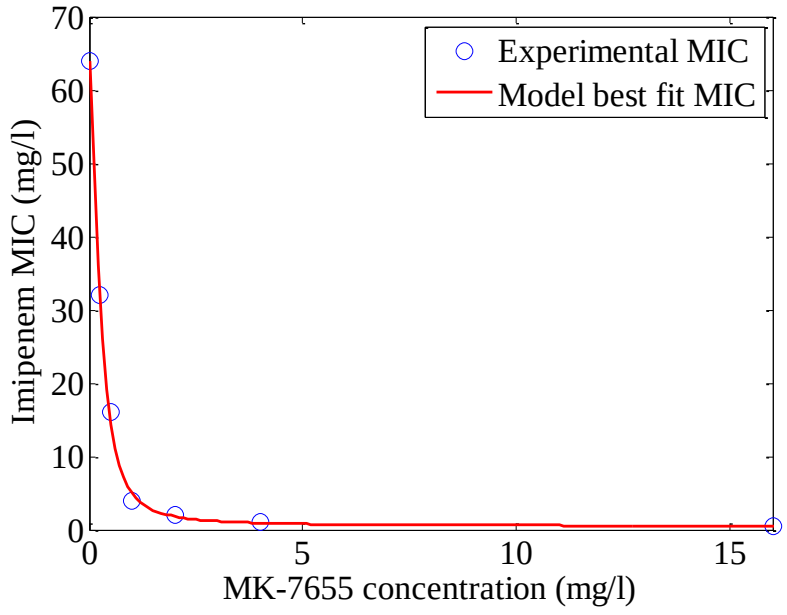

$r^2 = 0.99$

Figure 4-2 Model fit to experimental MIC data.

Open circles represent imipenem MIC in the presence of different MK-7655 concentrations. Solid line represents model fit with best fit parameters and 95% confidence intervals: I_{max} = 7.10(6.70-7.50) mg/l, H = 1.34(1.00-1.68), and I_{50} = 0.94(0.75-1.13) mg/l. When $I \rightarrow \infty$, MIC $\rightarrow$ 0.47 mg/l

Table 4-1 T>MIC_i for different MK-7655 dosing strategies

MK-7655 (mg/l)	Dosing interval (h)	MK AUC (0-24)	T>MIC_i (%)	AUC/Average MIC_i
0	-	0	0	0.22
2	6	0.71	45	0.86
6	6	2.12	69	3.19
20	12	3.54	69	1.10
20	6	7.06	99	13.71

*All regimens had an identical backbone IPM profile and AUC = 14.1

4.3.2 Experimental validation

Results of the HFIM experiments were in reasonable agreement with the model predictions. An apparent trend in bacterial response was observed as $T>MIC_i$ increased, as shown in Figure 4-3A. For the isolate investigated, $T>MIC_i$ greater than 69% was needed to suppress the bacterial population over time. Two experiments were performed with different MK-7655 dosing regimens resulting in a similar $T>MIC_i$. As shown in Figure 4-3B, the bacterial response in these experiments was comparable and within experimental errors.

A

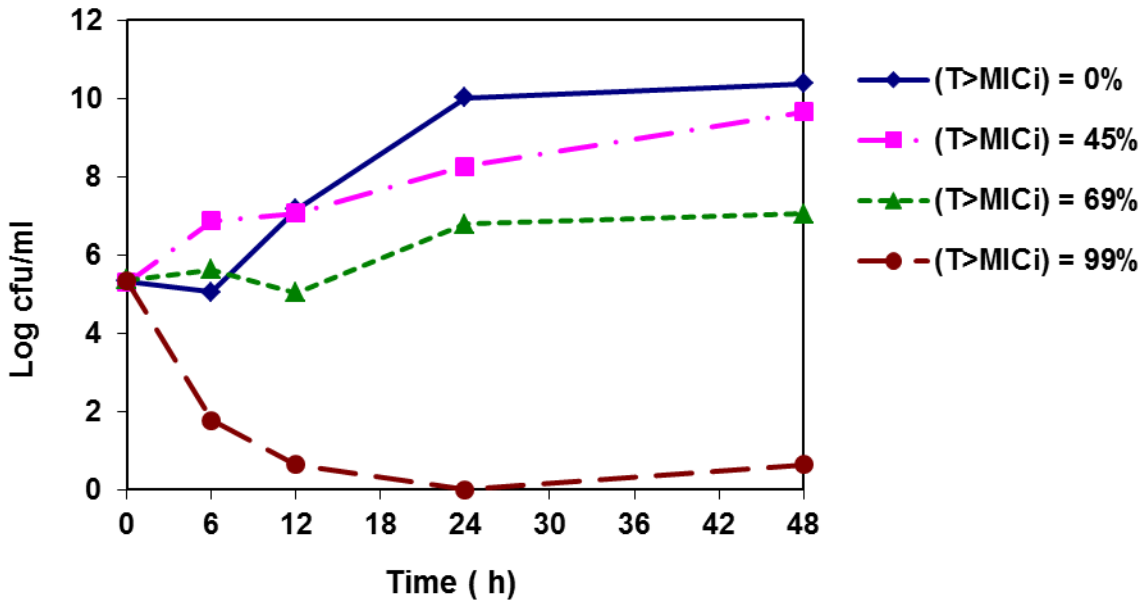

Figure 4-3 (A) Observed bacterial burden over time with different $T>MIC_i$ exposures.

B

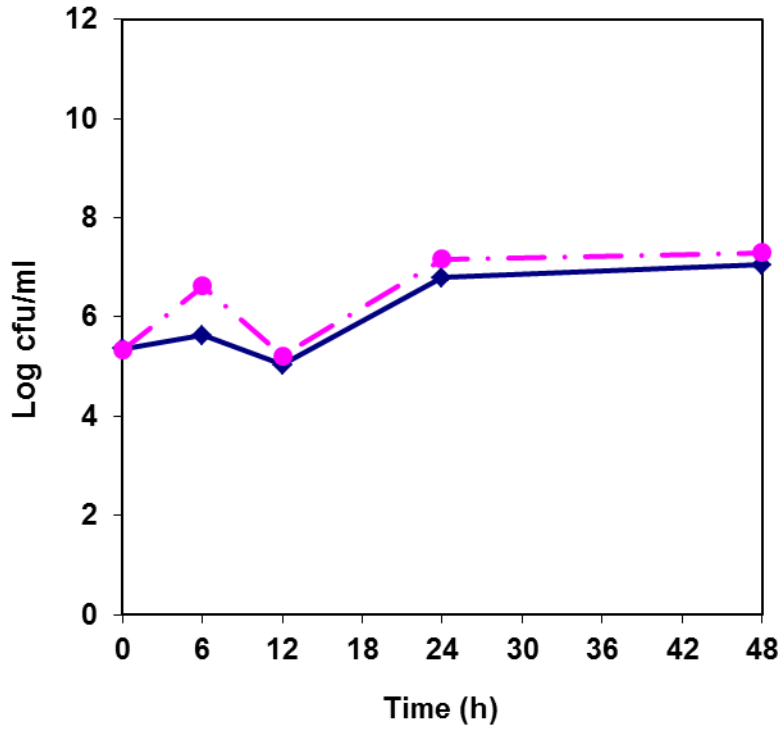

Figure 4-3 (B) Effect observed with different MK-7655 dosing regimens achieving similar T>MIC_i. Solid line: MK-7655 C_{max} = 6mg/l, q6h. Dashed line: MK-7655 C_{max} = 20mg/l, q12h. Simulated T>MIC_i was 69% in both cases.

A

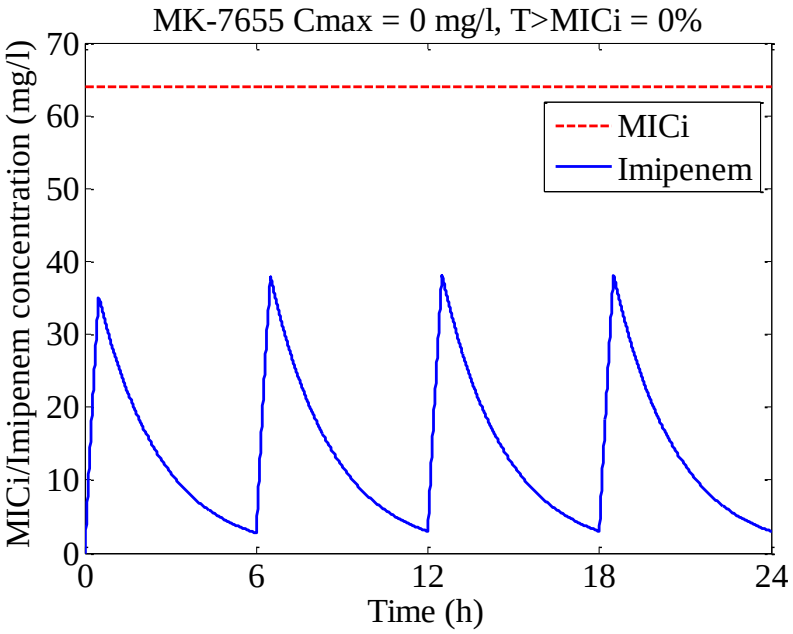

B

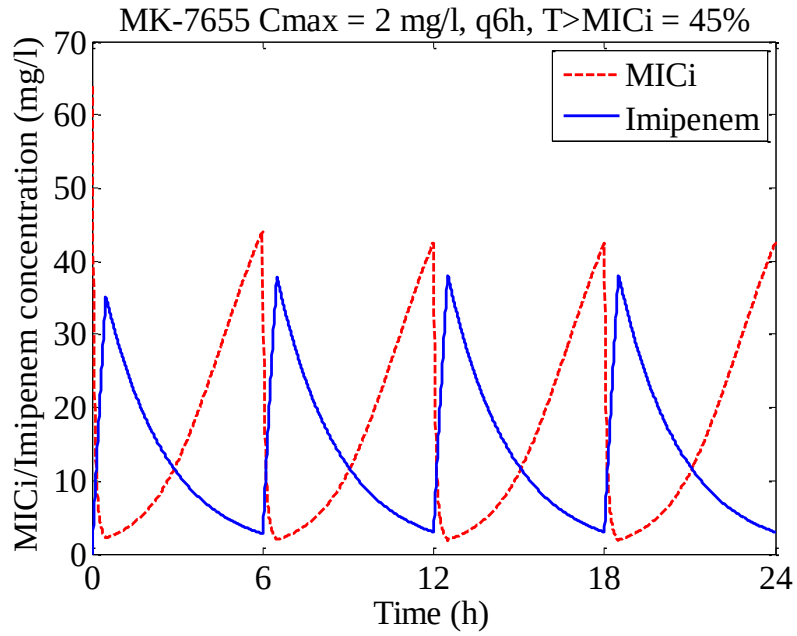

Figure 4-4 Superimposed imipenem concentration (solid line) and different MIC_i (dotted line) profiles. (A) $T>MIC_i = 0\%$. With no inhibitor MIC_i is constant at intrinsic MIC (B) $T>MIC_i = 45\%$.

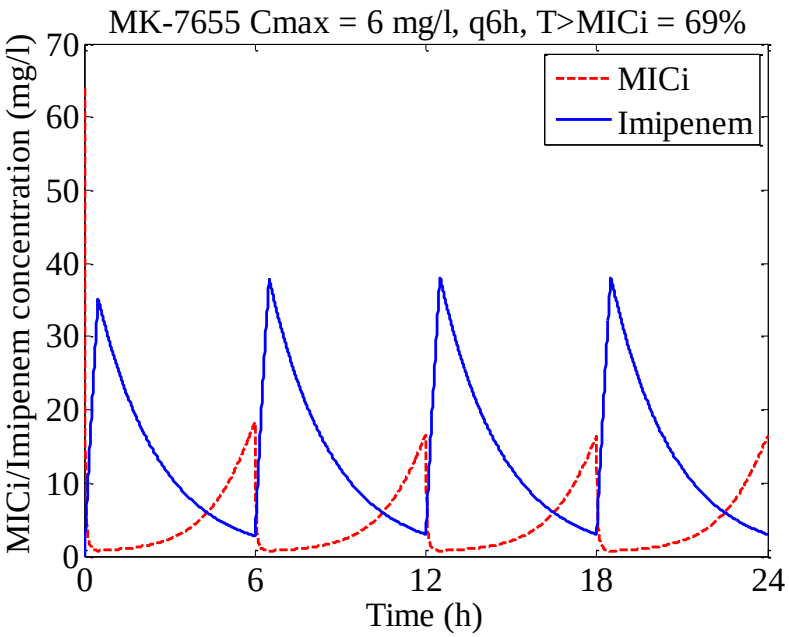

D

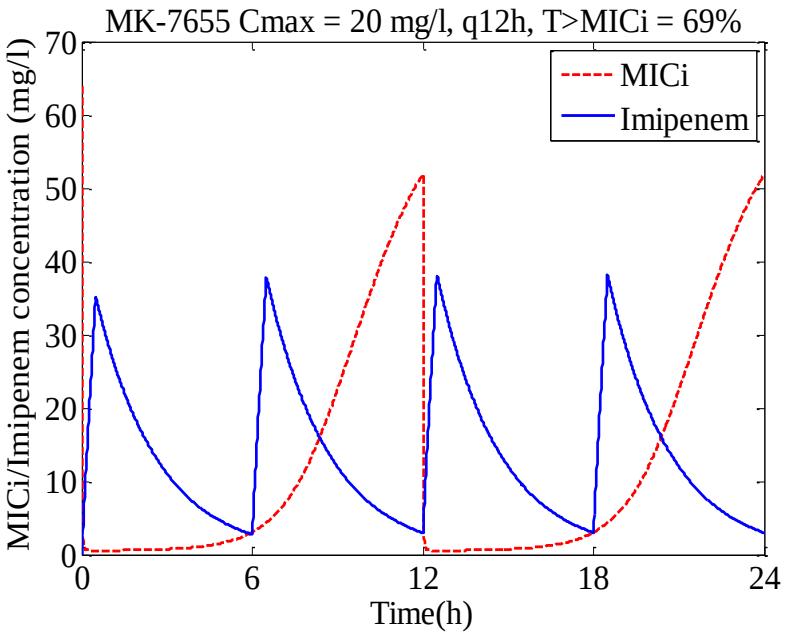

Figure 4-4 Superimposed imipenem concentration (solid line) and different MIC_i (dotted line) profiles. (C) T>MIC_i = 69%. (D) T>MIC_i = 69%.

E

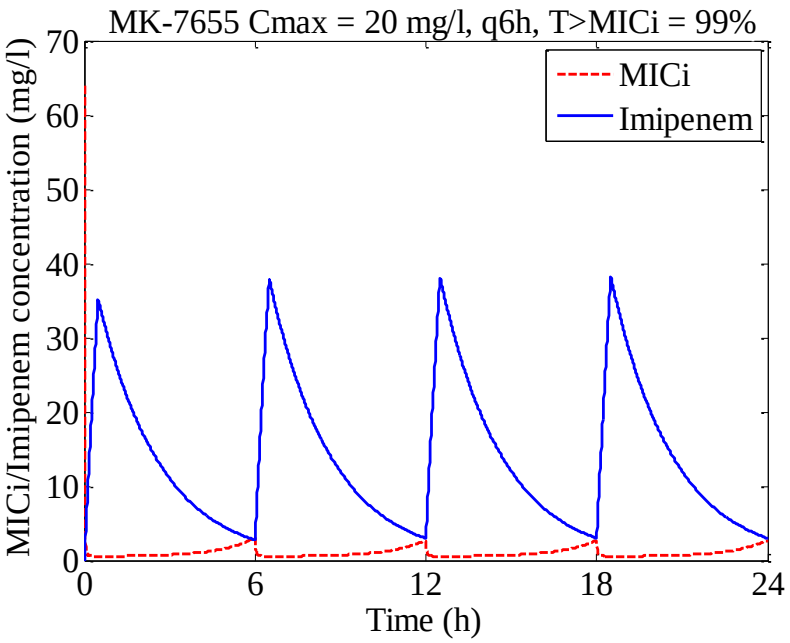

Figure 4-4 Superimposed imipenem concentration (solid line) and different MIC_i (dotted line) profiles. (E) $T>MIC_i = 99\%$.

4.4 DISCUSSION

Lack of antimicrobials with novel mechanisms against resistant bacteria has led to development of inhibitors which aim at restoring effectiveness of existing ones, by targeting specific resistance mechanism(s). Inhibitors intrinsically do not have significant antimicrobial activity and must be administered in combination with an antimicrobial agent. Intermittent dosing of an inhibitor typically results in fluctuating susceptibility (MIC) of the target pathogen over time; the use of conventional PK/PD indices such as AUC/MIC, T>MIC and C_{max}/MIC may not be directly applicable under these circumstances. Thus, optimal dosing strategy for inhibitors may require an unprecedented modeling and simulation approach to address the additional system complexity.

In our previous work, we have characterized the antimicrobial-bacteria interaction using a variety of modeling approaches, including conventional PK/PD indices (61). An approach that is simple enough yet provides us valuable insight into the system to meet the final objectives is most desired. Such an approach would have fewer computation requirements but would be novel enough to make useful predictions. Keeping this in mind, a mathematical modeling framework was proposed to guide the design of dosing regimens for drug/inhibitor combinations. The proposed modeling framework was based on the concept of fluctuating susceptibilities and was useful in predicting the *in vitro* activity of MK-7655 in combination with imipenem. With minimal modification of a standard MIC measurement procedure, the experimental setup was relatively straightforward and detailed knowledge of the mechanism of inhibitor action was not necessary. However, the framework was not completely empirical and useful information of the inhibition profiles could be indirectly captured irrespective of enzyme type,

expression level or inhibitor affinity. The efficiency and expression levels of an enzyme could have direct consequences on bacterial susceptibility, which in turn would affect intrinsic MIC (MIC_0). For example, the MIC_0 would be relatively low (e.g., 2 - 4× elevation from baseline level) for a bacterium poorly expressing a low-efficiency enzyme. On the other hand, for a highly efficient enzyme expressed at a high level, the corresponding MIC_0 would be much higher (e.g., 64 - 128× elevation from baseline level). Similarly, the potency and affinity of an enzyme inhibitor could be represented by the magnitudes of I_{50} and I_{max}. For instance, the high potency and affinity of MK-7655 against the KPC-2 enzyme was reflected in a high I_{max} and a low I_{50} value.

While the framework was simple and efficient in characterizing the activity of MK-7655, there were limitations. First, the pharmacological effect of the inhibitor (prevention of drug hydrolysis by the enzyme) was not explicitly characterized in the model. Instantaneous MIC is a theoretical concept used to reflect fluctuating susceptibilities over time, which may not be verified experimentally easily. Second, the novel pharmacodynamic index $T>MIC_i$ could be used as a surrogate to the conventional index T>MIC, when applying to fluctuating susceptibilities. Consistent with our expectation, an apparent trend was observed in bacterial response with increasing $T>MIC_i$. However, additional investigations are required to define a robust threshold of $T>MIC_i$ for optimal killing by applying the framework to a larger number of drug-inhibitor-pathogen combinations. To ascertain the robustness of the modeling approach studies of longer duration need to be carried out, which shall be considered in future investigations. Similarly, more comprehensive dose fractionation studies should be performed to ascertain if similar $T>MIC_i$ indeed correspond to a similar bacterial

response. If validated, the proposed framework could be generalized for a variety of inhibition mechanisms and used to screen multiple inhibitor dosing strategies. Instantaneous MIC could be extended to define C_{max}/MIC_i and AUC/MIC_i as surrogates to other conventional pharmacodynamic indices, in analogy to related indices used for assessment of antimicrobial agent effectiveness. The mathematical modeling framework could be used as a decision support tool to guide inhibitor dosing regimen design in both developmental as well as clinical stage.

In summary, an alternative computational approach is proposed for dosing strategy design of a beta-lactamase inhibitor. The results are promising and further *in vivo* investigations are warranted.

CHAPTER 5

SEMI-MECHANISTIC INTEGRATED DRUG EFFECT AND IMMUNE RESPONSE (GRANULOCYTE CLEARANCE) MODEL USING NAIVE AND NEUTROPENIC MICE

5.1 INTRODUCTION

Animal infection models such as the murine thigh and pneumonia models play a pivotal role in antimicrobial drug discovery and development by providing valuable pharmacokinetic and pharmacodynamic (PK/PD) insight. These infection models have been used to identify the PK/PD exposure targets for a given antibacterial agent associated with bacterial killing and magnitude of the PK/PD index required to achieve therapeutic effects facilitating the prediction of antimicrobial activity in humans. Although PK/PD infection models have been successfully used in early-stage drug evaluation, there are several factors that need to be delineated such as immune response, and resistance development before they can be used to predict dose in the clinical with high confidence. In the vast majority of these models used in drug discovery and development the animals are rendered severely neurtopeunic using cyclophosphamide to establish infection. Hence, the role of immune response and possible drug immune interactions are often not considered during human dose prediction using these models.

In an infected individual, the innate immune response primarily involving granulocytes often takes the first stand during an infection. Granulocytes play a key role in the clearance of many bacterial infections. There are very limited efforts to date to delineate the role of granulocytes to the ability to clear infection during chemotherapy (46, 47, 48) in the context of drug discovery using the neutropenic animal models. The contribution of the immune system is thus often not explicitly considered during drug dose and dose regimen determination.

The aim of the present work is to delineate antibacterial activity attributed to drug effect and host immune response (granulocyte activity) by using time course bacterial burden from naïve and nuetropeunic mice with and without drug treatment. First, granulocyte activity will be characterized with the help of a semi-mechanistic immune response model using data from untreated naive and neurtopenic mice infection mode against KP1490-07. The immune response model will then be integrated with semi-mechanistic drug effect pharmacokinetic / pharmacodynamic (PK/PD) model to describe time course in vivo data from treated neutropenic mice. The model will then be used to predict treated naive mice as validation step.

5.2 MATERIALS AND METHODS

5.2.1 Microorganisms and Reagents

Drug A, an LpxC inhibitor (in 40% sulfobutyl ether (SBE) cyclodextrin), was used against *Klebsiella pneumoniae* (KP-1490-07). The MIC of drug A versus KP-1490-07 is 0.5 mg/mL. The strain was incubated at 35°C in ambient atmosphere as described by the Clinical Laboratory Standards Institute (52). Cyclophosphamide monohydrate (Alfa Aesar Lot#K25U038) was used to achieve immune suppression.

5.2.2 In-vitro growth study

In vitro bacterial growth study was performed following CLSI methodology (12). Specifically, testing was carried out in 10 mL of Brain Heart Infusion medium (BHI) and incubated at 35°C with ambient atmosphere (n=2). Serial media samples (100 µL/sample) were collected at t=0, 2, 4, 6, 8, 12 and 24h.

5.2.3 In-vivo time-kill studies

All in vivo procedures were approved and reviewed by Pfizer's Institutional Animal Care and Welfare Committee. Female CF-1 mice (n=5) were rendered neutropenic with two oral doses of cyclophosphamide with150 and 100 mg/kg at -4 and -1 days prior to challenge to achieve immune suppression. Inoculum was prepared in 5 mL of BHI from frozen culture of KP-1490-07, incubated at 37^{o}C overnight and adjusted to an OD_{600} of 1.1 prior to challenge both to naïve and neutropenic mice. At time of challenge mice were anesthetized with isofluorane and inoculated intranasally with 50 mL of bacterial suspension (6.5 $\log_{10}$ cfu/mouse). At 2 hours post-challenge (T=0 hr in PD time course) naïve and neutropenic mice received single subcutaneous (SC) doses of

drug A dissolved in 40% SBE cyclodextrin at a dose volume of 10 mL/kg (ten-fold dose titration from 300 to 3 mg/kg). Bacterial burden was enumerated at predetermined time-points (0, 2, 4, 6, 8, and 24 hr post-dose). After the mice were euthanized at each time point lungs were aseptically harvested and homogenized in sterile saline. The samples were then serially diluted and plated on MacConkey plates to determine tissue burden.

5.2.4 Mathematical modeling

A semi-mechanistic model that integrates both the immune response and drug effects was employed. In this model as shown in Figure 5-1, the rate of change of bacterial growth over time was expressed as the difference between the intrinsic bacterial growth rate, kill rate by drug, kill rate by immune system and natural death rate. A one population drug effect model (49) was employed that assumes a continuous subpopulation of bacteria with adaptation estimated as a shift in EC_{50}. Using the in vitro growth data the growth parameters of the model were estimated. The immune response was modeled using a semi-mechanistic approach with a maximum saturable killing rate by granulocytes. The kill rate is maximum (K_{IM}) at very low to low bacterial burdens whereas it decreases as the bacterial burden increases. Such a decrease in kill rate with bacterial burden is necessary to account for inoculum effect (reduction in killing action as bacterial inoculum increases). The intensity of inoculum effect could be different for different for different bacteria and is modulated using the parameter S_{max}. Additionally the immune system takes time to kick off after an infection. This delay in onset of the immune response is accounted for by the parameter $dk_{I.}$ The immune response (granulocyte clearance) model was characterized using in vivo data from naïve and neutropenic mice at different starting inocula (no drug treatment). Integration of drug

effect was completed using time-kill data from drug treated neutropenic mice by utilizing fixed immune response parameters. PK from mice was fitted to a two compartment model. The integrated model was validated using time kill-data from neutropenic mice in a separate study. The model was further utilized to predict combined drug and granulocyte time kill from naïve mice observed in an additional study. The model was implemented in Monolix software (Paris, France).

Figure 5-1 Bacterial growth dynamics model with immune response and drug effect

Population balance for a bacterial population:

Rate of change of bacteria over time = Intrinsic growth rate – Kill rate by drug – Kill rate by immune response-Natural death rate

$$\frac{dN(t)}{dt} = G[N(t)] - K[C(t), N(t)] - K_I[N(t)] - K_N$$

where:

$$G[N(t)] = K_g\left(1 - \frac{N(t)}{N_{\max}}\right)(1 - e^{-dk_g t})N(t)$$

$$K[C(t), N(t)] = \left(\frac{K_k C(t)^H}{C(t)^H + (\alpha C_{50})^H}\right)N(t) \qquad \alpha = 1 + \beta(1 - e^{(-\tau C(t)t)})$$

$$K_I[N(t)] = K_{IM}\left(1 - \frac{S_{\max} N}{N + N_{50}}\right)(1 - e^{-dk_I t})N(t)$$

$$K_N = K_d N(t)$$

G – growth rate function

K_I – kill rate by immune response

K_N – kill rate by natural death

K_g – growth rate constant for bacterial population

$N(t)$ – concentration of bacterial population at time t

$N_{\max}$ – maximum population size

K_{IM} – maximal kill rate constant by immune response

K_d – maximal kill rate constant by natural death

dk_g – growth delay

dk_I – immune response delay

S_{max} – maximum reduction in immune response kill rate due to inoculum effect

N_{50} – Critical inoculum for the onset of inoculum effect

K – drug kill function

K_k – maximal drug kill rate constant

C_{50} – concentration to achieve 50% maximal kill rate

H – sigmoidicity constant for bacterial population

α – adaptation function

β – maximum extent of adaptation

τ – rate of adaptation

5.3 RESULTS

5.3.1 In-vivo time-kill studies

Time course of KP-1490-07 burden in lung as a function of initial inoculum burden in naïve and neutropenic mice without and with drug treatment is shown in Figure 5-2 and Figure 5–3 respectively. In naïve mice without drug treatment (Figure 5-2A), net kill attributed to granulocyte activity in naïve mice was demonstrated with initial inoculum burden ranging from $1.6x10^2$ to $4.0x10^7$ cfu/mL per lung challenges. Not unexpectedly, neutropenic mice demonstrated net killing for bacterial challenges less than $1.6x10^3$ cfu/mL, net growth for challenges greater than $2.4x10^4$ cfu/mL and stasis for burden level of $1.6x10^4$ cfu/mL (Figure 5-2B).

For naïve mice with drug treatment, at $1x10^7$ cfu/mL bacterial challenge, rapid initial killing was affected by the antibacterial drug for the mid and high dose treated groups (30 and 300 mg/kg, Figure 5–3A) to a final net 2-3 log-kill. For neutropenic mice at $1x10^7$ cfu/mL, bacterial burden containment of the bacteria was not achieved for the untreated and low dose groups while stasis and 3-log kill were achieved by the mid and high doses, respectively (Figure 5–3B). Similar results were also observed with 2×10^6 cfu/mL bacterial burden.

A

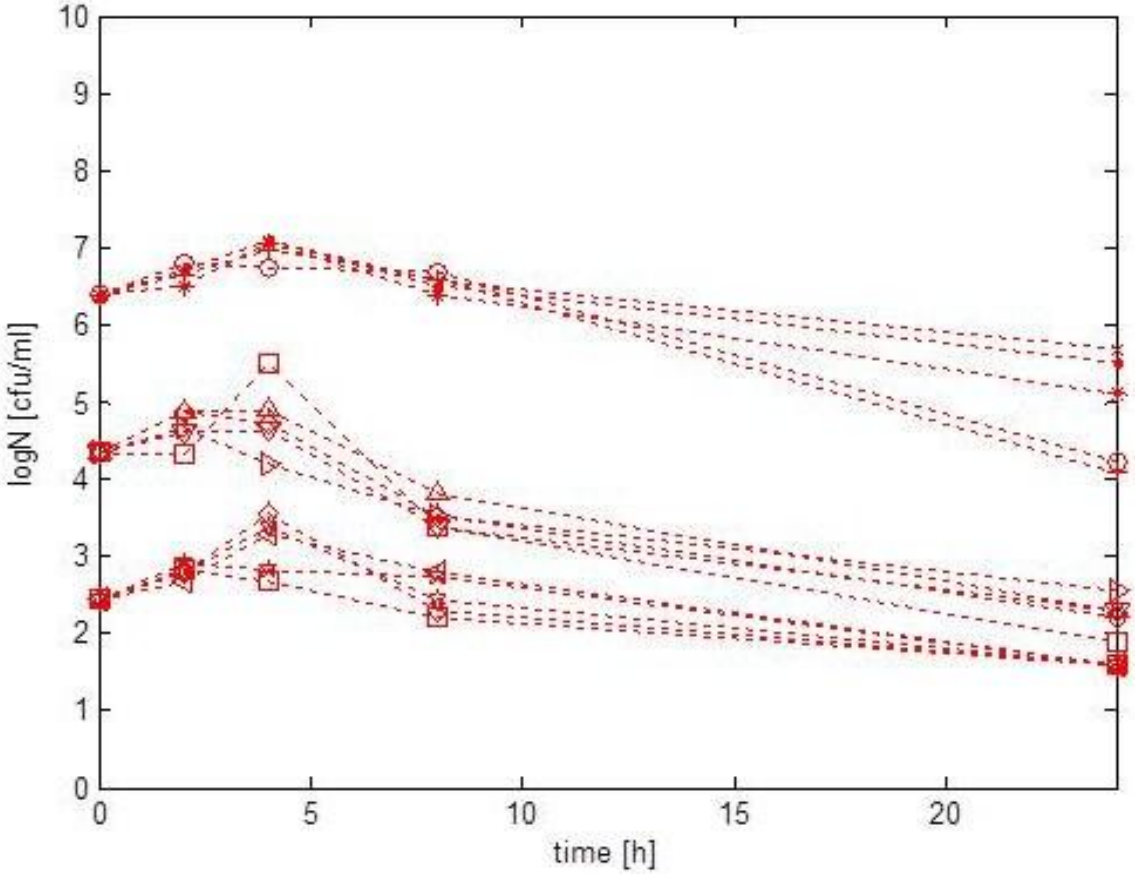

Figure 5-2 Time course of KP-1490-07 burden in lung as a function of initial inoculum burden without drug treatment in (A) naïve mice.

B

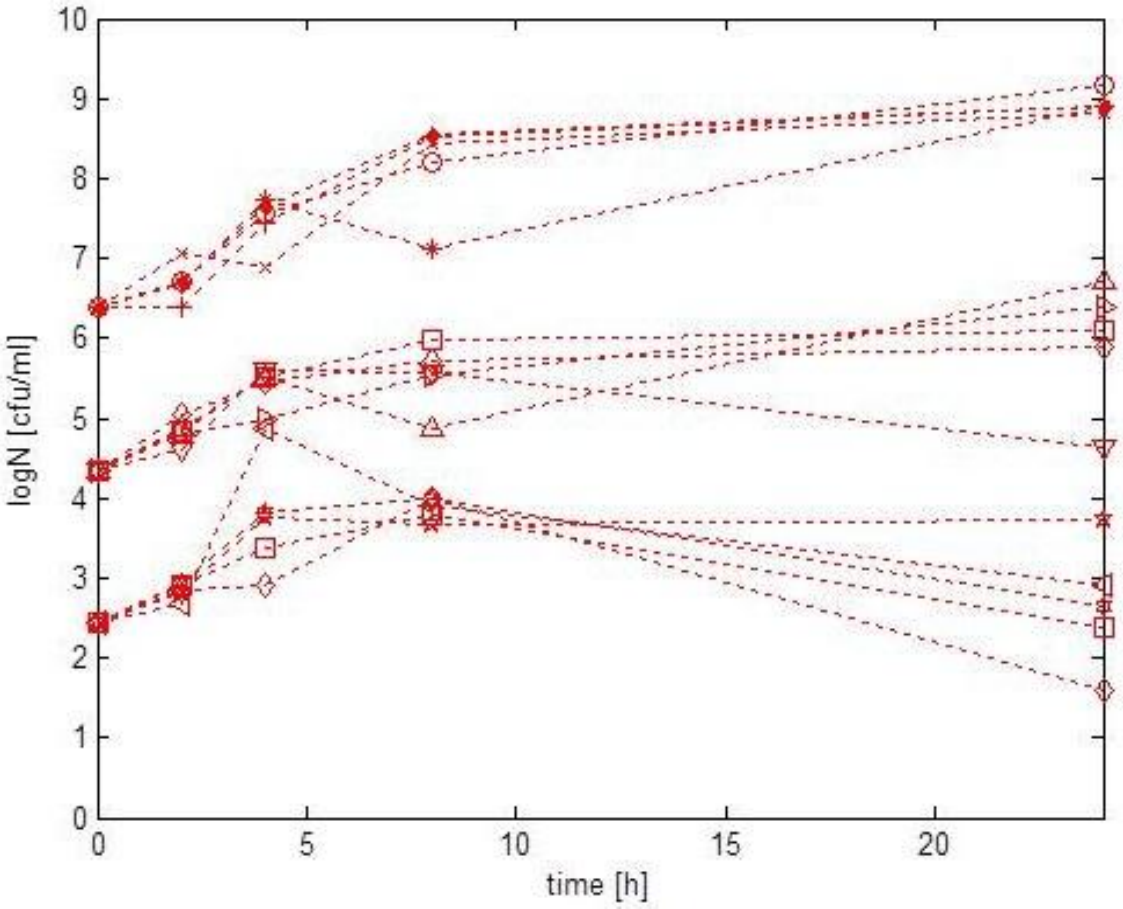

Figure 5-2 Time course of KP-1490-07 burden in lung as a function of initial inoculum burden without drug treatment in (B) neutropenic mice.

A

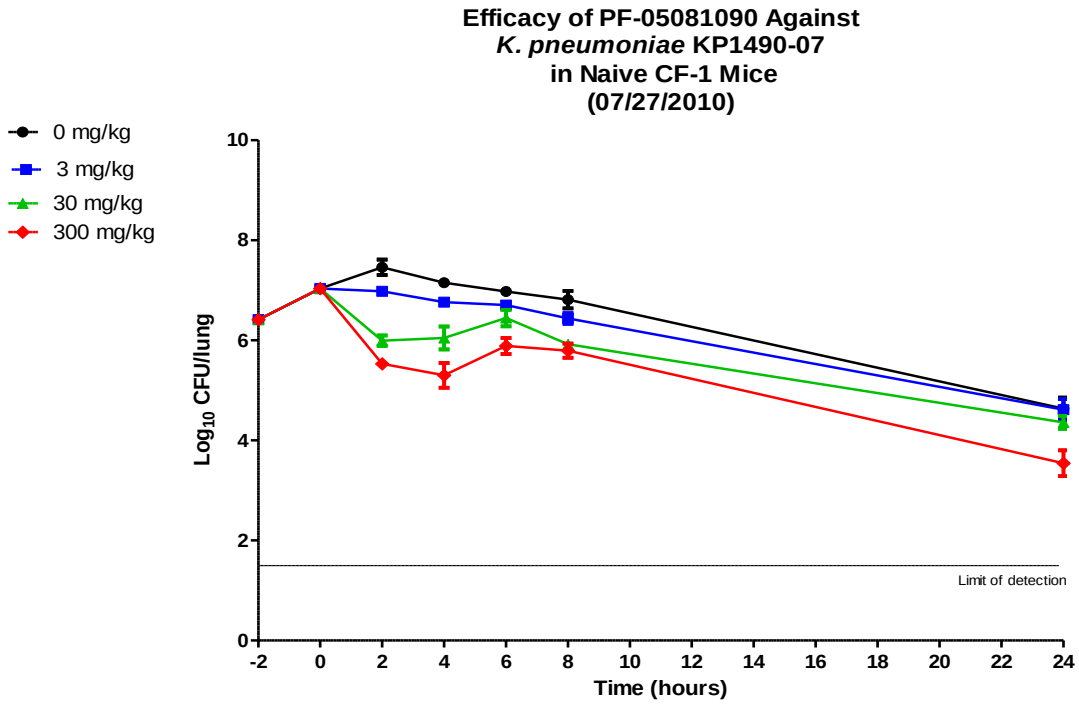

Figure 5-3 Data from in-vivo time kill studies with drug (PF-05081090) for mice infected with *Klebsiella Pneumoniae*, KP-1490-07. A) Naïve mice.

B

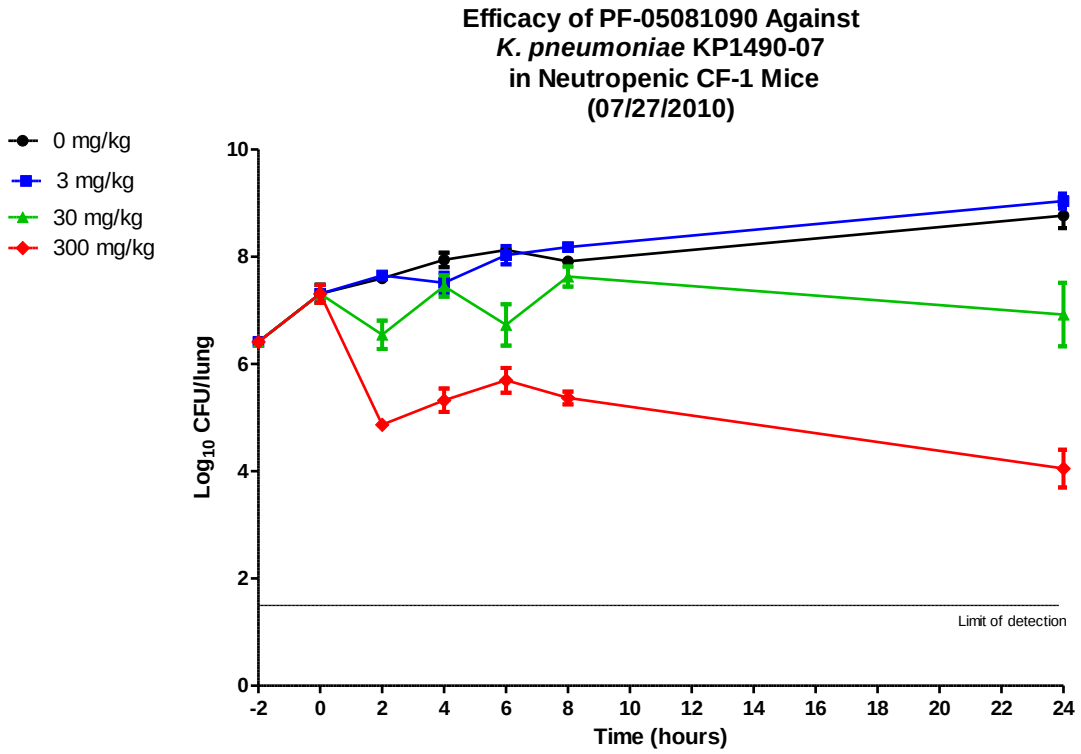

Figure 5-3 Data from in-vivo time kill studies with drug (PF-05081090) for mice infected with *Klebsiella Pneumoniae*, KP-1490-07. B) Neutropenic mice.

5.3.2 Mathematical model fitting and interpretation of results

The model-fit overlay plots with and without drug treatment is shown in Figure 5-4 and Figure 5-5 respectively for naïve and neuropenic mice. Granulocyte killing in naïve as well as neutropenic mice was well described by the proposed PK/PD model. A two-compartment pharmacokinectic model was used to characterize the drug pharmacokinetics. The drug PK paramters are as shown in Table 5–2. .The model parameter estimates for immune response and, with integrated immune reponse and drug effect are shown in Table 5–1 and Table 5–3 respectively. The granulocyte kill rate was estimated to be approximately 1.8 h^{-1} both for naïve and neutropenic mice. The effect of bacterial burden on the granulocyte killing rate was however different for naïve ($1.6x10^{10}$

cfu/mL) and for neutropenic ($2.8x10^6$ cfu/mL) mice. In order to quantify the drug effect in addition to the granulocyte activity drug treated naïve and neutropeunic mice data were employed using the the integrated PK/PD model. The model reasonably described the time kill data observed in naïve and neutropenic mice receiving drug treatment (Figure 5-5). Parameter estimates for the neutropenic mice suggests additional drug kill rate of 2.88 h^{-1} with EC_{50} of approximately 0.47 µg/mL and for the naïve mice an additional kill rate of 1.73 h^{-1} with EC_{50} of approximately 0.375 µg/mL.

A

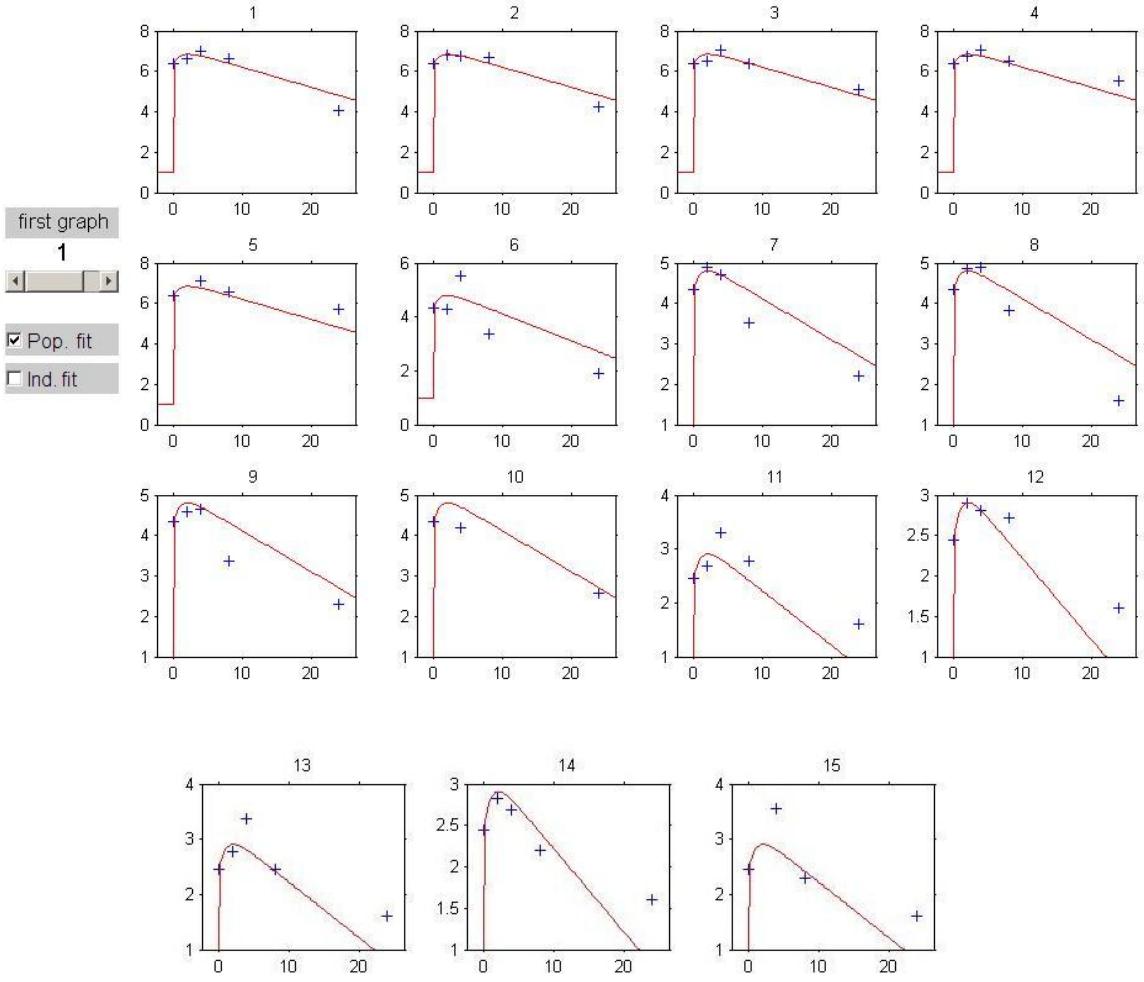

Figure 5-4 Model fits to experimental data in time kill studies for immune response without drug for mice infected with *Klebsiella Pneumoniae*, KP-1490-07. A) Naïve mice. Blue markers represent experimental data and red continuous lines represent model best-fit. For each box Y-axis is $\log_{10}$ cfu/lung and X-axis is time in hours. One box represents one experiment (initial inoculum).

B

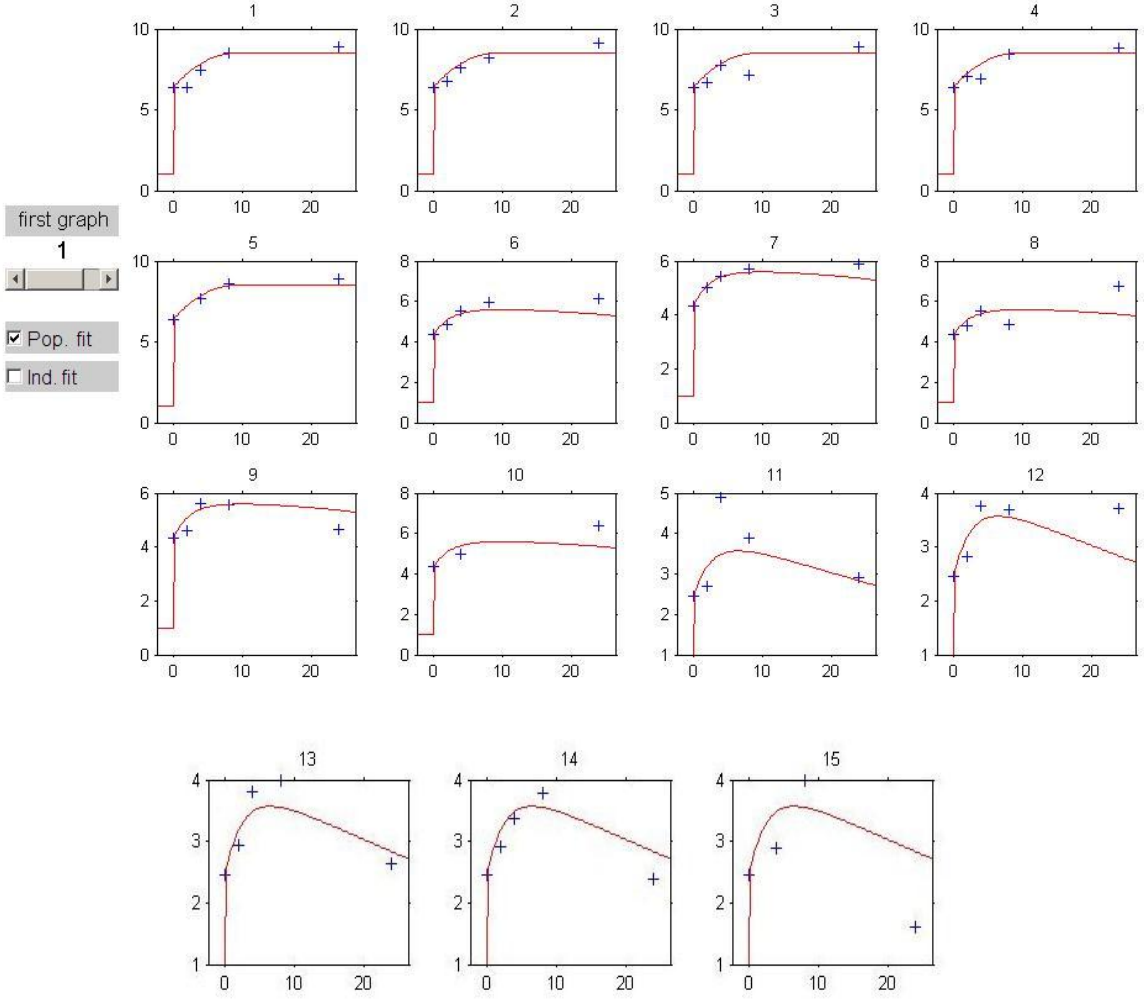

Figure 5-4 Model fits to experimental data in time kill studies for immune response without drug for mice infected with *Klebsiella Pneumoniae*, KP-1490-07. B) Neutropenic mice. Blue markers represent experimental data and red continuous lines represent model best-fit. For each box Y-axis is $\log_{10}$ cfu/lung and X-axis is time in hours. One box represents one experiment (initial inoculum).

Table 5-1 Parameter estimates to characterize immune response.

Parameter	*Naïve mice(SE %)*	*Neutropenic mice*
K_g (h^{-1})	1.85	1.65
N_{max} (CFU/ml)	$10^{9.3}$	$10^{9.3}$
K_{IM} (h^{-1})	1.7(1)	1.4(3)
K_d (h^{-1})	0.4	0.38
N_{50}	$1.6x10^8$	$2.8x10^6$
dk_g	-	-
dk_I	0.92(5)	0.78(7)
S_{max}	0.5	0.5

*growth delay was not required although there in the model. Data did not show much growth delay.

A

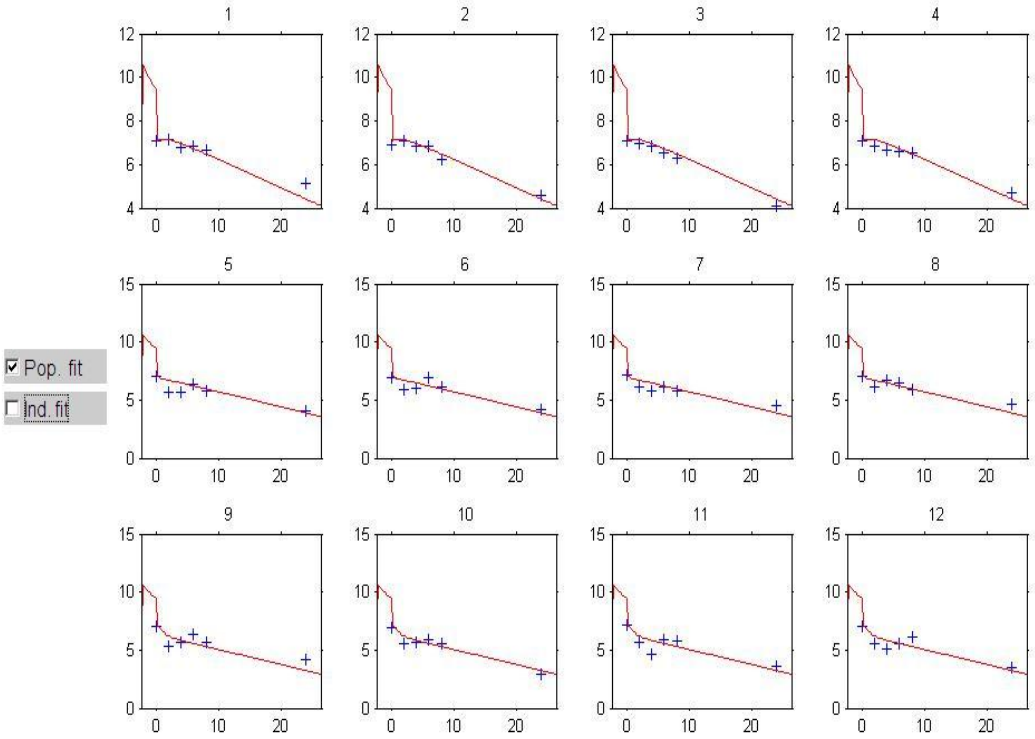

Data	Dose(mg/kg)
1,2,3,4	3
5,6,7,8	30
9,10,11,12	300

Figure 5-5 Model fits to experimental data in time kill studies for immune response with drug (PF-05081090) for mice infected with *Klebsiella Pneumoniae*, KP-1490-07. A) Naïve mice. Blue markers represent the experimental data. Red continuous lines are population fits to data. For each box Y-axis is $\log_{10}$ cfu/lung and X-axis is time in hours. One box represents one experiment.

B

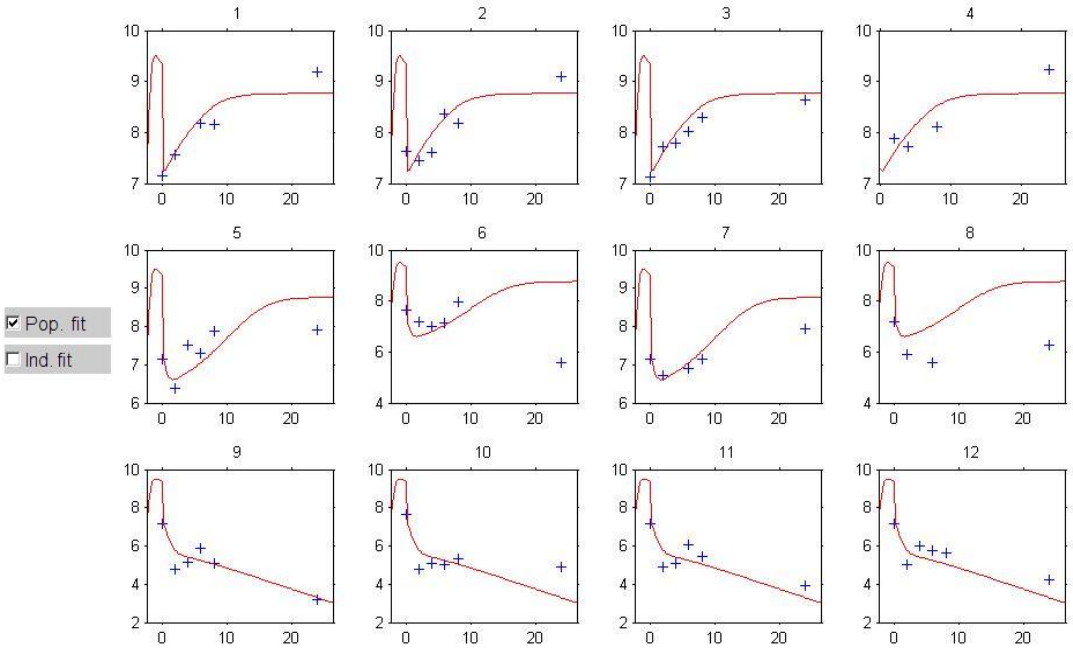

Data	Dose(mg/kg)
1,2,3,4	3
5,6,7,8	30
9,10,11,12	300

Figure 5-5 Model fits to experimental data in time kill studies for immune response with drug (PF-05081090) for mice infected with *Klebsiella Pneumoniae*, KP-1490-07. B) Neutropenic mice. Blue markers represent the experimental data. Red continuous lines are population fits to data. For each box Y-axis is $\log_{10}$ cfu/lung and X-axis is time in hours. One box represents one experiment.

Table 5-2 Parameter estimates of two compartment pharmacokinetic (PK) model for drug

PF-05081090

PK parameter	Estimate
Cl	4.59
V1	4.55
V2	15.1
Q	0.334

Table 5-3 Parameter estimates to characterize integration of drug (PF-05081090) effect and immune response in mice infected with *Klebsiella Pneumoniae,* KP-1490-07.

Parameter	*Naïve mice*	*Neutropenic mice*
K_g (h^{-1})	1.85(Fixed)	1.65(Fixed)
N_{max} (CFU/ml)	$10^{9.3}$(Fixed)	$10^{9.3}$(Fixed)
K_{IM} (h^{-1})	1.8(Fixed)	1.49(Fixed)
K_d (h^{-1})	0.4(Fixed)	0.38(Fixed)
N_{50}	$1.6x10^8$(Fixed)	$2.8x10^6$(Fixed)
dk_g	-	-
dk_I	1.43(Fixed)	1.1(Fixed)
S_{max}	0.5(Fixed)	0.5(Fixed)
K_k (h^{-1})	1.73(5)	2.88(5)
τ	0.0946(31)	0.0732(33)
β (h^{-1})	36.1(30)	28.1(18)
H (h^{-1})	3(Fixed)	3(Fixed)
C_{50}	0.375(20)	0.472(7)

5.4 DISCUSSION

From the early use of scaled serum half-life to the recent use of dynamic PKPD approaches, prediction of clinical dose and dosing regimen has gone through a couple of evolutions. The use of PKPD indices from preclinical infection models have scored a number of successful predictions for the clinic for new drugs. However, as new drug action mechanisms and combination therapy are needed to combat the menacingly increasing bacterial resistance, the use of PKPD indices which marry the efficacy to a single index (e.g AUC/MIC, %T>MIC) is incapable of dose and dosing regimen optimization for the clinic. The recent evolution thus requires the use of mechanism-based dynamic PK/PD approaches. These approaches leverage time course in vitro, and in vivo studies and incorporate the involved biochemical pathways of the antimicrobial agent(s) into the mathematical model.

It has been recognized that despite the higher dimensionality, thus more information into the interaction of bacteria and antibacterial agent, the main drawback of such approaches is that the missing of one component of the system, i.e. the immunity in the prediction of clinical dose. These models assume that if the antimicrobial agent can keep the bacterial burden in the manageable threshold (i.e. achieve stasis, 1-log reduction, 2-log reduction depending on the immunity suppression level of the patient), then the immune system can take care of the rest. Not only is this a hand waving exercise, but also the interaction of the antimicrobial agent with the immune system, either pharmacokinetically or pharmacodynamically, is completely ignored. Efforts to delineate the contribution of immune kill (mainly granulocyte) in the antimicrobial drug development, and the use of integrated immune and drug kill semi-mechanistic models

would be imperative in the future to accurately predict doses for immune-compromised and intact patients.

The pharmacokinetic and pharmacodynamic modulatory effects of antimicrobial agents to the innate and specific immunity have been well documented (31, 28). Microlides and specifically telithromycin is prime example that modulates the PK by distributing to the white blood cells that increases the exposure of the drug to the bacteria. Also telithromycine suppresses INF-γ production thus modulating the pro-inflammatory mediators (cytokines). These effects account for the effectiveness of telithromycin.

Leijh et al. (31) and Drusano et al. (18) have characterized the effect of bacterial burden on granulocyte clearance. Specifically Drusano et al. (18) have shown that granulocyte kill function is saturable with bacterial and the immune system would not be able to contain infection by high baseline bacterial burden. We also observed an effect of inoculum on immune response albeit in a different way. In our system, the kill rate by granulocytes decrease with inoculum, with the decrease saturating at high inocula. Additionally our observations showed a delay in the onset of immune response which was appropriately included in the immune response kill function. One of the efforts to integrate the immune response and drug effect is by Hope et al (28), where they characterized the change in burden of C. *albicans* in presence of drug and granulocyte kill. Our model is very similar to the model used by them except that we characterize the change in bacterial burden. However, similar to Drusano et al. they have characterized the inoculum effect as saturable function, which was modified in our case as described above.

The effect of bacterial inoculum on the granulocyte kill rate was different for naïve ($1.6x10^{10}$ cfu/mL) and for neutropenic ($2.8x10^{6}$ cfu/mL) mice. This is expected since in neutropenic mice we expect the decrease in maximal granulocyte kill rate would be faster because of their compromised immune system. However, the maximal granulocyte kill rate, being an intrinsic characteristic, remains unchanged in both the naïve and neutropenic settings, further attesting the consistency of the model. However, the model assumes that there is no interaction between drug and granulocytes which may not hold true. If there is indeed any interaction, then significant differences would be expected between naïve and neutropenic settings, since the change in immune response would eventually affect drug action. Additional investigations on different strains/species are necessary to ascertain if drug and immune response interaction is universal or species dependent phenomenon.

CHAPTER 6

CONCLUSIONS AND FUTURE DIRECTIONS

In our research we have applied novel mathematical modeling techniques to charactize diiferent phenomenon that are seen when antimicrobials are used to treat a bacterial infection both in-vitro and in-vivo.

In the first case study, we describe the phenomenon of inoculum effect using a simplified mathematical model. Specifically the cause of the phenomenon was attributed to the biofilm barrier that could develop as the bacterial cell density increases. This may be an over simplification of the actual mechanism. However, with respect to explaining the reduced kill at higher inoculum, our approach was found adequate enough. Starking features of the approach are a simple model with inoculum effect related to initial bacterial cell concentration (baseline inoculum). Not only was the model able to describe the data, we also characterized the statistics of the model parameters using novel ways to compute confidence intervals. This type of statistical analysis is novel in the sense we used the concepts of joint confidence regions to quantify uncertainity in the model paramteters. The assumptions of the model were validated using simple colorimetry experiments.

As a future direction, one may need to investigate the phenomena of inoculum effect much more mechanistically. Experiments could be designed to lyse the bacterial cells and actually see the concentration of drug inside the cell. That way transport equations could be used to describe the mass transfer limitations when drug passes from

bulk liquid to bacterial cell. Additionally, the phenomenon could be attributed to instantaneous bacterial population instead of baseline bacterial burden.

In the second case study, flouroquinolone pharmacodynamics were characterized using a mathematical model. The pharmacodynamics were studied for both gram-positive and gram-negative bacteria although on different drugs. Concepts of concentration dependency and time dependency were applied and was show that both types of dependencies were seen at different times (biphasic) of the drug exposure. The model parameters were again analysed statistically for joint confidence regions and non-linear type confidence intervals. Finally the model optimal parameters were used to make optimal predictions using surface plot methodology. As for predictions the numbers were very close to the clinically relevant doses for levofloxacin. While these predictions are for an early stage in-vitro study, they could be used as flags in the drug development process. For example, if the predictions from in-vitro expriments suggest that the dose required to suppress the bacterial population is much higher (orders of magnitude) than the permissible dose(based on toxicity/safety studies), then it is a possible red flag to decide upon the fate the of the candidate molecule (very early in the development stage)

As a future study one could investigate the role of persister populations and apply a relevant modeling framework to characterize the data. Better quantifying the susceptible, resiatant and dormant modes of the bacterial subpopulations could help in better model building and more optimal predictions.

In case study three, a novel mathematical framework and pharmacodynamic index was proposed to investigate the dynamics of antibitotic-inhibitor combinations. Such a framework could be very useful in designing optimal dosing strategy for the

combination.. A novel comcept of instantaneous MIC was introduced to capture fluctuating susceptibilities. This instantaneous MIC is hypothetical and ia a modeling convenience to capture fluctuating suscpetibilities. Nevertheless, the model could incorporate the properties of different inhibitors within its parameters. Additionally, the innovative surrogate index $T > MIC_i$ could be translated to concentration dependent drugs as C_{max}/MIC_i and AUC/MIC_i.

One could use such a approach to investigate a range of drug-inhibitor-bug combinations and test for robustness. Another important aspect is to define a robust threshold for the novel pharmacodynamic index such that its cut-off for efficacy is similar for a range of drug-inhibitor-bug combinations. Although it has been assumed in our approach that inhibitors inherently do not have any antimicrobial properties, it is very much possible that an inhibitor has significant antimicrobial properties. For example a beta-lactamase inhibitor may denature the beta-lactamase enzyme as well as bind itself to the penicillin binding proteins (PBPs). In such a case apart from studies to quantify fluctuating susceptibilities, one may need to incorporate the inhibitory effect into the pharmacodynamic model and characterize relevant combination data.

In the final case study immune response was characterized using a novel semi-mechanistic model and subsequently integrated with a drug effect model. Such a study is very important in quantifying the contribution of immune response in clearing bacterial infections. This in turn is crucial in designing optimal dosing regimens since neglecting the immune component may result in overprediction of the required dose to clear the infection. Such suboptimal dosing is not advised considering that suboptimal dosing results in amplification of resistance. In this case study, we were successfully able to

characterize the suppression or amplification of infection in both naïve and neutropenic mice. The model was robust in the sense that almost similar parameter values were obtained for the immune system component for both naïve and neutropenic mice. Additionally similar parameter values were used to when integrating with the drug component and the model was good enough.

In our study the model to characterize immune component was fairly simple. However, immune response is a highly complex phenomenon with various networks involved in it. Nevertheless our effort was amongst the first of its kind in integrating both components at semi-mechanistic level. The approach could be extended with inclusion of the immune system-drug interaction. Additionally, one could apply a very detailed systems biology/pharmacology approach to quantify exact mechanisms involved in the process.

In a nutshell, our use of mathematical modeling is very novel and includes all aspects of modeling, simulation, statistics and experimental validation. The mathematics as shown is useful in a variety of scenarios involving infection and therapy. Such models are useful in providing quick assessment of the drug candidate at early stage of development without being intensive. The demonstrated approach holds a lot of promise in preclinical and clinical drug development process.

REFERENCES

1. **Ambrose, P. G., S. M. Bhavnani, C. M. Rubino, A. Louie, T. Gumbo, A. Forrest, and G. L. Drusano.** 2007. Pharmacokinetics-pharmacodynamics of antimicrobial therapy: it's not just for mice anymore. Clin Infect Dis **44:**79-86.
2. **Ambrose. P. G., Grasela. D. M., Grasela. T. H., Passarell. J., Mayer. H. B., Pierce. P. F.** 2001. Pharmacodynamics of fluoroquinolones against Streptococcus pneumoniae in patients with community-acquired respiratory tract infections. Antimicrob Agents Chemother; **45**: 2793-7.
3. **Ambrose, P. G., Bhavnani. S. M. , Owens. R. C. Jr.** 2003. Clinical pharmacodynamics of quinolones. Infect Dis Clin North Am; **17**: 529-43.
4. **Andrews. J. M.** 2001. Determination of minimum inhibitory concentrations. J of Antimicrob Chemother 48 (Suppl. 1):5-16.
5. **Bhagunde. P., Chang. K. T., Hirsch. E., Ledesma. K. R., Nikolaou. M., Tam. V. H.** 2012. A novel modeling framework to guide design of optimal dosing strategies for beta-lactamase inhibitors. Antimicrob Agents Chemother; 56(5): 2237-40
6. **Bhagunde. P, Chang. K. T., Singh. R., Singh. V., Garey. K. W., Nikolaou. M., Tam. V. H.,** 2010. Mathematical modeling to characterize inoculum effect. Antimicrob Agents Chemother; 54(11): 4739-43
7. **Bhagunde. P., Singh. R., Ledesma. K. R., Chang. K. T., Nikolaou. M., Tam. V. H.** 2011. Modelling biphasic killing of fluoroquinolones: guiding optimal dosing regimen design. J Antimicrob Chemother; 66(5):1079-86

8. **Bedenic, B., N. Beader, and Z. Zagar.** 2001. Effect of inoculum size on the antibacterial activity of cefpirome and cefepime against Klebsiella pneumoniae strains producing SHV extended-spectrum beta-lactamases. Clin Microbiol Infect **7:**626-35.

9. **Bulitta, J. B., N. S. Ly, J. C. Yang, A. Forrest, W. J. Jusko, and B. T. Tsuji.** 2009. Development and qualification of a pharmacodynamic model for the pronounced inoculum effect of ceftazidime against Pseudomonas aeruginosa. Antimicrob Agents Chemother **53:**46-56.

10. **Burgess, D. S., and R. G. Hall, 2nd.** 2004. In vitro killing of parenteral beta-lactams against standard and high inocula of extended-spectrum beta-lactamase and non-ESBL producing Klebsiella pneumoniae. Diagn Microbiol Infect Dis **49:**41-6.

11. **Campion, J. J., P. J. McNamara, and M. E. Evans.** 2005. Pharmacodynamic modeling of ciprofloxacin resistance in Staphylococcus aureus. Antimicrob Agents Chemother **49:**209-19.

12. **Clinical and Laboratory Standards Institute.** 2007. Performance standards for antimicrobial susceptibility testing: seventeenth informational supplement. CLSI document M100-S17, Wayne, Pennsylvania.

13. **Cohen, M. L.** 1992. Epidemiology of drug-resistance - implications for a postantimicrobial era. Science, **257**, 5073, 1050-1055

14. **Craig. W. A., Ebert. S. C.** 1990. Killing and regrowth of bacteria in vitro: a review. *S*cand J Infect Dis Suppl; **74**: 63-70.

15. **Craig W.** 1993. Pharmacodynamics of antimicrobial agents as a basis for determining dosage regimens. Eur J Clin Microbiol Infect Dis 1993;12:Suppl 1:S6-8

16. **Drawz, S. M., and R. A. Bonomo.** 2010. Three decades of beta-lactamase inhibitors. Clin Microbiol Rev **23:**160-201.

17. **Drlica, K. A.** 2001.Strategy for fighting antibiotic resistance. ASM News, **67**, 1, 27-33.

18. **Drusano, G.L. Fregeau, C., Liu, W., Brown, D.L, Louie, A.** 2010. Impact of burden on granulocyte clearance of bacteria in a mouse thigh infection model.Antimicrob Agents Chemother; 54:4368-4372.

19. **Drusano. G. L., Preston. S. L., Fowler. C., Corrado. M., Weisinger. B., Kahn. J.** 2004. Relationship between fluoroquinolone area under the curve: minimum inhibitory concentration ratio and the probability of eradication of the infecting pathogen, in patients with nosocomial pneumonia. J Infect Dis; **189**: 1590-7.

20. **Dudley. M. N.** 1991. Pharmacodynamics and pharmacokinetics of antibiotics with special reference to the fluoroquinolones. Am J Med; 91:45S-50S.

21. **Eng, R. H., S. M. Smith, and C. Cherubin.** 1984. Inoculum effect of new beta-lactam antibiotics on Pseudomonas aeruginosa. Antimicrob Agents Chemother; 26**:**42-7.

22. **Etienne. M., Croisier. D., Charles. P. E., Lequeu. C., Piroth. L., Portier. H., Drlica. K., Chavanet. P.** 2004. Effect of low-level resistance on subsequent enrichment of fluoroquinolone-resistant Streptococcus pneumoniae in rabbits. J Infect Dis; **190**: 1472-5.

23. **Forrest. A., Nix. D. E., Ballow. C. H., Goss. T. F., Birmingham. M. C., Schentag. J. J.** 1993. Pharmacodynamics of intravenous ciprofloxacin in seriously ill patients. Antimicrob Agents Chemother; **37**: 1073-81.

24. **Fuhrmann. V., Schenk. P., Jaeger. W., Ahmed. S., Thalhammer. F.** 2004. Pharmacokinetics of moxifloxacin in patients undergoing continuous venovenous haemodiafiltration. J Antimicrob Chemother; **54**: 780-4.

25. **Garey, K. W., Q. P. Vo, R. E. Lewis, W. Saengcharoen, M. T. Larocco, and V. H. Tam.** 2009. Increased bacterial adherence and biomass in Pseudomonas aeruginosa bacteria exposed to clarithromycin. Diagn Microbiol Infect Dis **63:**81-6.

26. **Gold, H. S., Moellering, R. C.** 1996. Antimicrobial-drug resistance. N. Engl. J. Med.,**335**, 1444-1453.

27. **Gumbo. T., Louie. A., Deziel. M. R. , Parsons. L. M., Salfinger. M., Drusano. G. L.** 2004. Selection of a moxifloxacin dose that suppresses drug resistance in Mycobacterium tuberculosis, by use of an in vitro pharmacodynamic infection model and mathematical modeling. J Infect Dis; **190**: 1642-51.

28. **Hope, W. W., G. L. Drusano, C. B. Moore, A. Sharp, A. Louie, T. J. Walsh, D. W. Denning, and P. A. Warn.** 2007. Antimicrob. Agents Chemother. 51:285-295.

29. **Jumbe. N., Louie. A., Leary. R., Liu. W., Deziel. M..R., Tam. V. H., Bachhawat. R., Freeman. C., Kahn. J. B., Bush. K., Dudley. M. N., Miller. M. H., Drusano. G. L.** 2003. Application of a mathematical model to prevent in vivo amplification of antibiotic-resistant bacterial populations

during therapy. J Clin Invest; **112**: 275-85.

30. **Konig, C., H. P. Simmen, and J. Blaser.** 1998. Bacterial concentrations in pus and infected peritoneal fluid--implications for bactericidal activity of antibiotics. J Antimicrob Chemother **42:**227-32.

31. **Leijh. P. C., van. den. Barselaar. M. T., van. Zwet. T. L., Dubbeldeman-Rempt. I., V. F. R.** 1979. Immunology 37:453-465.

32. **Levy, S. B.** 1998. The challenge of antibiotic resistance. Scientific American.

33. **Liu, P., K. H. Rand, B. Obermann, and H. Derendorf.** 2005. Pharmacokinetic-pharmacodynamic modelling of antibacterial activity of cefpodoxime and cefixime in in vitro kinetic models. Int J Antimicrob Agents **25:**120-9.

34. **MacGowan. A. P., Rogers. C. A., Holt. H. A.** *et al.* 2003. Activities of moxifloxacin against, and emergence of resistance in, Streptococcus pneumoniae and Pseudomonas aeruginosa in an in vitro pharmacokinetic model. Antimicrob Agents Chemother; **47**: 1088-95.

35. **Mauldin, P. D., C. D. Salgado, I. S. Hansen, D. T. Durup, and J. A. Bosso.** 2010. Attributable hospital cost and length of stay associated with health care-associated infections caused by antibiotic-resistant gram-negative bacteria. Antimicrob Agents Chemother **54:**109-115.

36. **Meagher, A. K., A. Forrest, A. Dalhoff, H. Stass, and J. J. Schentag.** 2004. Novel pharmacokinetic-pharmacodynamic model for prediction of outcomes with an extended-release formulation of ciprofloxacin. Antimicrob Agents Chemother **48:**2061-8.

37. **Mizunaga, S., T. Kamiyama, Y. Fukuda, M. Takahata, and J. Mitsuyama.** 2005. Influence of inoculum size of Staphylococcus aureus and Pseudomonas aeruginosa on in vitro activities and in vivo efficacy of fluoroquinolones and carbapenems. J Antimicrob Chemother **56:**91-6.

38. **Morens, D. M., Folkers, G. K., Fauci, A. S.** 2004. The challenge of emerging and re- emerging infectious diseases. Nature; **430**: 242 - 249.

39. **Mouton, J. W., M. N. Dudley, O. Cars, H. Derendorf, and G. L. Drusano.** 2005. Standardization of pharmacokinetic/pharmacodynamic (PK/PD) terminology for anti-infective drugs: an update. Journal of Antimicrobial Chemotherapy **55:**601-607.

40 **Neu, H. C.** 1992. The crisis in antibiotic resistance. Science, **257**, 1064-1073.

41. **Nielsen, E. I., A. Viberg, E. Lowdin, O. Cars, M. O. Karlsson, and M. Sandstrom.** 2007. Semimechanistic pharmacokinetic/pharmacodynamic model for assessment of activity of antibacterial agents from time-kill curve experiments. Antimicrob Agents Chemother **51:**128-36.

42. **Nikolaou, M., A. N. Schilling, G. Vo, K. T. Chang, and V. H. Tam.** 2007. Modeling of microbial population responses to time-periodic concentrations of antimicrobial agents. Ann Biomed Eng **35:**1458-70.

43. **Nikolaou, M., and V. H. Tam.** 2006. A new modeling approach to the effect of antimicrobial agents on heterogeneous microbial populations. J Math Biol **52:**154-82.

44. **Norrby, S. R., B. Bjornegard, F. Ferber, and K. H. Jones.** 1983. Pharmacokinetics of imipenem in healthy volunteers. J Antimicrob Chemother **12 Suppl D:**109-124.

45. **Painter, R. E., and K. Young.** 2007. Carbapenem-hydrolyzing beta-lactamases KPC-2 and KPC-3 in *Klebsiella pneumoniae* isolates from Florida, abstr. A-016, Abstr. 107th Gen. Meet. Am. Soc. Microbiol., American Society for Microbiology, Toronto, Ontario, Canada.

46. **Pea. F., Di. Qual. E., Cusenza. A., Brollo. L., Baldassarre. M., Furlanut. M.** 2003. Pharmacokinetics and pharmacodynamics of intravenous levofloxacin in patients with early-onset ventilator-associated pneumonia. Clin Pharmacokinet; **42**: 589-98.

47. **Preston. S. L., Drusano. G. L., Berman. A. L., Fowler. C. L., Chow. A. T., Dornseif. B., Reichl. V., Natarajan. J., Corrado. M.** 1998. Pharmacodynamics of levofloxacin: a new paradigm for early clinical trials. Jama; **279**: 125-9.

48. **Schuck, E. L., A. Dalhoff, H. Stass, and H. Derendorf.** 2005. Pharmacokinetic/pharmacodynamic (PK/PD) evaluation of a once-daily treatment using ciprofloxacin in an extended-release dosage form. Infection **33 Suppl 2:**22-8.

49. **Singh. R, Ledesma. K. R., Chang. K. T., Hou. J. G., Prince. R. A., Tam V. H.** 2009. Pharmacodynamics of moxifloxacin against a high inoculum of Escherichia coli in an in vitro infection model. *J Antimicrob Chemother*; **64**: 556-62.

50. **Singh. R, Ledesma. K. R., Chang. K. T., Tam. V. H.** 2010. Impact of recA on levofloxacin exposure-related resistance development. Antimicrob Agents Chemother; **54**: 4262-8.

51. **Stass. H., Kubitza. D., Schuhly. U.** 2001. Pharmacokinetics, safety and tolerability of moxifloxacin, a novel 8-methoxyfluoroquinolone, after repeated oral administration. Clin Pharmacokinet; **40 Suppl 1**: 1-9.

52. **Standards., N. C. f. C. L.** Methods for determining bactericidal activity of antimicrobial agents, Approved Guideline.

53. **Stevens, D. L., S. Yan, and A. E. Bryant.** 1993. Penicillin-binding protein expression at different growth stages determines penicillin efficacy in vitro and in vivo: an explanation for the inoculum effect. J Infect Dis **167:**1401-5.

54. **Talbot, G. H., J. Bradley, J. E. Edwards, Jr., D. Gilbert, M. Scheld, and J. G. Bartlett.** 2006. Bad bugs need drugs: an update on the development pipeline from the Antimicrobial Availability Task Force of the Infectious Diseases Society of America. Clin Infect Dis **42:**657-668.

55. **Tam, V. H., K. R. Ledesma, K. T. Chang, T. Y. Wang, and J. P. Quinn.** 2009. Killing of Escherichia coli by beta-lactams at different inocula. Diagn Microbiol Infect Dis **64:**166-71.

56. **Tam. V. H., Louie. A., Deziel. M. R., Liu. W., Drusano. G. L.** 2007. The relationship between quinolone exposures and resistance amplification is characterized by an inverted U: a new paradigm for optimizing pharmacodynamics to counterselect resistance. Antimicrob Agents Chemother; **51**: 744-7.

57. **Tam, V. H., A. Louie, M. R. Deziel, W. Liu, R. Leary, and G. L. Drusano.** 2005. Bacterial-population responses to drug-selective pressure: examination of garenoxacin's effect on Pseudomonas aeruginosa. J Infect Dis **192:**420-8.

58. **Tam, V. H., A. N. Schilling, D. A. Melnick, and E. A. Coyle.** 2005. Comparison of beta-lactams in counter-selecting resistance of Pseudomonas aeruginosa. Diagn Microbiol Infect Dis **52:**145-51.

59. **Tam. V. H., Ledesma. K. R., Vo. G., Kabbara. S., Lim. T. P., Nikolaou. M.** 2008. Pharmacodynamic modeling of aminoglycosides against Pseudomonas aeruginosa and Acinetobacter baumannii: identifying dosing regimens to suppress resistance development. Antimicrob Agents Chemother; **52**: 3987-93.

60. **Tam, V. H., A. N. Schilling, and M. Nikolaou.** 2005. Modelling time-kill studies to discern the pharmacodynamics of meropenem. J Antimicrob Chemother **55:**699-706.

61. **Tam, V.H., Schilling, A.N., Nikolaou, M. J.** 2005. Antimicrob. Chemother. 55:699-706.

62. **Tam, V. H., A. N. Schilling, K. Poole, and M. Nikolaou.** 2007. Mathematical modelling response of Pseudomonas aeruginosa to meropenem. J Antimicrob Chemother **60:**1302-9.

63. **Udekwu, K. I., N. Parrish, P. Ankomah, F. Baquero, and B. R. Levin.** 2009. Functional relationship between bacterial cell density and the efficacy of antibiotics. J Antimicrob Chemother **63:**745-57.

64. **Varaldo, P. E.** 2002. Antimicrobial resistance and susceptibility testing: An evergreen topic. J of Antimicrob Chemother; **50:** 1-4.

65. **William. M. M. K.** 1945. Bacteriostatic and lytic actions of penicillin on sensitive and resistant staphylococci. J Clin Invest; 24(2): 165–169.

66. **Yano, Y., T. Oguma, H. Nagata, and S. Sasaki.** 1998. Application of logistic growth model to pharmacodynamic analysis of in vitro bactericidal kinetics. J Pharm Sci **87:**1177-83.

67. **Zhanel. G. G., Walters. M., Laing. N., Hoban. D. J.** 2001 In vitro pharmacodynamic modeling simulating free serum concentrations of fluoroquinolones against multidrug-resistant Streptococcus pneumoniae. J Antimicrob Chemother; 47:435-440.

68. **Zinner. S. H., Lubenko. I. Y., Gilbert. D., Simmons. K., Zhao. X., Drlica. K., Firsov. A. A.** 2003. Emergence of resistant Streptococcus pneumoniae in an in vitro dynamic model that simulates moxifloxacin concentrations inside and outside the mutant selection window: related changes in susceptibility, resistance frequency and bacterial killing. J Antimicrob Chemother; **52**: 616-22.